



ALUMINUM LIGHTWEIGHT ORTHOTROPIC DECK EVALUATION PROJECT



FLORIDA DEPARTMENT OF TRANSPORTATION
M. H. ANSLEY STRUCTURES RESEARCH CENTER
WRITTEN BY: CHRISTINA FREEMAN, P.E.
REVIEWED BY: WILLIAM POTTER, P.E.
2017

Table of Contents

Introduction.....	4
Acknowledgement	5
Background.....	6
Test Specimen.....	7
Visual and Non-Destructive Inspections.....	8
Visual Inspection and Photographic Inventory	8
Generation II Panel Weld.....	13
Faying Surface	15
Bolt Torque	17
Discussion.....	18
Structural Testing.....	20
Test Setup Description.....	20
Static Testing	25
Data Analysis and Processing	25
Results.....	26
Cyclic Testing	31
Data Analysis and Processing	31
Fatigue Results.....	36
Deflection Results	37
Discussion.....	38
Heavy Vehicle Simulation Testing	40
Test Setup Description.....	40
Simulation Testing	44
Data Analysis and Processing	46
Fatigue Results.....	49
Deflection Results	50
Slip Deflection Results.....	51
Wearing Surface Testing.....	54
Bond Testing.....	54
Friction Testing.....	57
Discussion.....	58
Corrosion Testing.....	59
Conclusions.....	62

Bibliography	63
Appendix A: Structural Testing Procedure	64
Appendix B: Heavy Vehicle Simulator Testing Procedure	85
Appendix C: Material and Weld Certifications	93
Appendix D: Visual Inspection Records.....	106
Appendix E: Visual Inspection Photo Inventory	118
Appendix F: Bond Test Location Plan and Photo Inventory	250
Appendix G: Friction Testing Report	263

Introduction

The majority of bascule bridges in Florida have been constructed with lightweight open grid steel decks, which leave substantial steel surface area exposed to corrosive debris, resulting in significant maintenance costs during their service life. The existing decks also have fatigue prone details, limited skid resistance resulting in reduced safety for bicycles, and are noisy. Replacement options for lightweight open grid steel decks must be a similar weight and depth as the existing bridge deck, so that rehabilitation is not required for the bascule bridge foundations, mechanical systems or roadway profile.

An existing concept for aluminum bridge deck panels for use on moveable bridges was further refined by the Florida Department of Transportation in consultation with AlumaBridge, LLC and Hardesty & Hanover, LLC. The aluminum material of the deck is inherently less corrosive than steel in coastal environments, providing for better maintainability. The solid riding surface allows for better skid resistance, reduction in noise levels, and provides protection to the structural members. Because the aluminum deck panel has an equivalent weight and depth as lightweight open grid steel decks, it can easily be used to replace those decks and may prove to be an ideal replacement alternative.

Thorough evaluation of any new structural system is required prior to placement on a bridge in order to ensure safety of the travelling public. The Florida Department of Transportation conducted a thorough in-house research-based evaluation of the deck system, including visual inspection, structural testing, heavy vehicle simulation, wearing surface evaluation and corrosion testing. This report provides some details of the deck system and presents the findings of the Florida Department of Transportation's evaluation.

Acknowledgement

This research has been made possible by many people. Credit is due to Alberto Sardinas, FDOT District 4 Maintenance, for his forward thinking and drive to find an alternative to open grid steel decks. The thorough evaluation of this deck system would not have been possible without the FDOT Pavement Materials Group, led by Bouzid Choubane. Under his direction, heavy vehicle simulation testing was performed and the friction surface evaluated. Specific thanks goes to Wayne Allick, Jacob McDonald and Richard Smith, in Pavement Research. Their expertise in accelerated testing was invaluable and their effort to help another office achieve their objectives is commendable. Charles Holzschuher and the Pavement Performance Group provided a thorough wearing surface friction evaluation. Thanks is due to Ivan Lasa, Ronald Simmons and Adrian Steele, of the FDOT Corrosion Research Laboratory for testing the wearing surface bond strength. Their job continues due to ongoing corrosion evaluation and their effort is appreciated from now until the corrosion evaluation is complete. Finally, credit is due to of all members of the FDOT Structures Research Center for their assistance during the testing described in this report.

Background

The Florida Department of Transportation initiated research in the 2000s to identify or develop a structural deck system for replacing open grid steel decks on bascule bridges. Several research reports were completed by Florida International University and the University of Central Florida.

The first research project considered three deck systems: SAPA aluminum deck by SAPA Group of Sweden, Ductal®-MMFX steel deck and Ductal®-fiber reinforced polymer (FRP) tube deck [1]. At the conclusion of the research project, SAPA aluminum deck was deemed ready for implementation, the Ductal®-MMFX steel deck required development of a few additional components, and the Ductal®-fiber reinforced polymer (FRP) tube deck required additional experimental and analytical work prior to recommendation for field application.

The second research project, Phase II, with Florida International University and the University of Central Florida further developed the UHPC-HSS deck (previously referred to as Ductal®-MMFX) and introduced a fourth alternative – a FRP deck system [2]. The research determined further weight reduction is needed for the UHPC-HSS deck. The FRP deck was evaluated, but the wearing surface did not perform satisfactorily.

A separate research project with URS Corporation, Inc. (with Hardesty & Hanover, LLC as sub consultant) provides a comparative evaluation of several deck types previously researched, using a value engineering approach considering cost, functionality and safety, maintenance, durability and constructability. URS recommended the aluminum orthotropic deck system be developed further as it scored highest among the deck systems considered. [3]

Through a continued contract with URS/ Hardesty & Hanover with George Patton as Principal Investigator and through consultation with supplier AlumaBridge, LLC, the aluminum orthotropic deck system was refined and made more constructible and economical. The extruded panel shape was revised to enable an infinite number of widths to be constructed and the friction stir welding process was used to join extruded panels, improving weld quality. The research project resulted in two different panels which were given to FDOT for testing and evaluation. [4]

Test Specimen

The test specimen provided to FDOT by AlumaBridge, LLC includes two extruded aluminum panels attached to three steel beams. The two panels are designated generation I and generation II, representing different stages in conceptual development. Both panels are 14 feet wide. The generation I panel is 7'-7½" long and the generation II panel is 8'-3" long. The panels were bolted to the three steel beams with a 1" joint between panels, forming a 15'-11½" long by 14' wide test specimen. The panels, including a ¼" wearing surface, are 5¼" thick and the steel beams are 1'-4" tall, for a total test specimen height of 1'-9¼". The panel dimensions were set so the test specimen could be installed on the North Bridge in FDOT District 4. The bolts joining the panels to the beams are at varying spacing designed specifically for the test specimen to be placed on that bridge. A Flexolith wearing surface was applied to the test specimen prior to joining the beams and panels at Seacoast, Inc. in Tampa, FL. The Flexolith wearing surface is an aggregate epoxy overlay manufactured by Euclid. The test specimen was delivered to FDOT fully fabricated.

The generation II panel is a more efficient and constructible design than the generation I panel, due to refinement of welding methods. The generation I panel extrusions were joined together by double sided friction stir welds at the top and bottom flanges of the extrusion. The generation II panel has single sided friction stir welds on the top and bottom flange with permanent backing material. The single-sided welds are faster to construct and have lower weld distortion. [4] In addition, the generation I panel has 7 lines of welds, whereas the generation II panel has only 5 lines of welds. Figure 1 shows both panel types with the weld locations circled. The generation II panel also has a different cross-section, required to enable weld efficiencies.

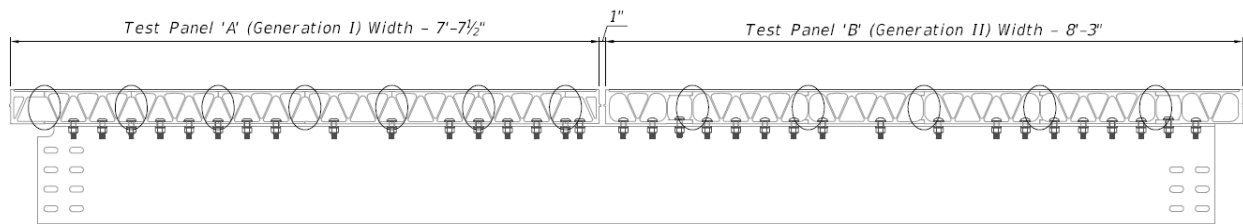


Figure 1: Test Specimen

Material certifications were provided by AlumaBridge, LLC. Aluminum alloy 6063-T6 was used for the panels, per ASTM Specification B221-14. Welding inspections were performed by Western Inspection Services, Inc. using ultrasonic inspection techniques. Machining inspection records were performed by HF Webster. Material certifications, welding inspection reports and machining inspection reports are provided in Appendix C. Note that the Weld Inspection report includes a second generation I panel, which was rejected by the weld inspection and therefore not included in the test specimen.

Visual and Non-Destructive Inspections

A thorough inspection was conducted prior to the start of structural testing to establish a baseline for the test specimen condition and is hereafter referred to as the preliminary inspection. Visual inspections were conducted two more times – after structural testing (intermediate) and again after heavy vehicle simulation (final). The conditions documented during the inspections indicate if any damage, structural changes or degradation occurred during testing.

Visual Inspection and Photographic Inventory

A thorough photographic inventory was completed for each inspection to document the condition of each weld. The welds are designated by panel, A or B, and by weld number 1-7 for panel A and 1-5 for panel B. Panel A is the generation I panel and Panel B is the generation II panel, described previously. The position along the length of the weld is numbered 1.1 to 1.5 between stringers 1 and 2 and 2.1 to 2.5 between stringers 2 and 3. To the outside of the steel stringers, the welds are designated as left or right. When labeled “top”, the weld is on the top plate of the aluminum panel while a “bottom” label indicates a weld on the bottom plate of the panel. Figure 2, below, shows the weld naming convention.

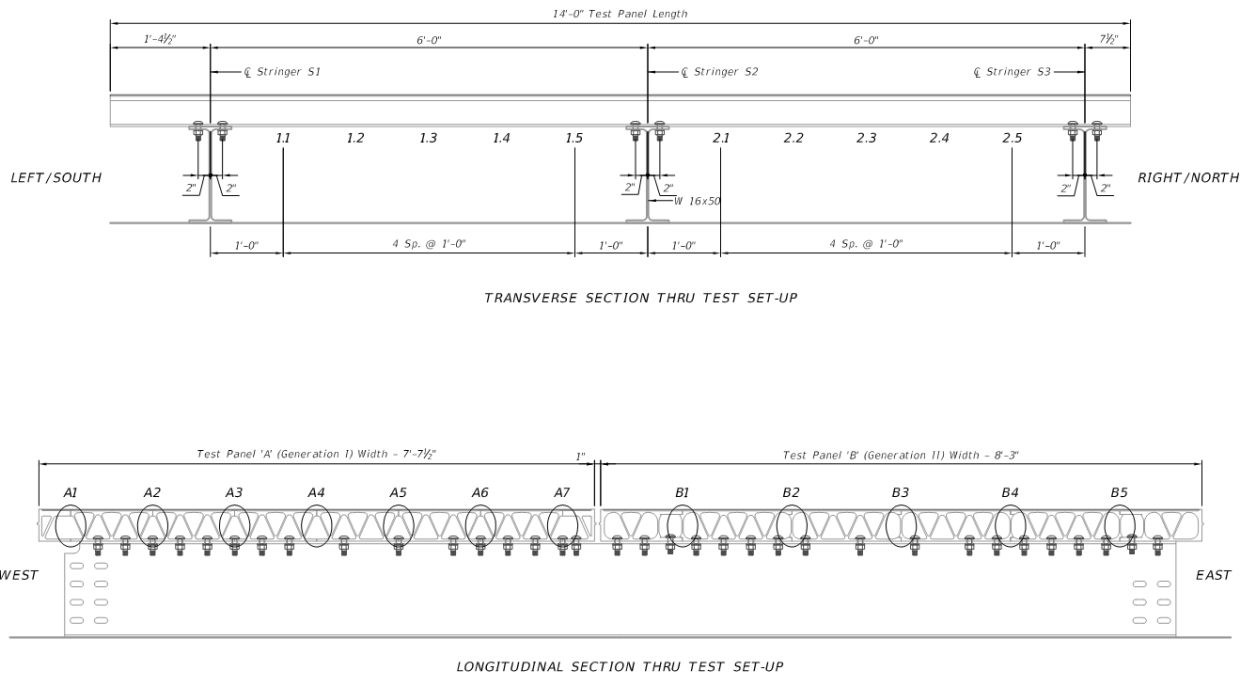


Figure 2: Weld Key

The welds on the top plate of the aluminum panels could not be inspected due to the wearing surface. The entire visible length of each weld on the bottom plate of the aluminum panels was inspected and photographed for the preliminary, intermediate and final inspections. The entire photo inventory is available in Appendix E: Visual Inspection Photo Inventory. The condition of the top of the welds on the bottom plate of panel A (generation I) was documented by bore scope video from within the panel voids during the

preliminary inspection only. The photographic inventory and bore scope video showed some very minor general corrosion, visible as white spots in the photographic inventory in Appendix E: Visual Inspection Photo Inventory and in Figure 3.

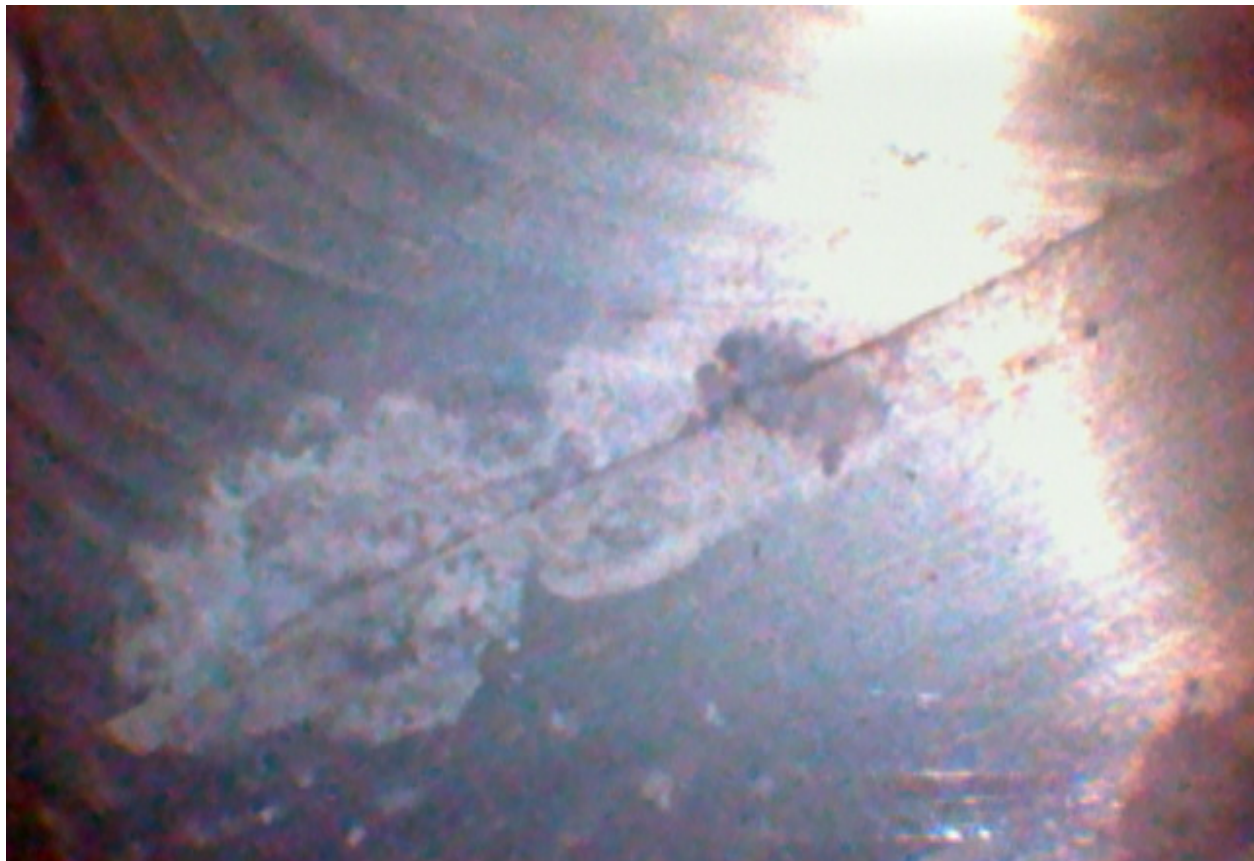


Figure 3: Bore Scope Screenshot at Internal Weld

The photographic inventory documented brown colored corrosive stains along the bottom of welds 2 through 6 in the generation I panel and the bottom of welds 1-3 in the generation II panel. Staining varied from severe, covering the entire weld surface for several inches, to minor, covering part of the weld surface. Examples of each are shown in Figure 4 and Figure 5. In general, the staining was more severe for the generation I panel than the generation II panel. The stains do not appear to be active corrosion and no section loss was measured. The extent and severity of the brown colored corrosive stains did not increase between the preliminary and final inspections. The stains are most likely due to contact with bare steel, which could result in galvanic corrosion due to the dissimilar metal. The weld material appears to be more susceptible to corrosion than the adjacent unaffected material. The aluminum plate adjacent to the weld rarely had corrosion stains as severe as at the weld. An exception is shown in Figure 6. In general, any weld is more electrochemically active than surrounding metal, potentially because of a different microstructure, residual stress or loss of temper. Texture of the weld seam could also allow water to pool or bead. Metallographic analysis would require destructive testing and if it were performed the deck could not be placed in service for a trial period in an existing bridge. Therefore, growth of current staining should be monitored during the trial installation of this deck. If required, metallographic analysis could be performed

after the test specimen is removed from service. For future manufacturing, minimizing contact with steel, a dissimilar metal, could reduce or eliminate this type of staining.



Figure 4: Corrosive Staining at Weld A4



Figure 5: Corrosive Staining at Weld A2



Figure 6: Corrosive Staining at Weld A7

Additional evidence of galvanic corrosion documented during the preliminary photographic inventory consisted of a diagonal affected area approximately 2 inches wide and eighteen inches long, located between stringers 2 and 3 on the generation I panel. Galvanic corrosion is evident by rust colored staining and minor pitting, shown in Figure 7. Figure 8 shows the aluminum panel was supported by bare steel during storage. The location of the supports coincides with the documented galvanic corrosion, therefore the corrosion is likely due to contact with dissimilar metals during fabrication. For future use, Specifications should be incorporated to ensure proper handling during fabrication and installation. The manufacturer and contractor should have proper quality controls in place to verify the aluminum does not come in contact with dissimilar metals during the fabrication process. If proper controls are not in place, service life of the product could be reduced.

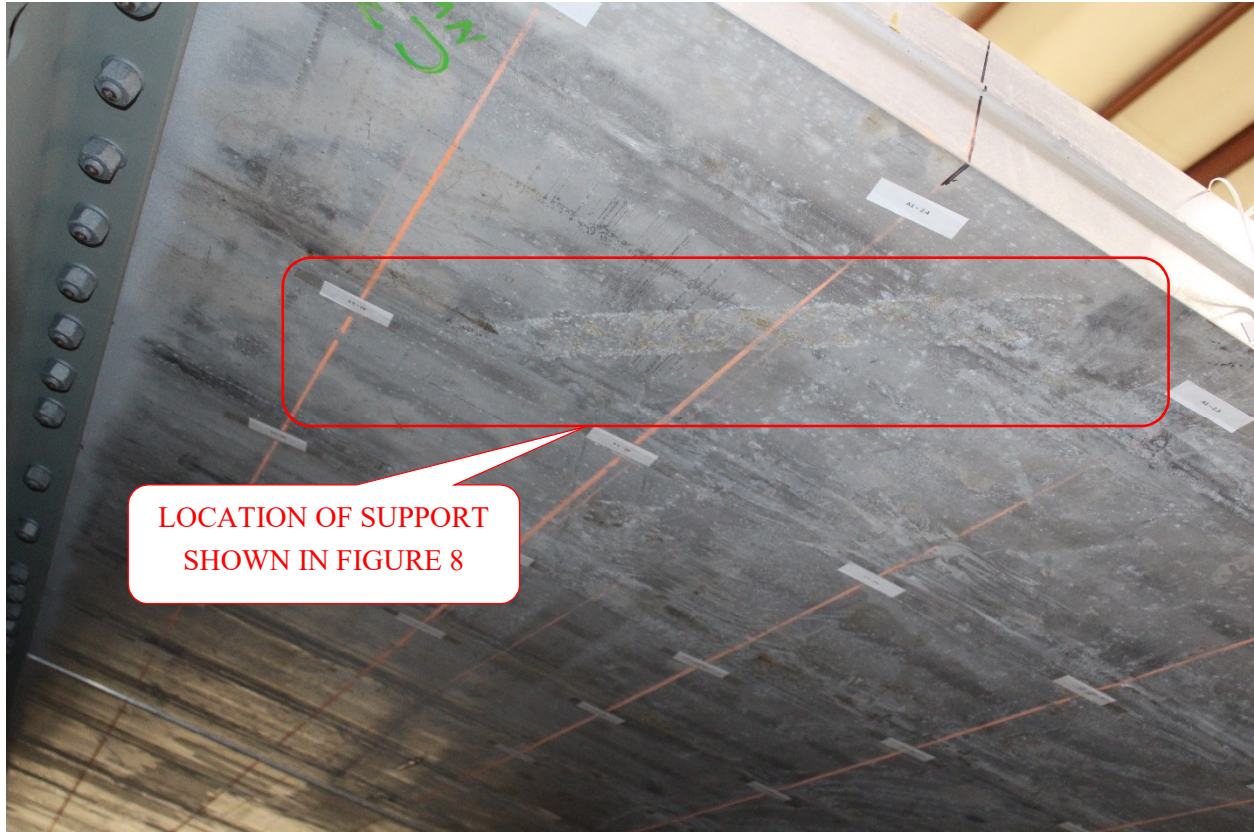


Figure 7: Corrosive Staining at Generation I Panel



Figure 8: Fabrication Support Conditions

Generation II Panel Weld

The single sided friction stir weld used for the generation II panel was a development by AlumaBridge, LLC. The detail has not been used before on aluminum deck panels subjected to traffic loads. The weld is single sided with a vertical web providing backer material. The backing must remain solid during the welding process to contain the plasticized material, therefore not all of the backing material is stirred into the weld. The final product has a small gap between the top or bottom plate and vertical web of the panel. That gap is shown in Figure 9. The final product also has a visible seam between the top or bottom plate and the web, shown in Figure 10. The seam is generally most visible close to the gap and becomes non-detectable towards the middle of the weld. The friction stir weld joint was evaluated by Hardesty & Hanover, LLC in [4]. Their analysis concluded the seam tip remains in compression due to the low tension component of the applied stress range and the presence of residual compression, but the report recommends the fatigue detail receives scrutiny during laboratory testing. To determine if this type of single sided weld has the propensity to separate when loaded, the gap size and the length of visible seam was documented at each inspection phase.

The gap width at the open end of the seam was documented using a Helios Feeler Gage with 10 blades ranging from 0.0015 to 0.025 inches. In general, the gap was very small, although more measureable at the weld between the end extrusion and adjacent extrusion.

Gap widths were measured at the left and right end and top and bottom of each weld on the generation II panel, for a total of 20 different measured locations. The results are shown in Appendix D: Visual Inspection Records. In general, the readings are highly variable at each inspection stage. The weld gaps are larger at each end of the panel, at welds B1 and B5. The gap size at weld B1 shows very little change, while the gap size at weld B5 appears to have decreased during the Heavy Vehicle Simulator testing. Weld B5 is at the end of the panel and the impact of the heavy vehicle simulator tire may have caused the weld gap to close over the duration of HVS testing. However, the results are not conclusive due to variability in measurements at the other weld locations.

The visible seam length was documented using a ruler accurate to 1/64 inch. The measurement did not change significantly between the preliminary and final inspections. The preliminary inspection was conducted in February 2016 at an ambient temperature of 52 degrees F. The final inspection was conducted in August 2016 at an ambient temperature of 85 degrees F. The data is included in Appendix D: Visual Inspection Records. From the recorded data, the average change in measurement is $-3/64$, but the standard deviation is double that value, $7/64$. Due to the small measurement values, measurement variation influences the results and therefore measurement of the visible seam length is not useful for determining the rate of structural degradation.

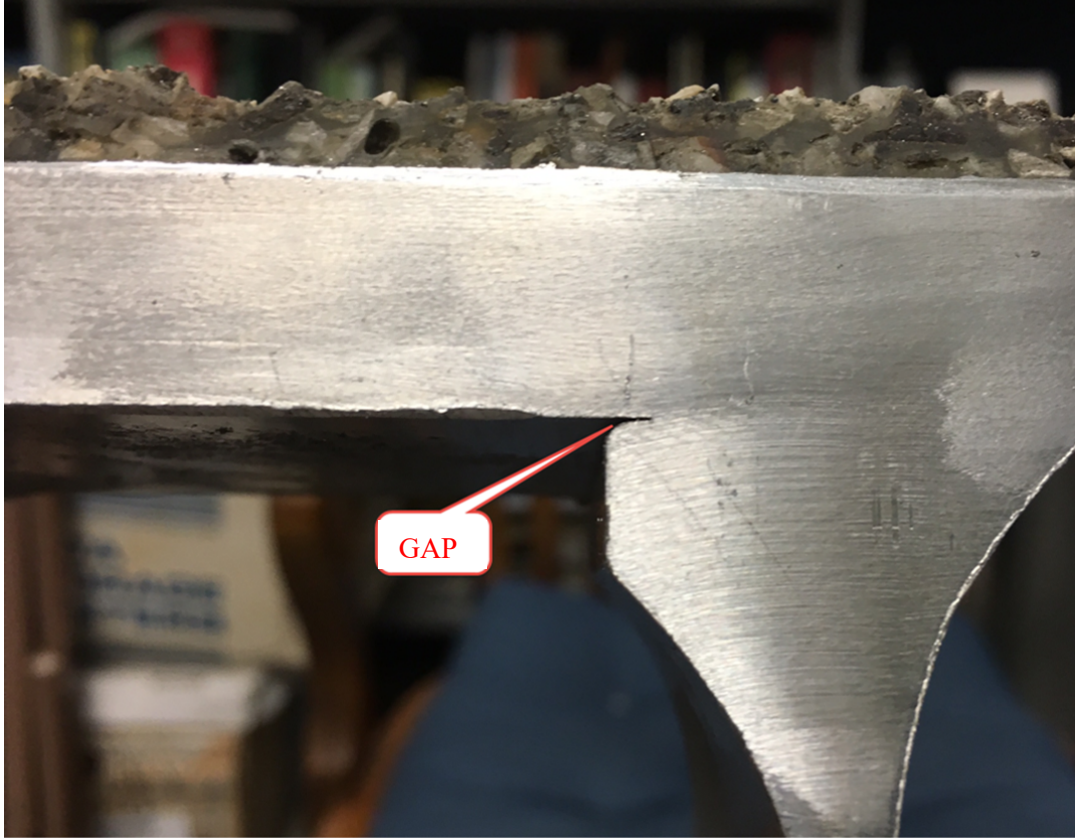


Figure 9: Gap between Top Plate and Backer Material at Weld

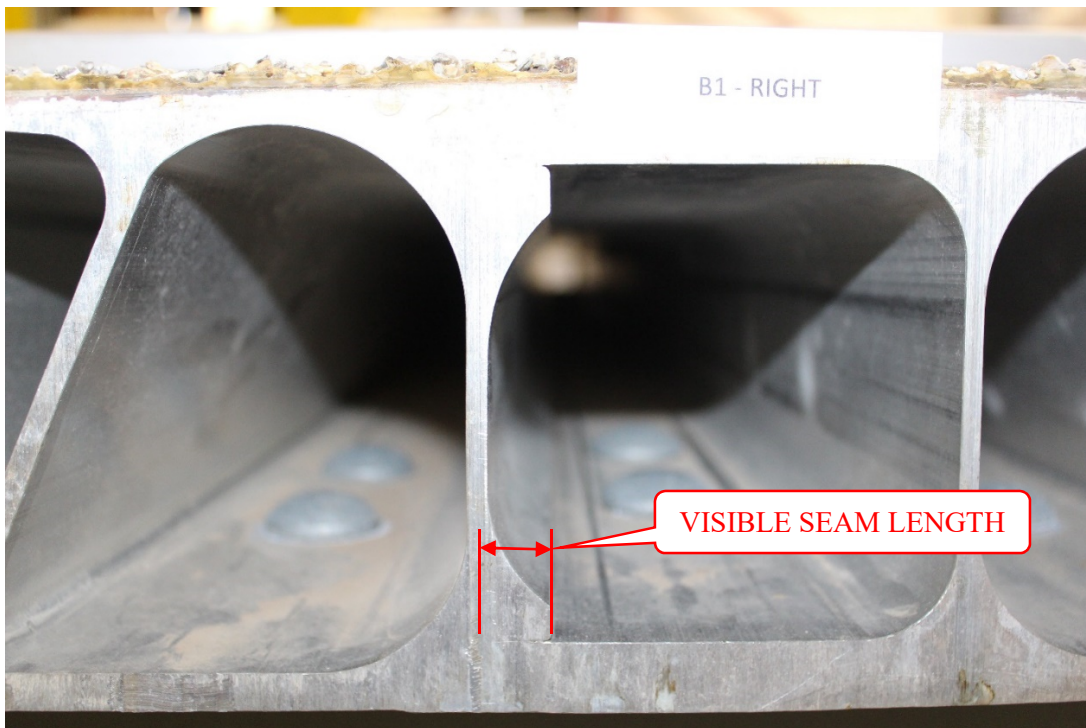


Figure 10: Visible Seam Length

Faying Surface

The generation I panel has a top and bottom plate with unequal thickness. The differential stiffness between the top and bottom plates caused minor distortion upon welding the extrusions together. The stiffer top plate contracted, resulting in a negatively cambered shape. During attachment to the steel stringers, the aluminum panel was forced down for contact with the stringers. The force was enough to cause local distortion of the panel around the bolt hole. Contact was achieved between the panel and stringer at each bolt, but not between bolts. The result is uneven contact between the panel and beam, as shown in Figure 11. In general, the gap is more pronounced close to the free end of the aluminum panel. Although the generation II panel did remain flat during the welding process, a gap between the panel and stringer is still present, as shown in Figure 12. To compensate for the loss of material during the friction stir weld process, the extrusions were thickened directly adjacent to the planned weld location. At welds where not all of the extra material was used during the weld process, the width of the weld remained raised compared to the surrounding aluminum deck panel, preventing complete contact between the aluminum panel and steel stringer.

During each of the inspections, the gap between the panel and stringer was documented for the left side of stringer 1 and the right side of stringer 3. Due to ease of access during the intermediate and final inspection, the gap was documented along each side of all stringers. The gap was measured using a BlackHawk MT-1049 feeler gage with 25 blades ranging from 0.0015 inches to 0.035 inches. For gaps exceeding 0.035 inches, a Tritan Digital Caliper was used. Between the preliminary and intermediate inspection, during which structural testing was conducted, there was very little change in the measured gap. Of the 54 locations measured along the left side of stringer 1, six had a recorded measurement change. The maximum difference in measurement between the two inspections was 0.01 inches, and the average difference was 0.005 inches. Of the 70 locations measured along the right side of stringer 3, three had a recorded measurement change. The maximum difference in measurement between the two inspections was 0.008 inches, and the average difference was 0.006 inches.

Between the intermediate and final inspection, during which heavy vehicle simulation (HVS) testing was conducted, there was more change. Measurement changes were noted for 32 out of 108 locations at stringer 1, away from the heavy vehicle simulator load, 98 out of 124 locations at stringer 2 and 85 out of 140 locations at stringer 3. The maximum increase in the gap was 0.06 inches for stringer 1, 0.08 inches for stringer 2, and 0.08 inches for stringer 3. Most of the measured gap changes occurred near the edges of the generation I panel, where the gap was more pronounced, as shown in Figure 11. Impact from the heavy vehicle simulator load may have caused the recorded change. Although the rate of change was more notable during the HVS than the structural testing, the magnitude is small and is not an impediment to using this structural system.

The design for the aluminum panel and steel stringer bolted connection is a faying surface with slip critical bolts. The design assumes the connection slips during thermal movements but not during typical traffic loading. If slippage occurs frequently enough, the inorganic zinc coating on the steel stringers may wear off and cause galvanic corrosion between the aluminum panel and steel stringers. The faying surface was inspected after all structural testing was completed. There was no evidence of corrosion at the faying surface at that time. However, after HVS testing, several areas of black discolorations were noted. An

example is shown in Figure 13 and evaluation of the noted problem is discussed in the Corrosion Testing section.



Figure 11: Gap between Steel Stringer and Generation I Aluminum Panel



Figure 12: Gap between Steel Stringer and Generation II Aluminum Panel

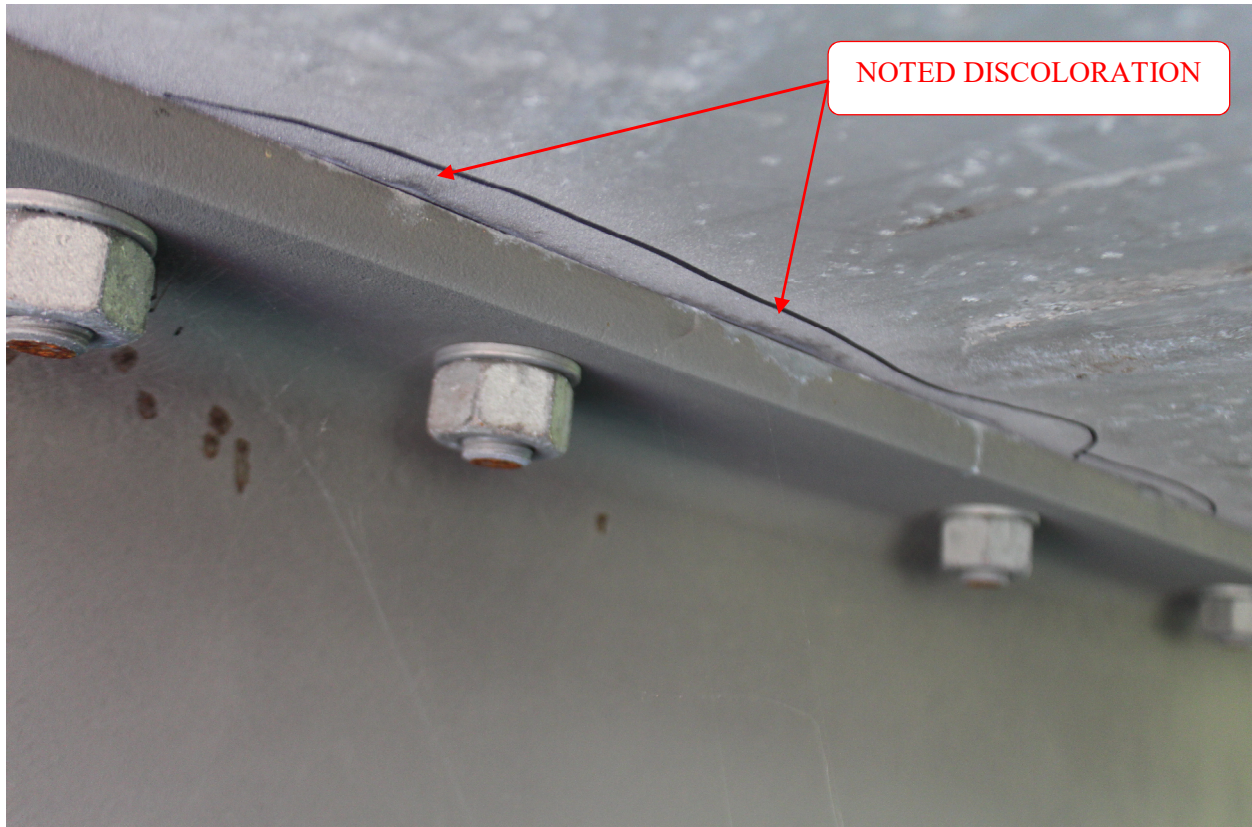


Figure 13: Black Discoloration Noted during Final Inspection

Bolt Torque

Bolt torque was checked at each of the inspections to determine if testing loads caused the bolts connecting the generation I panel to the stringer to loosen. Only the bolts on the left side of stringer 1 and the right side of stringer 3 connecting to the generation I panel were checked due to ease of access and because those bolts would be most likely to loosen due to the bending shape of the panel. The torque was checked at increments of 30 ft.-lbs. from 210 ft.-lbs. to 300 ft.-lbs. A Stanley Proto Model J6018AB torque wrench with +/- 3% clockwise and +/- 6% counterclockwise certified accuracy was used. At each increment, the wrench was applied to the nut and movement of the nut indicated the applied torque exceeded the torque present in the bolt.

Correlation between measured bolt torque and tension present in the bolt depend upon the condition of the fastener assembly. Testing is typically performed as part of the bolt installation process. Portland Bolt & Manufacturing Company and SC Fastening Systems, LLC provide estimated torque values on their websites, although the Portland Bolt & Manufacturing Company, Inc. provides the following disclaimer: “Due to many variables that affect the torque-tension relationship like human error, surface texture, and lubrication the only way to determine the correct torque is through experimentation under actual joint and assembly conditions.” [5] [6] The predicted torque required for installation of the bolts, provided by the AlumaBridge, LLC supplier is 437 ft.-lbs. Since torque measurements vary due to a number of different factors, the measured torque value for an in-service bolt is not an effective measure of the residual tension

in the bolt. However, a decrease in torque readings over time could represent a change in the residual tension. As the coating on the bolt deteriorates, the torque reading for a constant tension should increase.

During the preliminary inspection, prior to structural testing, one bolt on stringer 3 had an existing torque between 240 and 270 ft.-lbs. Another bolt on stringer 3 had a torque between 270 and 300 ft.-lbs. Two bolts at stringer 1 had a torque between 270 and 300 ft.-lbs. All other bolts inspected had an existing torque above 300 ft.-lbs. At the completion of measurements, every bolt had a torque reading of 300 ft.-lbs. or higher as a function of the torque measurement method. After structural testing, the bolt torque was measured again and all bolts still had a torque reading at or above 300 ft.-lbs. After HVS testing, bolt numbers three and four on the right side of Stringer 3, near the end of the generation I panel had a torque reading between 270 and 300 ft.-lbs. The same bolts to the right side of stringer 1 and bolt ten (numbered from the end of the stringer) also had a torque between 270 and 300 ft.-lbs. Bolts three and four for the right side of stringer 1 and the left side of stringer 2 were checked and had an existing torque of 300 ft.-lbs. or higher. Since most of the affected bolts were at the end of the generation I panel where the gap is more pronounced, and structural testing didn't cause any effect on the bolts, the torque may have decreased due to the effect of a moving load or impact from the heavy vehicle simulator.

Discussion

Thorough inspections were conducted prior to the start of structural testing (preliminary), after structural testing (intermediate) and again after heavy vehicle simulation (final) to determine if any damage or structural deterioration occurred during testing. The inspections included visual inspections documented with a photographic inventory, feeler gage and visible length measurements for welds on the generation II panel, feeler gage measurements for the gap between the panel and stringer, and bolt torque for the generation I panel. The inspections did not uncover any significant damage or structural deterioration between the start and conclusion of physical testing. However, findings during the inspections did indicate improvements could be made during the fabrication process for the aluminum deck panels. Both generation I and II panels showed some sign of past galvanic corrosion action at some welds and temporary support points. It is unclear if the corrosion along certain welds is due to handling during fabrication, contact with temporary support points or material composition. Although further testing is necessary to determine why the welds were more susceptible to corrosion than the surrounding aluminum plate, galvanic corrosion could be limited by preventing contact between aluminum and steel. When contact is required, the steel could be coated or directly separated by an approved means.

The inspections uncovered several areas of discoloration along the faying surface between the generation I panel and steel stringers, discussed further in the Corrosion Testing section. The contact between the generation I panel and steel stringers is slightly uneven due to the weld fabrication method. The combination of a flat panel constructed using single-sided friction stir welds and the inorganic zinc coating on the steel stringers appears to be effective at limiting galvanic corrosion as there was no indication of corrosion at the faying surface between the generation II panel and stringer.

The gap between the panels and stringers was documented during inspections using a feeler gage or digital caliper. The gap changed minimally during testing. A full contact connection between the panel and stringer

is preferred so that the finished product matches the conditions assumed for design. The varying gaps between the generation I panel and stringers is due to the weld fabrication process. The generation II panel has a small gap between the panel and stringer due to the buildup of material required for the weld connection. Welds are typically ground after friction stir welding to remove residual burs and fins. For the generation II panels, it may be possible to grind the welds flush on the bottom of the panel where the panel will be in contact with the supporting steel beams. Although the gap is much smaller for the generation II panel than for the generation I panel and may not be fully correctable due to required fabrication tolerances, it should be minimized as much as possible.

Torque measurements were taken at a select number of bolts considered particularly susceptible to loosening during testing. 32 bolts were checked for the generation I panel, only. The torque readings did not change as a result of structural testing. Torque readings for five bolts (15%) changed as a result of heavy vehicle simulation (HVS). Because the change was only observed after HVS and not after structural testing, the behavior can be assumed to be due to the effects of a moving load or impact from the heavy vehicle simulator. Due to deterioration of lubricants, torque readings should theoretically increase or remain the same for a constant bolt tension. The change in torque was an unknown value less than 30 ft-lbs, or 10% of the original torque. The measured change is close in magnitude to the accuracy of the torque wrench and can therefore be considered negligible.

Structural Testing

Structural testing of both the generation I and generation II panel was completed in Tallahassee, FL at the FDOT Structures Research Center. The testing program included nine static tests (tests 1-6 and 8-10) and one cyclic test (test 7). The number of loading points for the static tests varied from one to four and the cyclic test was completed with four loading points. The support conditions for the steel stringers varied. In some tests, the steel stringer was rigidly supported and restrained by the laboratory strong floor and for other tests, the test specimen and steel stringer was supported on bearing pads. Instrumentation for the testing included 92 bi-axial strain gages and 20 deflection gages. Of primary interest was the generation II panel because it is the most efficient design and the latest development. There are no plans to implement the generation I panel. Therefore during six of the static tests, the generation II panel was loaded and during the remaining three tests, the generation I panel was loaded. During cyclic testing, only the generation II panel was loaded.

Test Setup Description

The purpose of structural testing was to verify the test specimen performs as per the analytical model/calculation in conjunction to proving that it could be placed in service on a bridge with safety for the travelling public maintained. Loads were applied corresponding to the factored Service II, Strength I and Strength II limit states. Both the HL-93 truck and tandem design loads were used for the Service II and Strength I limit state, in loading patterns to induce maximum positive and negative moment. The permit truck loading (FL-120) was used for the Strength II limit state. The applied loads include a multiple presence factor of 1.2, impact factor of 1.33, and live load factors corresponding to the appropriate limit state.

For the HL-93 truck loading, the Service II load at each load point was 33.2 kips and the Strength I load was 44.7 kips. For the HL-93 tandem loading, the Service II load at each load point was 25.9 kips and the Strength I load was 34.9 kips. For the HL-93 truck loading, during test 1, one load application point was used to represent one half of a single axle and to induce maximum positive bending. During tests 3, 4, 9 and 10, two load application points were used to represent both wheel lines for a single axle of the design truck and to induce maximum negative moment. The spacing between the two load application points was 6 feet, corresponding to the spacing between wheel lines for the HL-93 design truck, per AASHTO LRFD Figure 3.6.1.2.2-1 [7]. Loads applied for the Strength II limit state correspond to the FDOT permit FL-120 truck. The load application points are in the same position as the HL-93 design truck with a 57.5 kip load at each application point. For the HL-93 tandem loading, during test 2, two load application points were used to represent both axles along one wheel line and to induce maximum positive bending. During tests 5, 6 and 8, four load application points were used to represent the entire design tandem and to induce maximum negative moment. The spacing between the four load application points was 4 feet in the longitudinal direction of the steel stringers and 6 feet in the transverse direction, corresponding to the design tandem per AASHTO LRFD Article 3.6.1.2.3 [7]. Further details are provided in Appendix A: Structural Testing Procedure.

For each test except test 10, the load was applied using a rectangular steel plate and bearing pad with a 10 inch by 20 inch footprint. That area is specified in AASHTO LRFD Article 3.6.1.2.5 as the tire contact area. [7] When the test included multiple load application points, one or three spreader beams were added to achieve the required load layout, as shown in Figure 14. During each test, the aluminum panel was loaded close to its edge to induce maximum bending perpendicular to the steel beams. The bearing pad was placed directly against the aluminum lip at the panel edge, providing ½” between the extreme edge of the aluminum panel and the loading area, as shown in Figure 15. For static test 10, the load was applied with a 4 inch by 20 inch footprint to simulate tire loading at the extreme edge of the panel and to exercise the weld between the exterior and adjacent aluminum extrusions.

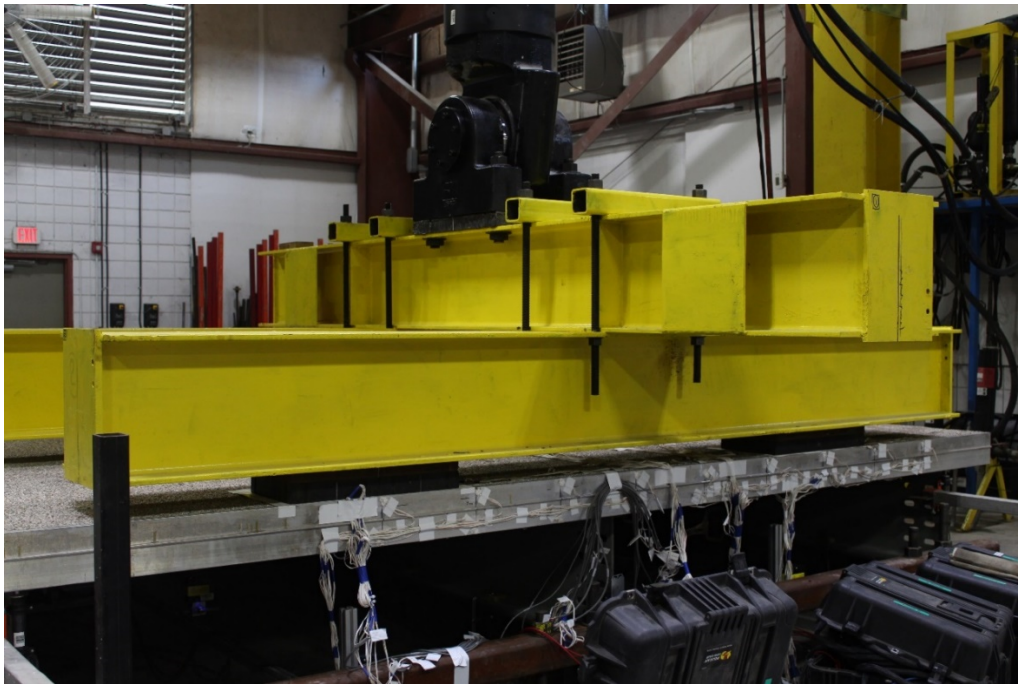


Figure 14: Four Point Loading



Figure 15: Single Point Loading

To induce maximum bending in the aluminum panel itself, for static tests 1-3 and 5, the test specimen was rigidly attached to the laboratory floor. Three 14 inch tall support beams were placed under each stringer of the test specimen and leveled with grout poured between the beam and floor. Structural tubes were placed at each end of the support beams and anchored to the laboratory floor to prevent movement during testing. The support and anchor system is shown in Figure 16. The test specimen was clamped to the steel support beams on each side of all three stringers, at 2 foot spacing as shown in Figure 17. The inorganic zinc coating on the test specimen stringer was protected from the clamping force with a small piece of wood. In locations where the test specimen stringer was not in firm contact with the support beam, shims were added to fill the gap.



Figure 16: Test Specimen Support



Figure 17: Clamp

For static tests 4, 6 and 8-10 and for cyclic test 7, the test specimen was supported with bearing pads at each end of each steel stringer. The bearing pads provide more flexibility than would be present for the in service conditions where the stringer is bolted to the floor-beam of a bascule bridge. However, the rigid connection to the laboratory floor provides a stiffer support condition than would be present in a bridge. The actual support conditions would be between the two laboratory support methods used. By testing and evaluating the test specimen behavior under both support conditions, in service behavior is enveloped.

As stated earlier, one of the goals of the testing was to verify the preliminary structural analysis results presented by the researcher in [4]. The deck design presented in that report was completed using finite element analysis and manual calculations. The maximum stresses due to positive and negative flexure were presented, along with maximum deflections. Good correlation between the analytical and test results would provide confidence that the deck is satisfactorily designed. Strain gage placement was set based on the structural analysis results to measure strain at locations which would provide a meaningful comparison of analytical and experimental results. The proposed strain gage locations were provided to FDOT in [4].

Instrumentation consisted of 92 bi-axial strain gages and 20 deflection gages. At each top surface location where the strain gages were installed the wearing surface was removed using a 1 inch diameter hole saw and careful chiseling to avoid damage to the aluminum. The aluminum surface was sanded to remove any residual epoxy, then it was cleaned with Acetone and dried. The strain gages were 5 mm aluminum specific bi-axial rosette gages manufactured by KYOWA. The gages were adhered to the aluminum surface with super glue provided by KYOWA. Wax and SB-Tape was applied over the strain gage for waterproofing and to seal the gage from weather. The leads to the gages were taped to the test specimen to provide strain relief.

Deflection gages consisted of MTI LTC-300 laser displacement gages. The gages were attached to T slot aluminum or steel frames, supported by the laboratory floor. The frames supporting the deflection gages were independently supported and were not in contact with the test specimen or support beams.

The gages were assigned names based on their type, location and direction. The first letter of the gage designates its Location or Type (T for Top Rosette, B for Bottom Rosette, GD or D for Deflection). The second letter and the number indicates its Transverse Location (Alphabetical Mark) and Longitudinal Location (Numerical Mark) according to the Instrumentation Plan, included in Appendix A: Structural Testing Procedure. The final letter in the gage name indicates its direction, either 'X' for the transverse direction, in the direction of panel voids, or 'Y' for the longitudinal direction, in the direction of the attached steel beams. For example, gage T_F11_X is a rosette located on the top of the panel, at transverse grid location F and longitudinal grid location 11, measuring strain in the transverse direction. Designation 'D' deflection gages located at lines 'C' and 'J' and the gages located at F1 and F20 are attached to the bottom of the panel. Designation 'D' deflection gages located at line 'F' (except F1 and F20) are attached to the bottom of the steel beam. Gage Z is deflection of the actuator.



Figure 18: Installed Strain Gage

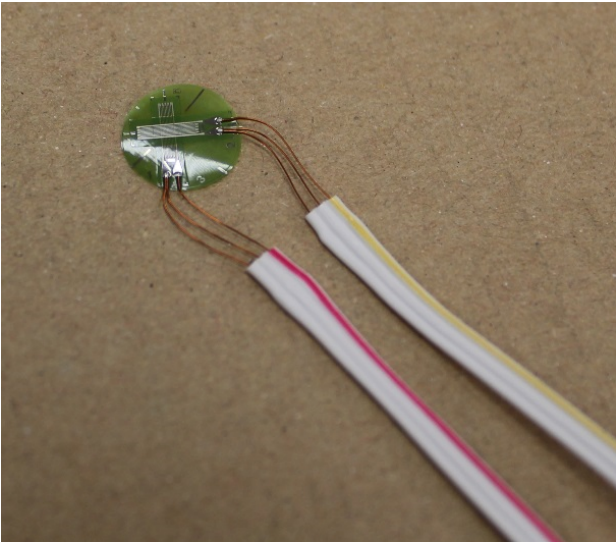


Figure 19: KYOWA Rosette Strain Gage

Static Testing

For each of the static tests, the target loads were applied and removed for five iterations. The target loads correspond to the Service II, Strength I and Strength II limit states, explained previously. During each iteration, the zero load level and each target load level was held for 10 seconds. Load was applied at a rate of 250 lbs. per second and removed at a rate of 500 lbs. per second or less. The data sampling rate was at least 5 Hz. Further details are provided in the test procedure, in Appendix A: Structural Testing Procedure.

Data Analysis and Processing

Data was processed manually using Microsoft Excel. For each load stop during each of the five iterations, the first 2.5 seconds and final 2.5 seconds of recorded data was removed from the data set. The remaining recorded strain and deflection data for each load stop and iteration was averaged and then corrected by the initial average recorded zero. The coefficients of variation between each load stop for the five iterations was calculated to determine the variability in gage readings over the duration of the test. The results of the coefficient of variation analysis are shown in Table 1. Gages with average absolute value microstrain readings less than 50 were not considered because error may be a significant cause of the variation. During all testing, only three gages had variations over 20% and in all tests, less than 11% of gages had variations over 10%. Because the readings for the majority of gages did not vary significantly during the test, the five iterations were averaged for each load stop. Additionally, deflection readings were corrected by subtracting the recorded deflections at the stringer supports. In general, the gages survived the testing regimen well and the data is reliable. However, gage T_H9_Y and GD_1 became defective during test 6. Gage T_H9_Y was not used for any subsequent tests. Gage GD_1 was fixed for tests 8-10.

Table 1: Data Coefficient of Variation

Test	Total Number of Gages	Gages with Average Absolute Value Reading over 50 Microstrain and Coefficient of Variation of:	
		10% to 20%	Over 20%
1	100	T_C4_Y, T_B9_X, T_C6_Y, T_C7_Y, B_C10_Y	T_C4_Y (112%)
2	100	-	T_C4_Y (30%), B_E1_X (46%)
3	104	T_F4_Y (Service II load level only)	-
4	104	T_D9_X, B_E10_X, T_F2_Y, T_F5_X, T_F6_X, T_F11_X, T_G2_Y, T_H9_X (Service II load level only), T_E9_X, T_F9_X, T_G9_X	T_E1_Z (57%)
5	104	-	-
6	104	T_F5_X, T_F11_Y, B_H2_X (Service II load level only), B_D1_Z, B_E1_Z, T_F13_Y,	-
8	64	-	-
9	64	-	-
10	64	-	-

During testing, the behavior of the panel remained linear elastic. The maximum strain readings were taken during test 3. Select gages with high strain readings from that test are shown in a load versus microstrain

plot in Figure 20. Strain readings returned close to zero for each ramp of testing, indicating minimal to no permanent deformation during the test. The slope of the load-strain line also remained fairly constant throughout testing. Determined by statistical analysis, the lowest Pearson product moment correlation coefficient for any of the gages shown in Figure 20 is 0.997 for gage T_F2_X, indicating very close to total positive linear correlation.

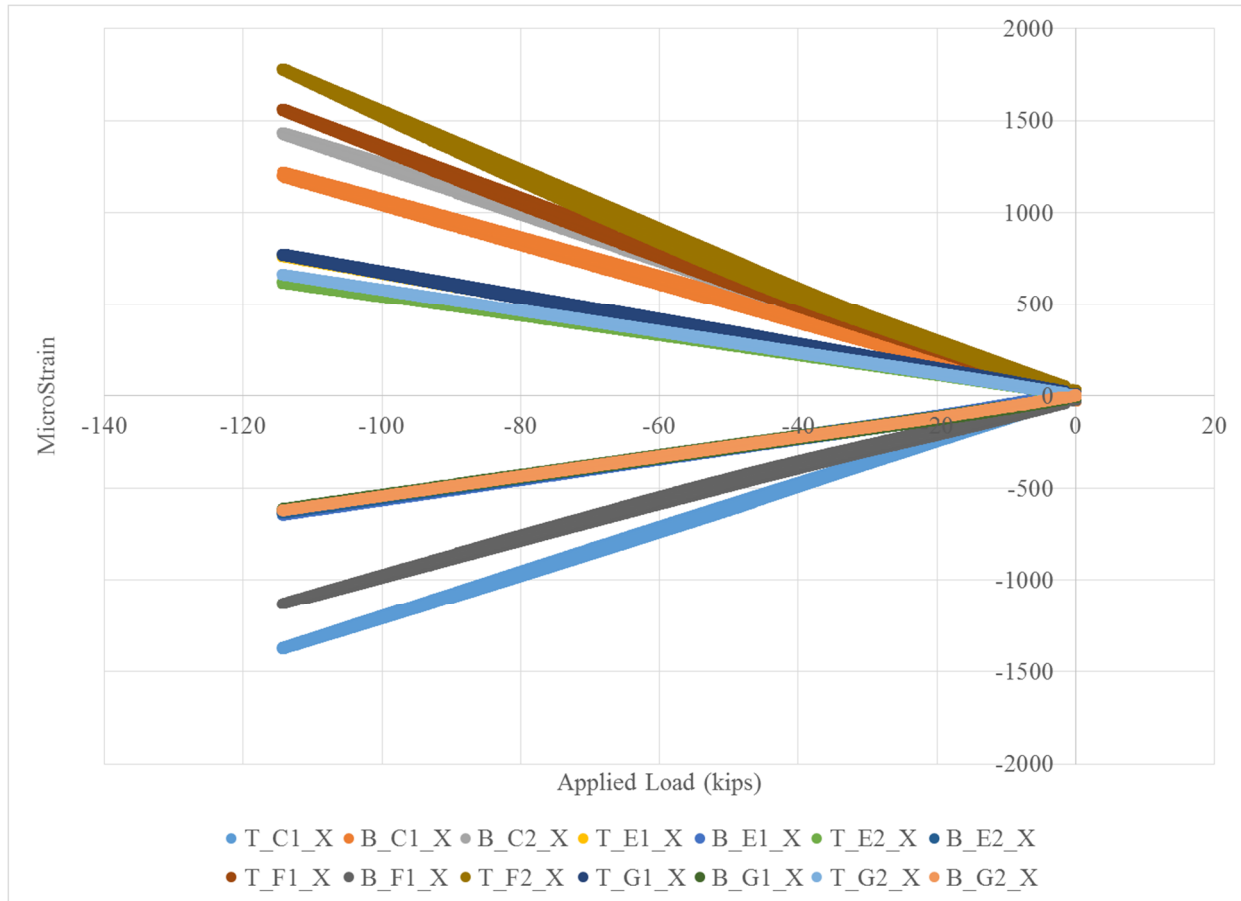


Figure 20: Load vs. MicroStrain for Test 3

Results

A summary of the data from all static tests is included in Table 2. The summary shows the maximum compression and tension measured for each of the tests, along with maximum deflection. Deflection readings were corrected for support deflection for all tests, including the tests which utilized bearing pads as support (tests 4, 6-10). Therefore, the deflection for those tests represents the system deflection, a combination of stringer and panel deflection. All gages were considered in order to summarize results.

The results are used to compare required capacity to actual panel capacity. The maximum tensile strain measured during any of the structural tests is 1747 microstrain. The calculated factored nominal resistance for design of the aluminum deck panel for flexural tension is 25.3 ksi, per information provided in [4]. Per AASHTO LRFD Table 7.4.1-3, the modulus of elasticity for aluminum is 10,100 ksi. So, the microstrain corresponding to the factored nominal resistance is 2505. The maximum measured tensile microstrain is

30% lower than the microstrain corresponding to factored nominal resistance, resulting in a demand to capacity ratio of 0.70. The maximum measured compressive strain for any test is 1482 microstrain. Per [4], the factored nominal resistance for design of the aluminum deck panel for flexural compression is 26.3 ksi. So, the microstrain corresponding to the factored nominal resistance is 2603. The maximum measured compressive microstrain is 43% lower than the microstrain corresponding to factored nominal resistance, resulting in a demand to capacity ratio of 0.57. The demand to capacity ratios for tension and compression strain are very low.

Table 2: Static Test Summary and Design Predictions

Test	Description	Limit State	Maximum MicroStrain or Deflection								
			Tension			Compression			Deflection (in)		
			Measured	Predicted	Error	Measured	Predicted	Error	Measured	Predicted	Error
1	Generation II Panel, Truck Positive Moment	Service II	887	812	9%	-853	-861	-1%	-0.14	-0.117	20%
		Strength I	1196	1099	9%	-1148	-1158	-1%	-0.19	-0.158	20%
		Strength II	1548	1416	9%	-1482	-1485	0%	-0.25	-0.203	23%
2	Generation II Panel, Tandem Positive Moment	Service II	773	723	7%	-707	-733	-4%	-0.14	-0.107	31%
		Strength I	1047	960	9%	-960	-990	-3%	-0.19	-0.144	32%
3	Generation II Panel, Truck Negative Moment	Service II	942	812	16%	-771	-1119	-31%	-0.11	-0.09	22%
		Strength I	1319	1089	21%	-1042	-1495	-30%	-0.15	-0.121	24%
		Strength II	1747	1406	24%	-1346	-1931	-30%	-0.18	-0.156	15%
4	Generation II Panel, Truck Negative Moment (Bearing Pad)	Service II	877	-	-	-833	-	-	-0.14	-	-
		Strength I	1187	-	-	-1123	-	-	-0.18	-	-
		Strength II	1533	-	-	-1450	-	-	-0.22	-	-
5	Generation II Panel, Tandem Negative Moment	Service II	756	644	17%	-619	-871	-29%	-0.08	-0.073	10%
		Strength I	1055	861	23%	-832	-1178	-29%	-0.12	-0.097	24%
6	Generation II Panel, Tandem Negative Moment (Bearing Pad)	Service II	770	-	-	-698	-	-	-0.13	-	
		Strength I	1009	-	-	-923	-	-	-0.17	-	
8	Generation I Panel, Tandem Negative Moment (Bearing Pad)	Service II	619	-	-	-625	-	-	-0.13	-	
		Strength I	803	-	-	-808	-	-	-0.15	-	
9	Generation I Panel, Truck Negative Moment (Bearing Pad)	Service II	694	-	-	-633	-	-	-0.10	-	
		Strength I	907	-	-	-821	-	-	-0.13	-	
		Strength II	1159	-	-	-1033	-	-	-0.18	-	
10	Generation I Panel, Truck Negative Moment at Panel Edge (Bearing Pad)	Service II	880	-	-	-758	-	-	-0.11	-	
		Strength I	1194	-	-	-1021	-	-	-0.16	-	
		Strength II	1567	-	-	-1315	-	-	-0.19	-	

The deflection limit for decks which do not carry pedestrian load is $\text{Span}/800$ per AASHTO LRFD 9.5.2. As stated in AASHTO LRFD C9.5.2, “the primary objective of curtailing excessive deck deformation is to prevent breakup and loss of the wearing surface.” [7] In this case, the span between stringers is 6 feet, so the deflection limit is 0.09 inches. Tests 1-3 and 5 are most appropriate for evaluating deflection because the stringers were secured and the measured deflections during those tests represent deflection of the panel itself, not overall superstructure deformation. The maximum measured deflection of 0.144 inches was observed for the Service II limit state, which includes a 1.30 factor on live load. Deflection is to be evaluated at the Service I limit state, which has a 1.0 factor on live load. Since the results are linear, the Service I deflection can be predicted as the measured deflection divided by the Service II live load factor of 1.3. The resulting value is 0.11 inches, 0.02 inches above the limit. Since the measured deflection exceeds the limit by less than $1/32$ ”, it can be considered acceptable pending wearing surface testing.

The panels were designed using finite element analysis. The results including screenshots are shown in [4]. For comparison, design information from [4] is shown in Table 2. The design stress is converted to strain, using the aluminum modulus of elasticity (10,100 ksi).

The experimental results show that maximum tensile strain is higher than maximum compressive strain. The prediction from design is different, with maximum compressive strain higher than maximum tensile strain. The maximum experimental tensile strain is approximately 24% higher than the design tensile strain and the experimental compressive strain is approximately 30% lower than the maximum design compressive strain. It is observed that different loading cases control the maxima. The design predicted that maximum tension would occur at the load application point when one load is applied. Experimental results show that maximum tension occurs perpendicular to the stringers on the top surface of the deck at the middle stringer when two loads are applied equidistant from that stringer, inflicting negative moment. For compression, experimental results show that maximum compression occurs at the load point for a single applied load. However, the design predicted maximum compression occurs at the middle stringer due to negative bending moment. The maximum deflection determined experimentally was located at the edge of the panel and is approximately 20% higher than the deflection calculated for design.

Experimental results are presented graphically for Tests 1 and 3 in Figure 21 to Figure 24. Those specific tests are shown because the highest strain was recorded during those tests and because the test specimen was clamped to the laboratory floor, matching the boundary conditions for the finite element analysis. The graphs show strain values along transverse sections in the panel, at the line where gages were installed and where the finite element analysis provides corresponding results. The legend numbers represent the longitudinal gage location. The letters along the x axis represent the transverse gage location. Single points indicate where only one gage per line was installed. Refer to the Instrumentation Plan in Appendix A: Structural Testing Procedure for gage line locations.

Analytical results are presented graphically for select tests in Figure 25 and Figure 26. The Figures are based on LUSAS Finite Element results extracted by FDOT using LUSAS files provided to FDOT by George Patton, of Hardesty & Hanover. The LUSAS files were opened, solved and the design strain was extracted at each gage point. The LUSAS files were not modified in any way which would affect the results. Note that the geometry in LUSAS is different than the test specimen panel geometry. For comparison

between the experimental and analytical figures, the analytical figures must be mirrored. In general, the shape of the graphs showing experimental and analytical results is similar. An exception is at the top of the panel, over the middle girder. For that region which has negative bending moment, the experimental results show a more rounded shape than the analytical results.

Differences between predicted and experimental results are typical for structural testing. Several factors could have contributed to the differences apparent in Table 2 and Figures 21 through 26. Although the generation II panel was the primary interest of this research effort, the finite element analysis was completed for the generation I panel, before the generation II panel was developed. For positive moment bending the finite element analysis included only two supports (with the third support released), while three supports were activated for the negative moment bending analysis. Those boundary control differences for the positive and negative moment analyses could explain why the analytical and experimental results are closer for positive moment than negative moment. Maximum strains and deflections occurred at the edge of the panel and the results could be affected because the two panel types have different end extrusions.

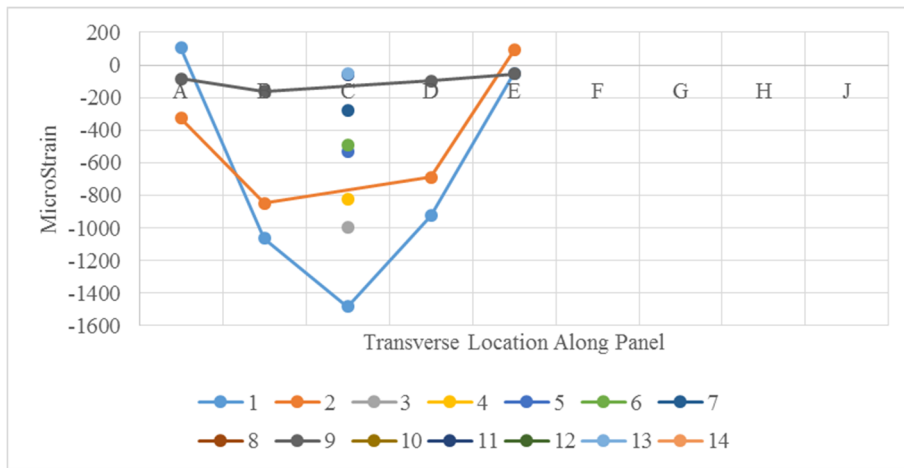


Figure 21: Experimental Results for Test 1, Strength II, Top of Panel

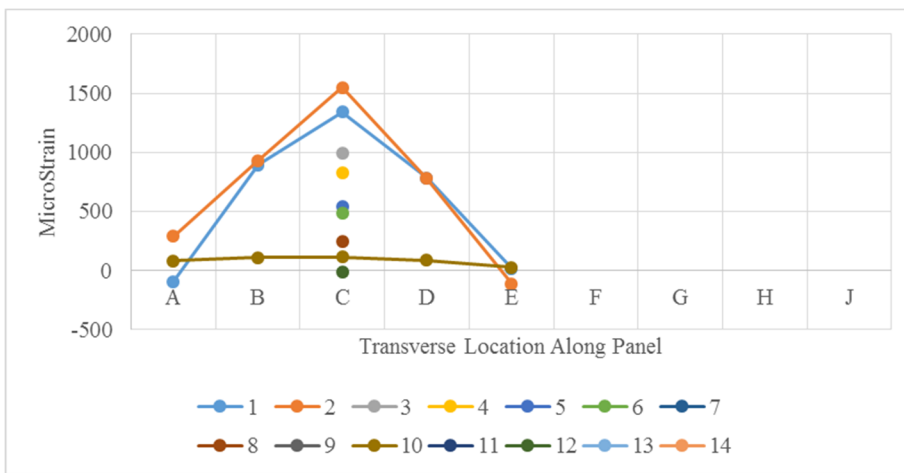


Figure 22: Experimental Results for Test 1, Strength II, Bottom of Panel

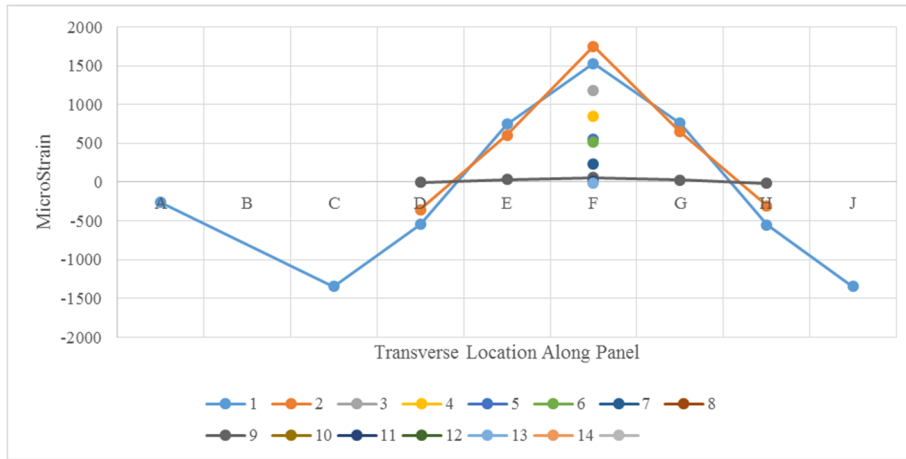


Figure 23: Experimental Results for Test 3, Strength II, Top of Panel

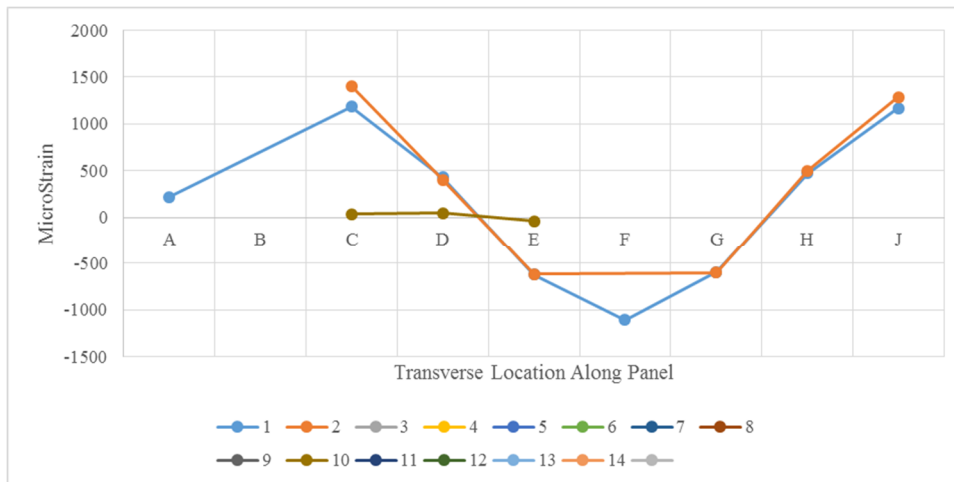


Figure 24: Experimental Results for Test 3, Strength II, Bottom of Panel

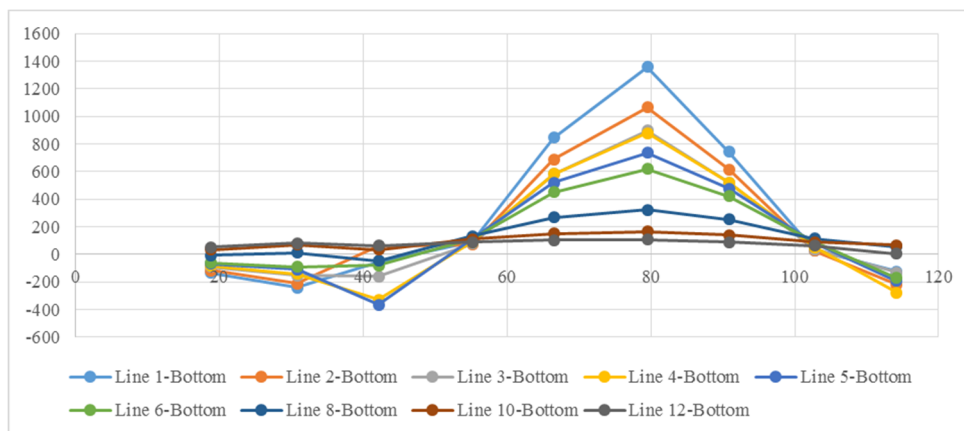


Figure 25: Analytical Results for Test 1, Strength II, Bottom of Panel

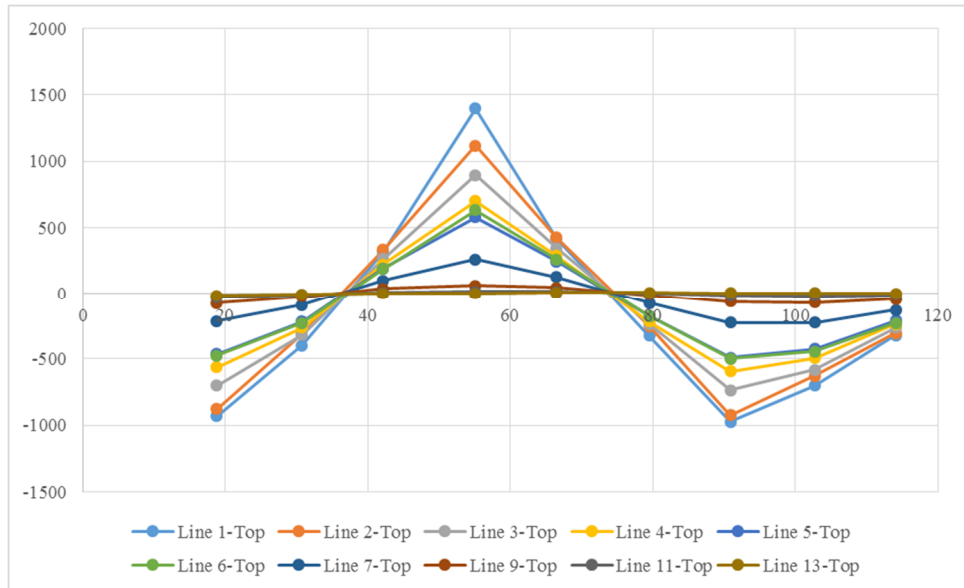


Figure 26: Analytical Results for Test 3, Strength II, Top of Panel

Cyclic Testing

The intent of test 7 was to verify satisfactory fatigue performance through a cyclic test. A load range corresponding to the design fatigue load per AASHTO LRFD Article 3.6.1.4 was applied. [7] The applied load range of 55 kips included a 1.15 impact factor and the 1.5 infinite life fatigue live load factor per the Fatigue I limit state. A 5 kip minimum load was maintained during the test to keep the test assembly stable. The maximum load applied during the cyclic test was the sum of the minimum load and load range, 60 kips. The load was applied as a sinusoidal function at a rate of 0.75 Hz for two million cycles. Load application points were positioned per the loading pattern for the fatigue load per AASHTO LRFD Figure 3.6.1.4.1-1. [7] The geometrical loading pattern for the fatigue load is the same as the loading pattern for the HL-93 tandem design load, previously discussed.

Data Analysis and Processing

Data was recorded for the cyclic test at a rate of 50 Hz for 10 seconds once each hour during the month-long test. The maximum, minimum and average readings from each data recording were extracted and summarized in a comprehensive Excel file. Results from previous static test 6 were used to determine which strain gages were in tension (positive) or compression (negative). The strain range for each data recording is the difference between the maximum and minimum value in each 10 second recording period. The strain range is positive (maximum minus minimum) for gages in tension and negative (minimum minus maximum) for gages in compression. Figure 27 shows the results for all gages in the test.

At approximately cycle 330,000, the support bearing pad closest to gage location F1 failed. The test was stopped and the bearing pad replaced. The bearing pad had increased deflection prior to failure, therefore the results presented in Figure 27 show high variability before the bearing pad replacement. However, after the bearing pad was replaced, the results show good, consistent strain readings for the remainder of the test.

Prior to replacement of the failed bearing pad, the stresses generally increased in the positive bending region and decreased in the negative bending region. The behavior is logical as the deterioration of the bearing pad essentially reduced the support of the center stringer. As a result of the failed bearing pad, the panel resisted a higher fatigue demand than planned.

The strain growth rate was estimated based on a linear regression analysis of the strain range between the bearing pad replacement and the end of the test. The largest strain growth rate in the data set was approximately 10 microstrain. Since the strain growth is insignificant, minimal to no structural degradation occurred during the cyclic test.

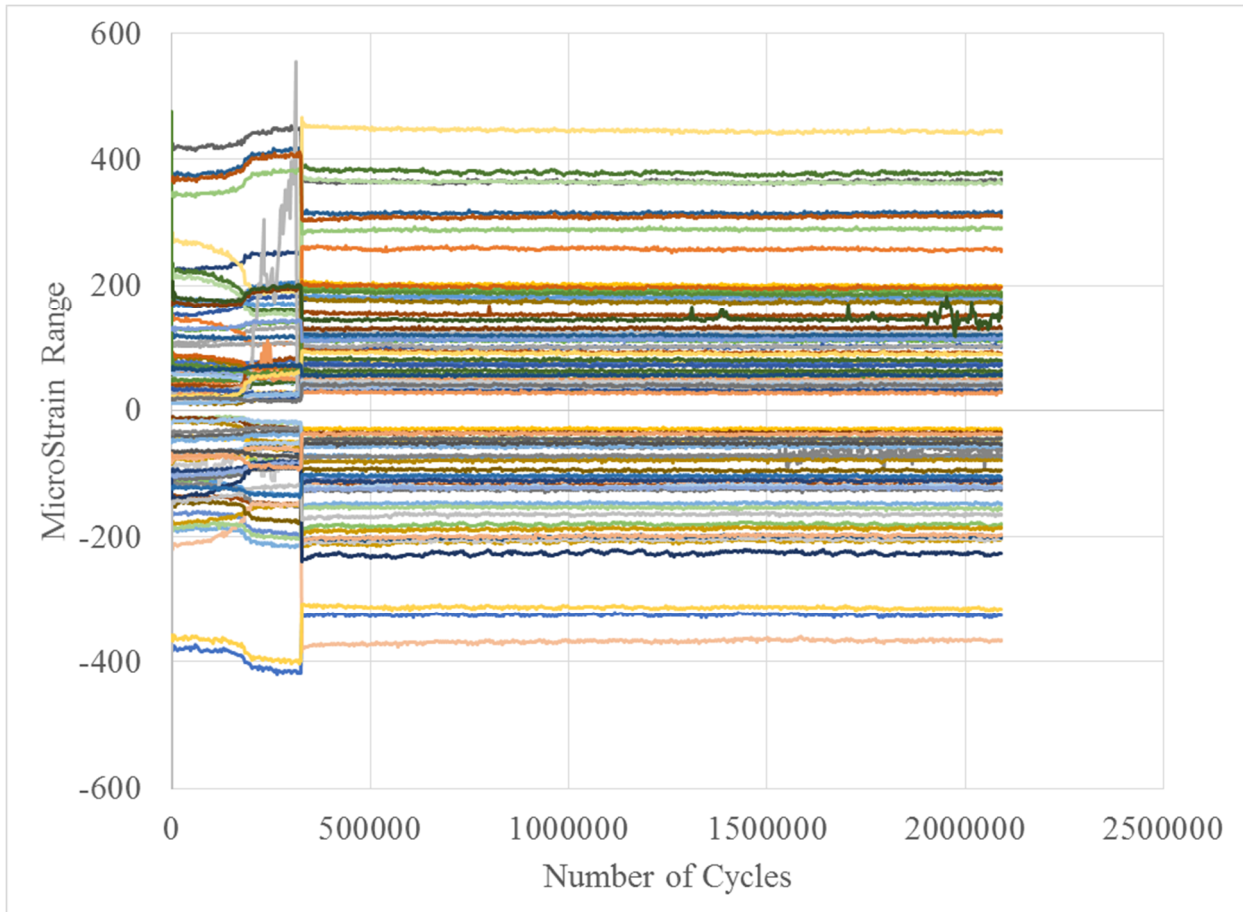


Figure 27: Strain Range versus Number of Cycles

Further evidence that minimal structural degradation occurred during the cyclic test is shown in Figure 28 through Figure 33. The figures show strain measurements recorded at the beginning of the test, after the bearing pad was replaced, at the middle of the test and at the end of the test. Gages B_C2_X, T_F1_X and B_J2_X are shown because those gages have the highest tensile (positive) strain range. Gages T_C1_X, B_F1_X and T_J1_X are shown because those gages have the highest compressive (negative) strain range. For all gages, the strain readings at the initial cycle are different than at the subsequent cycles due to the inadequate bearing pad which was replaced at approximately cycle 330,000. Gage T_F1 shows some drift in the three recordings after the bearing pad was replaced, but the slope remains constant at each discrete

cycle count. For all other gages shown, the three recordings after the bearing pad was replaced are very close in both magnitude and slope.

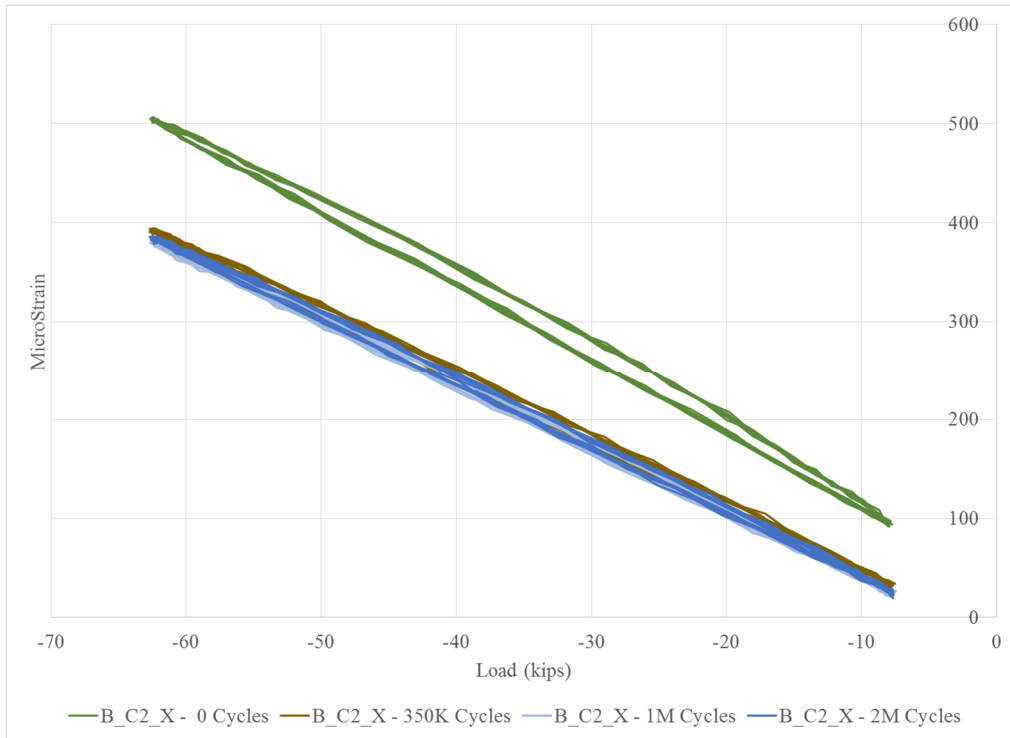


Figure 28: Strain at Gage B_C2_X vs. Load

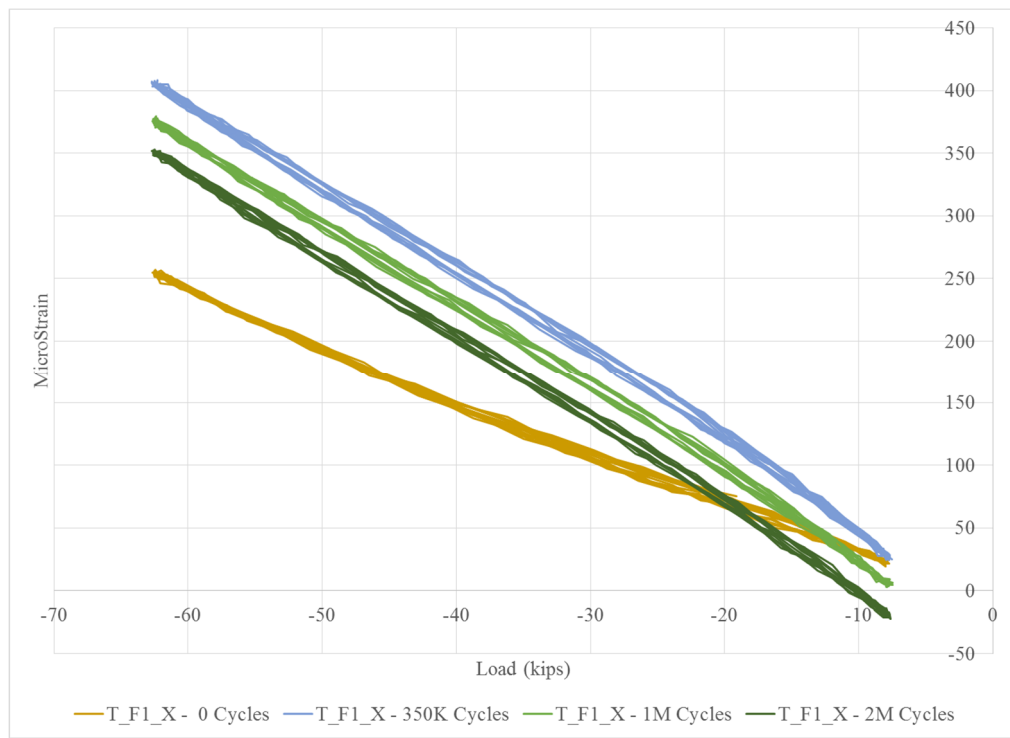


Figure 29: Strain at Gage T_F1_X vs. Load

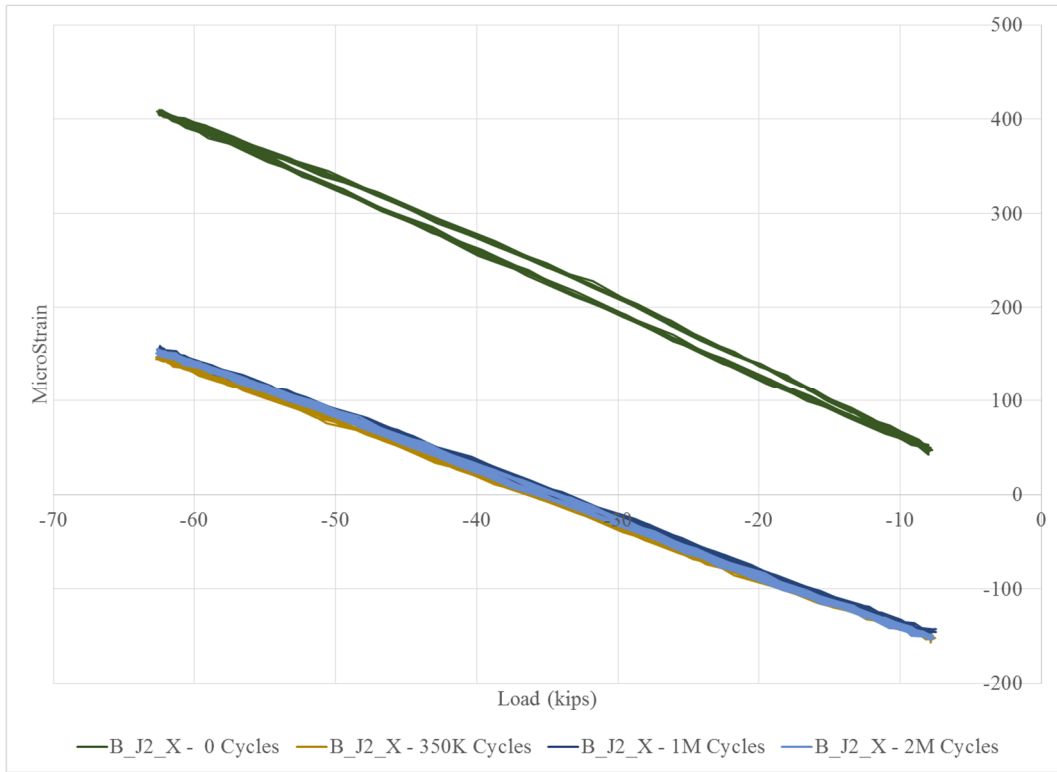


Figure 30: Strain at Gage B_J2_X vs. Load

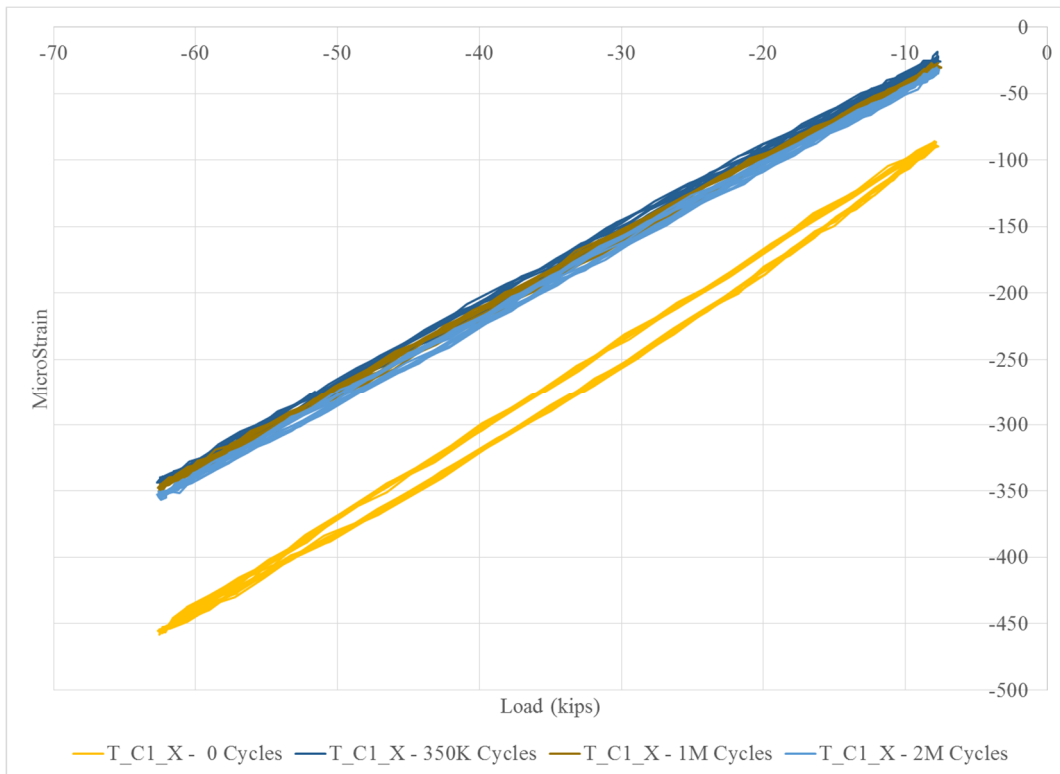


Figure 31: Strain at Gage T_C1_X vs. Load

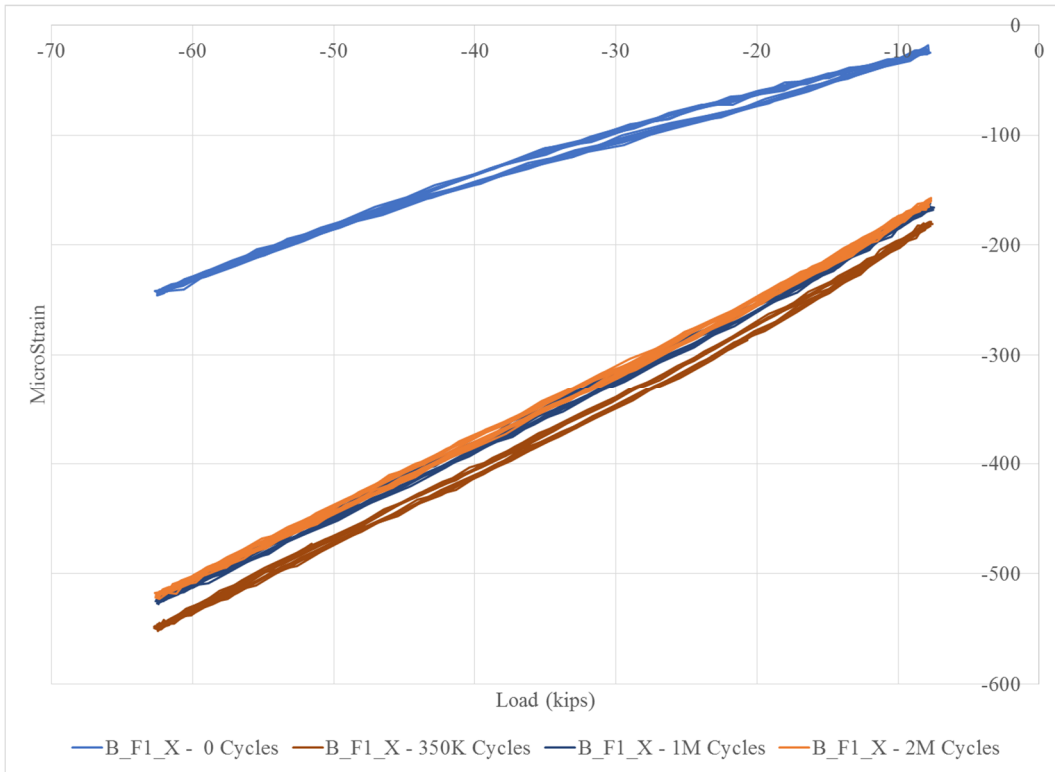


Figure 32: Strain at Gage B_F1_X vs. Load

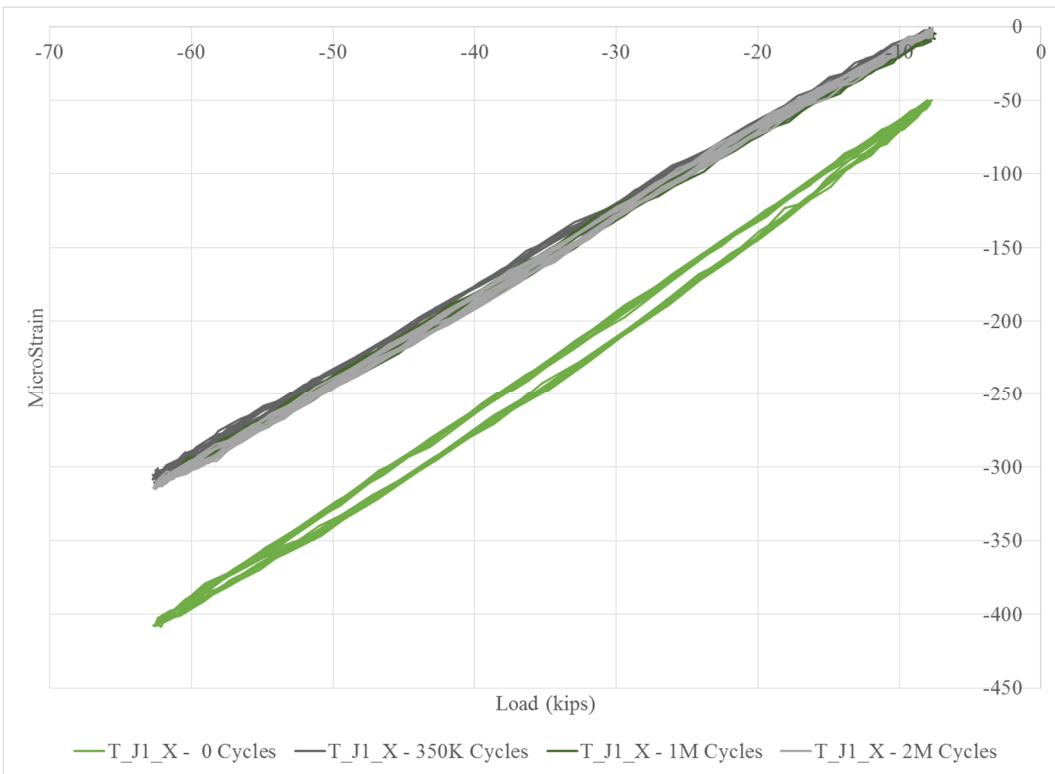


Figure 33: Strain at Gage T_J1_X vs. Load

Fatigue Results

The friction stir weld joining the aluminum panel extrusions is classified as a Category E detail per AASHTO LRFD Table 7.6.2.3-1. [7] Category E details have a constant amplitude fatigue threshold of 1.8 ksi per AASHTO LRFD Table 7.6.2.5-1, equivalent to 178 microstrain for the aluminum material tested. A higher constant amplitude fatigue threshold for friction stir welds may be appropriate based on limited research, but available design codes do not yet provide guidance for the types of single-sided friction stir welds with permanent backing used for the test specimen. [8] Figure 34 shows the strain range measured in the direction transverse to the weld over the duration of two million loading cycles. The strain range shown is the difference between the maximum and minimum strain recorded in each ten second data set.

Gages on the top of the panel indicated higher longitudinal strain ranges than those on the bottom of the panel. The behavior is consistent for static tests 5 and 6 as well as the cyclic test, indicating it is due to the bending action of the panel. Composite behavior would result in higher strain at the top of the panel than the bottom of the panel because the top of the panel is at the extreme fiber location of the composite section.

Figure 34 provides a comparison between the constant amplitude fatigue threshold and maximum recorded strain range, for fatigue evaluation purposes. Gage T_F4 is positioned directly at the weld seam on the top plate of the panel. Gage T_F3 is located 2 inches from the weld seam on the top of the panel. None of the other longitudinal gages on the top of the panel were located close to a weld. All other longitudinal gages on the top of the panel and all longitudinal gages on the bottom of the panel have tensile strain ranges below 120 microstrain. Gage T_F3_Y has the highest recorded longitudinal tensile strain range. The measured value is close and slightly higher than the constant amplitude fatigue threshold. The average strain range measured at gage T_F3_Y is within 1% of the constant amplitude fatigue threshold and therefore the weld detail for this test specimen can be considered to be within the infinite fatigue life stress limit. However, this particular test specimen has been subjected to a significant number of loading cycles during the testing regimen representing approximately half of its fatigue life and non-ferrous metals such as aluminum do not have distinct endurance limits like ferrous materials such as steel. Therefore, the remaining fatigue life for this test specimen should be evaluated and it should be inspected on a regular basis if placed in service for a trial period.

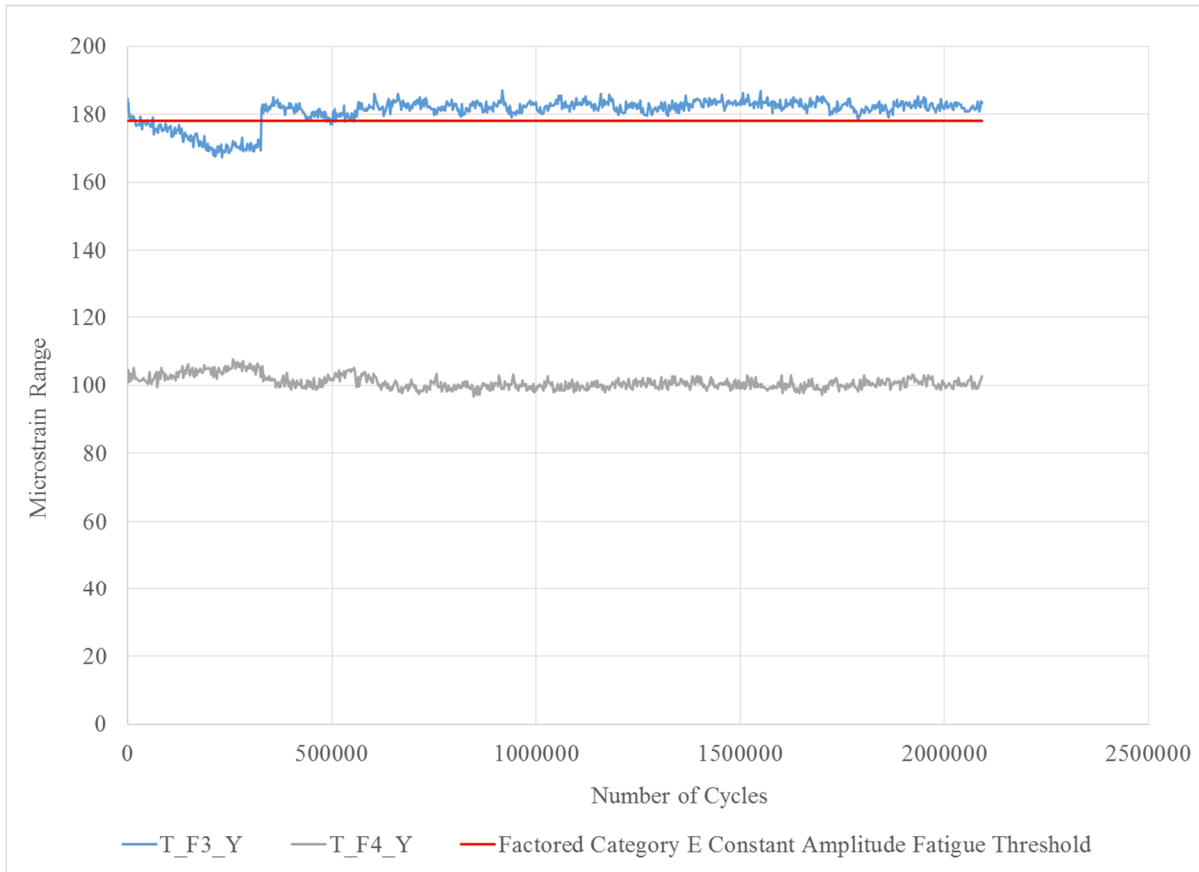


Figure 34: Tensile Strain Range Transverse to Weld vs. Number of Cycles

Deflection Results

The maximum deflection occurs directly under each loading point, at mark C1 and J1. The deflection readings at those locations were corrected by the support deflection readings to remove the deflection due to the bearing pad supports. The deflection at mark C1 was corrected by the average of the deflections at gages GD1 and D_F1. The deflection at mark J1 was corrected by the average of the deflections at gages D_F1 and GD3. Refer to the Instrumentation Plan in Appendix A: Structural Testing Procedure for those gage locations. The corrected data is presented in Figure 35. The increased deflection from zero to cycle 330,000 is due to failure of a support bearing pad. Gage D_J1 also appears to have malfunctioned between cycles 330,000 and 550,000. Although noisy, the deflection readings are stable over the cyclic loading test, after cycle 550,000.

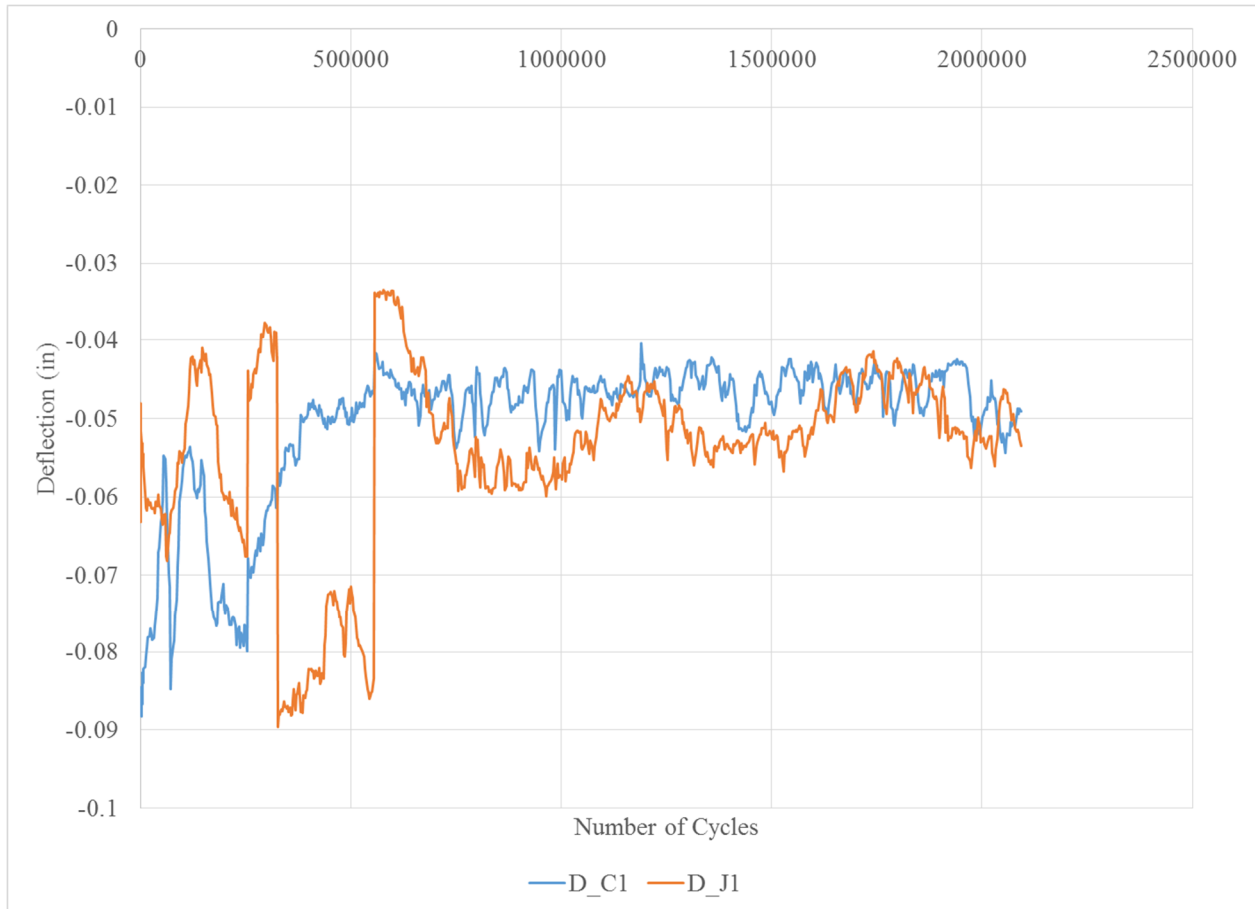


Figure 35: Deflection vs. Number of Cycles

Discussion

The aluminum lightweight deck test specimen was subjected to a thorough structural testing regimen including nine static tests and one cyclic test. The loading magnitude, footprint and layout were set based on requirements per AASHTO LRFD and FDOT Structures Manual. [7] [9] The target limit states were Service II, Strength I and Strength II, with loads corresponding to the HL-93 truck and tandem and the FL-120 permit truck. Instrumentation consisted of 92 bi-axial strain gages and 20 deflection gages, placed according to structural analysis results to provide a valuable comparison of analytical and experimental results.

Structural adequacy of both the generation I and II panel were verified before the test specimen is placed in service for a trial period. Test results show the deck panel meets the design requirements of AASHTO LRFD, with demand to capacity rates of 0.7 for tension and 0.57 for compression. The design is controlled by deflection at the edge of the panel, with a measured deflection exceeding the deflection limit by 0.02 inches. The measured deflection was 0.11 inches and the limit per AASHTO LRFD (Span/800) is 0.09 inches.

The experimental results show higher tensile strain and deflection and lower compressive strain than predicted by analytical methods. The controlling locations are also different. Experimental results show maximum tension at the negative moment region and maximum compression at the loading point. Analytical results predicted maximum tension at the loading point and maximum compression at the negative moment region. However, the recorded strains have a conservative demand to capacity ratio and therefore an acceptable design.

Results from the cyclic test show the panel deflection and strain were stable during two million cycles of fatigue loading. No significant structural degradation occurred during that test. Results from that test show the friction stir weld for the tested panel under the applied fatigue loading condition (representing the maximum design case) is predicted to have a sufficient fatigue life, although the measured strain range is slightly (1%) above the constant amplitude fatigue threshold.

The test results are valid for the dimensions of the particular specimen tested. Numerical analysis would be required to verify the adequacy of panels with different lengths or widths. Since the panel is deflection controlled, if the span is adjusted to over 6 feet or the number of supports is decreased, the panel deflection may exceed recommended limits. Also of concern for future numerical analysis is the strain range at the welds. The measured strain was very close to the constant amplitude fatigue threshold. Dimensional changes to the panel and/or support system would need to be offset by a change in panel resistance to ensure that the strain range remained acceptable for the fatigue detail.

Heavy Vehicle Simulation Testing

The lightweight aluminum extruded deck specimen was tested using a Heavy Vehicle Simulator (HVS) to simulate real-world traffic loading. The movement of the single loaded tire in the HVS can uncover problems which are not exposed in conventional structural testing. The structural testing conducted at the Structures Research Center, discussed in the previous section, loaded the panels to a higher level than the HVS capabilities, therefore, structural capacity was not an intended outcome of the HVS testing. Instead, the primary focus was on performance of the wearing surface, however, monitoring for potential structural implications continued. Friction and bond measurements for the wearing surface were collected before and after the heavy vehicle simulation (HVS) testing.

Heavy Vehicle Simulator (HVS) testing was conducted at the FDOT State Materials Office in Gainesville, FL. The Heavy Vehicle Simulator owned by FDOT is a HVS-A Mark V, with consulting services provided by Dynatest. The machine is capable of completing 29,000 bi-directional test passes within a 24 hour period, although 23,000 passes per day was typical during this particular test. The tire runs at approximately 8 miles per hour over a test length of 20 feet. The HVS can be programmed to include wheel wander in its loading pattern, but that wasn't desired for this particular test. Due to HVS tire limitations, the target tire load was 11 kips.

Test Setup Description

600,000 loaded tire passes were conducted using the Heavy Vehicle Simulator. The tire was run along gage line 'C' shown on the Instrumentation Plan in Appendix A: Structural Testing Procedure. To aggressively test the wearing surface, heat was applied for the first 300,000 tire passes. Thereafter, the heating elements were removed and water was applied for the remainder of the test. During preliminary bond tests of the wearing surface, the epoxy bonding the wearing surface failed at a lower load when the specimen was heated to 120 degrees Fahrenheit (50 degrees C). Therefore, that target temperature was applied during the first half of HVS loading. Heat was applied via built in heaters on the HVS, to the left and right of the tire path. The heaters are programmed to turn on and off based on preset limits. To retain heat, an enclosure was built around the HVS loading path, as shown in Figure 37. During testing, the measured temperature varied between 100 and 120 degrees Fahrenheit (40 and 50 degrees C), as shown in Figure 39. Some variation in thermal measurements is due to the geometric placement of the thermocouples and their proximity to heaters, as shown in Figure 38 (black line indicates tire path). Gage T-SE1 was originally installed incorrectly and was recording ambient temperature until the error was corrected, see Figure 39.



Figure 36: Heavy Vehicle Simulator Wheel Path



Figure 37: Heavy Vehicle Simulator Enclosure

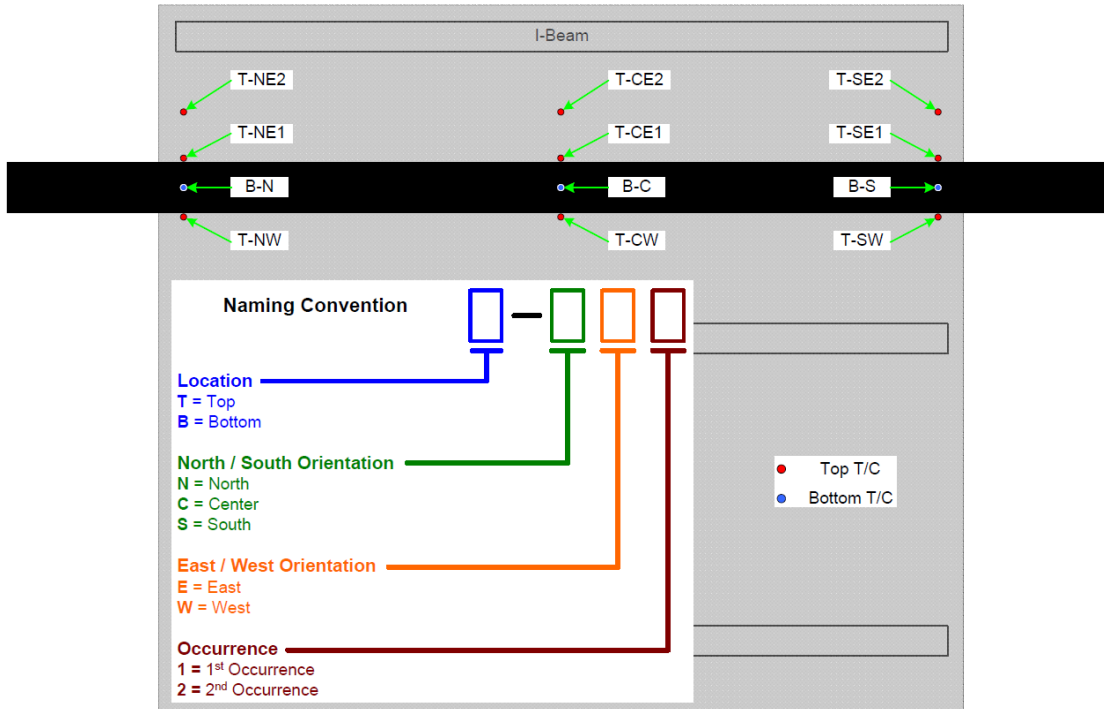


Figure 38: Bridge Deck Thermocouple Names and Locations

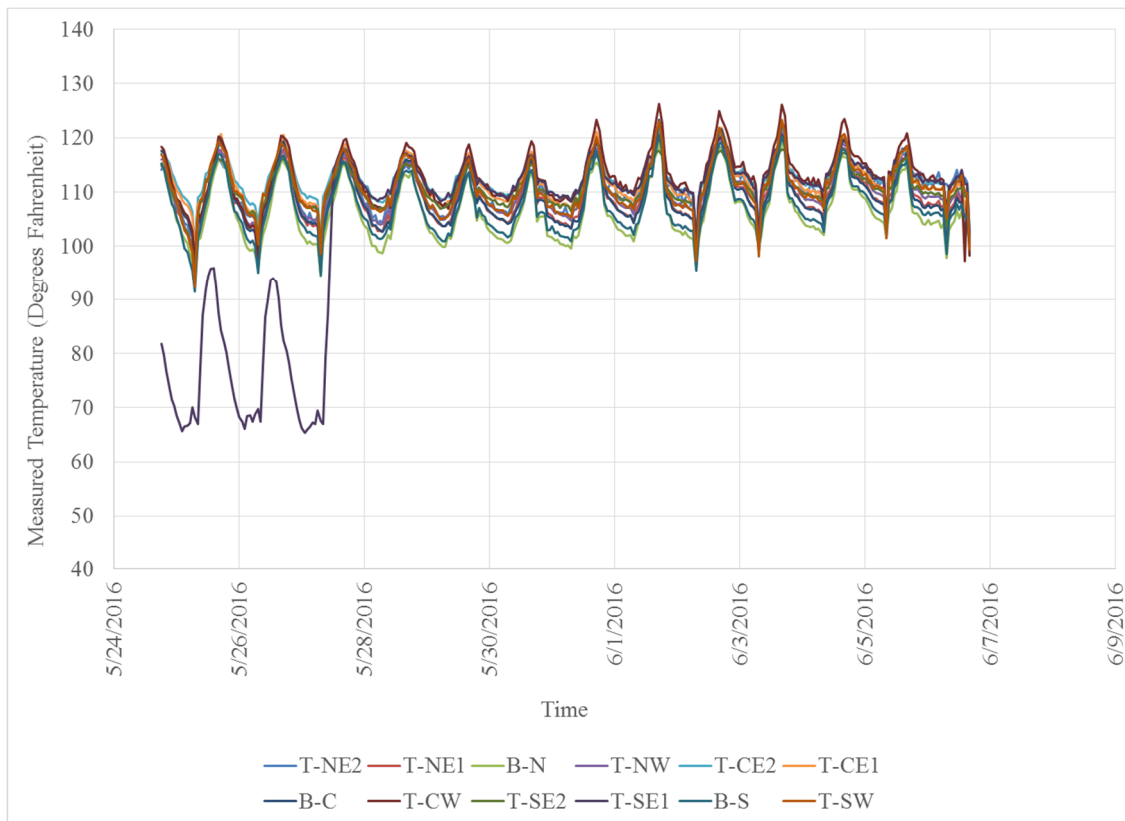


Figure 39: Measured Temperature during HVS Testing

During the second half of testing, corresponding to the second 300,000 bi-directional passes, the wearing surface was saturated in and around the HVS tire path. Tap water, at typical temperatures, was applied to the deck as needed using soaker hoses to maintain a saturated condition. Heat was not applied during the second half of HVS testing.



Figure 40: Heavy Vehicle Simulator Water Saturated Test

The maximum target load allowed for the tire installed in the Heavy Vehicle Simulator is 11 kips. That maximum load was selected to maximize the effects of testing. The maximum load applied at any one location during static testing at the Structures Research Center was 57.5 kips, approximately five times higher than the moving load applied. The applied moving load is approximately equal to the resulting single tire load for an HL-93 truck with tandem axles, including the Service I limit state load factor and impact factor, but not the multiple presence factor. Figure 41 shows the tire load variation over the duration of the test. The data points less than zero kips indicate instances when the HVS was shut down for temporary maintenance. The average load applied was 11.1 kips.

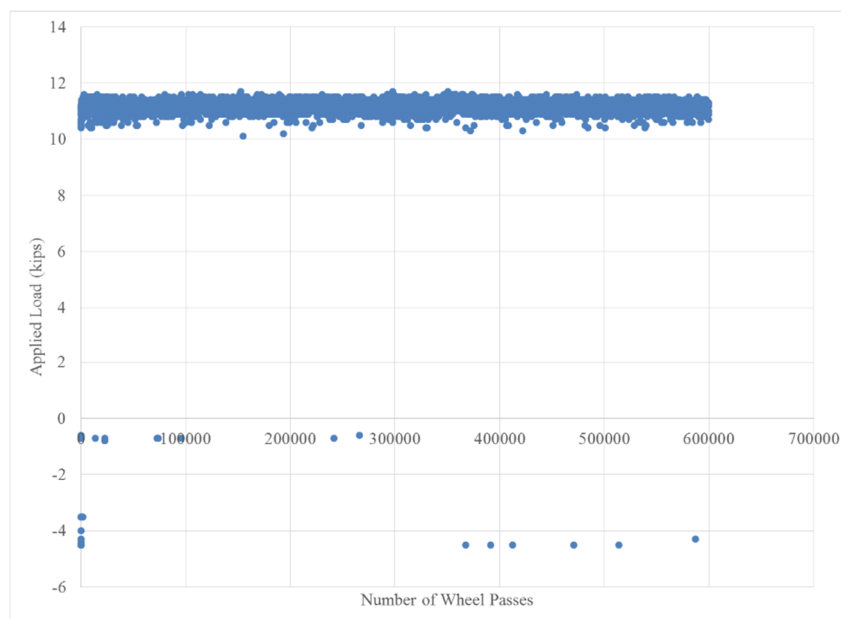


Figure 41: Applied Load vs. Number of Wheel Passes

Instrumentation consisted of 38 bi-axial strain gages and 15 deflection gages. For locations, refer to the Instrumentation Plan included in Appendix B: Heavy Vehicle Simulator Testing Procedure. Installation and naming convention for the strain gages was previously discussed in the Structural Testing section of this report and remained consistent for the HVS testing. Thirteen of the fifteen deflection gages were used to measure deflection of the aluminum panel and steel stringers. For those locations, Firstmark Controls Position Transducers, model number 60-25-54C1 with a 13.5" range were used. The gages were attached to a frame constructed of structural steel and aluminum double T-slot. The frame was bolted to the steel stringers for transportation to the testing site. Upon arrival, the bolted connection to the steel stringers was removed. During testing, the frame supporting the deflection gages was independently supported and not in contact with the test specimen or support beams. For details, see Figure 42. Two of the deflection gages were installed at each end of stringer 2 to measure horizontal slip between the aluminum panel and steel stringer. ETI Systems LCP8S-10 linear motion potentiometers were used for those locations.

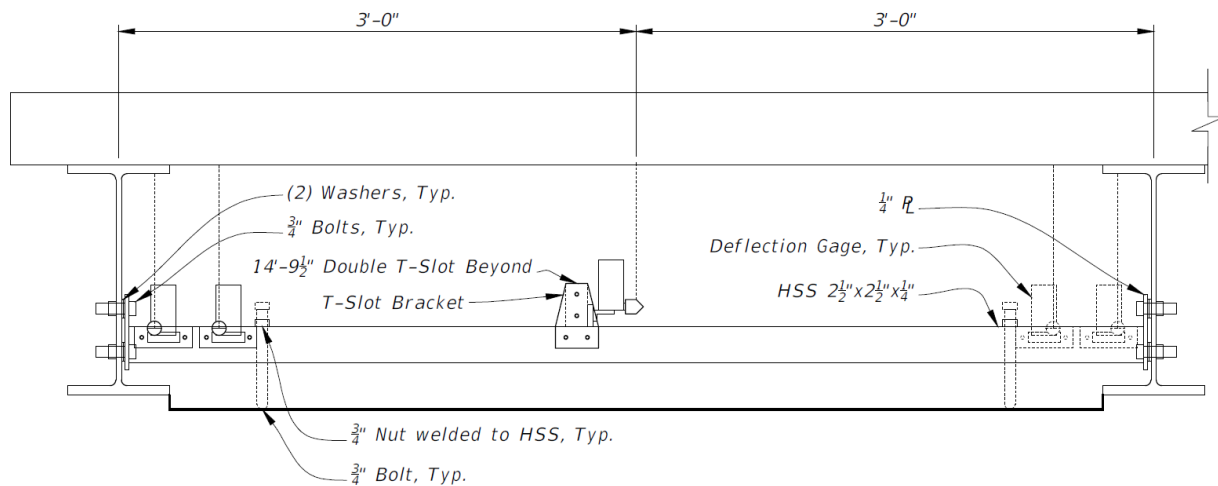


Figure 42: Deflection Frame

Simulation Testing

Data was recorded for the heavy vehicle simulation (HVS) test at a rate of 100 Hz for 1 minute once each hour during the 27 day long test. The maximum, minimum and range of each data file was extracted and collected in a comprehensive Excel file. Due to the moving nature of the HVS load, stress reversal occurred for some locations in the deck and some gages showed both tensile and compressive strain according to the tire location. Therefore, the strain range was not corrected to be either positive for tension or negative for compression, as was previously done for the Test 7 data. The strain range presented is an absolute value of the maximum reading minus the minimum reading. For the aggregate presentation of strain range data, refer to Figure 43 and Figure 44. Due to a malfunction of the data acquisition machine, no data was recorded between HVS passes 67,814 - 152,720 and between passes 566,508 - 599,504 although the HVS was operating. Gage B_C20_Y became faulty during the first phase of testing (0 - 300,000 HVS passes). During the second phase of testing (300,000 - 600,000 HVS passes), gages B_A10_X, B_C1_Y, B_C2_X,

T_C20_X, T_C20_Y, B_C20_Y, B_D2_Y, B_E16_Y, B_F1_X and T_F11_X became faulty. None of those gages are shown in Figure 43 or Figure 44.

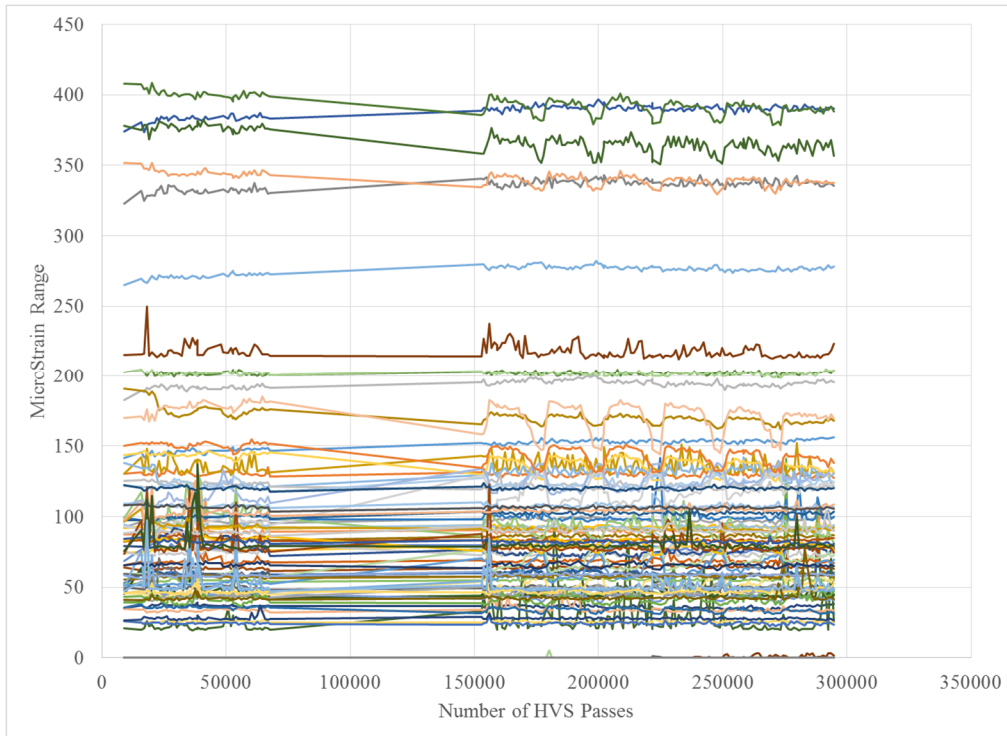


Figure 43: Strain Range versus Time for Heat Applied Testing

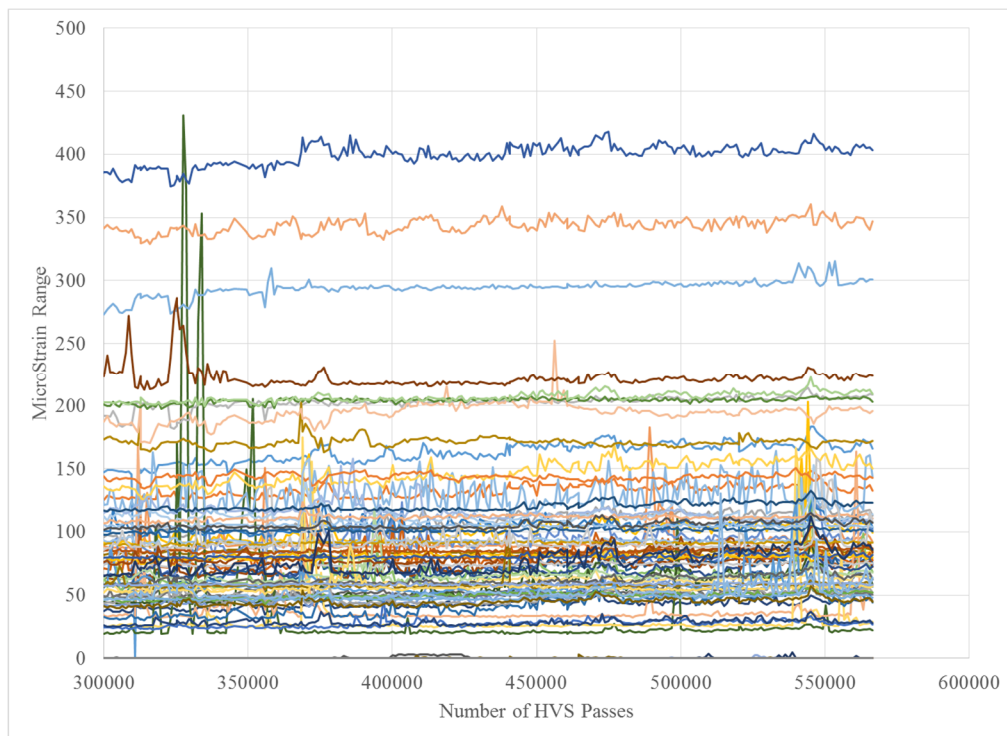


Figure 44: Strain Range versus Time for Water Applied Testing

Data Analysis and Processing

Although the primary intent of Heavy Vehicle Simulator testing was to evaluate the wearing surface, strain and deflection readings were analyzed to provide information regarding the structural response of the deck and stringer system to a moving load. Comparisons are made between the effects of static/cyclic structural testing and the effects due to a moving load. Growth in the strain range over the testing period is an indication of structural change and was calculated as the difference between the average strain range for the first 50,000 cycles and the last 50,000 cycles. The strain range growth was less than 10 microstrain for 88 percent of the gages, excluding faulty gages. The six gages with strain growth over 20 microstrain were B_C16_X, B_D16_X, B_C18_X, B_E18_X, B_C20_X and T_F7_X. Five of the six gages are located on the bottom of the generation II panel close to the HVS wheel path and all of the gages with strain growth over 20 microstrain measured bending in the transverse direction of the panel. The largest growth in strain range was 30 microstrain, occurring at gage B_C18_X. For gage B_C18_X and adjacent gage B_C20_X, the recorded behavior is presented in Figure 45 to Figure 48. The behavior at the beginning and end of the test is similar, although the magnitudes and range differ at the end of the test compared to the beginning of the test. The primary difference between the magnitude of recorded strain at the beginning and end of the test is due to sensor drift. There is moderate to strong correlation between strain and temperature readings over the duration of the test. Therefore, sensor drift is assumed to be primarily due to thermal effects. Variation of the difference between the minimum and maximum data point in each recording (range) is a more appropriate assessment of structural change than the magnitude of the maximum or minimum.

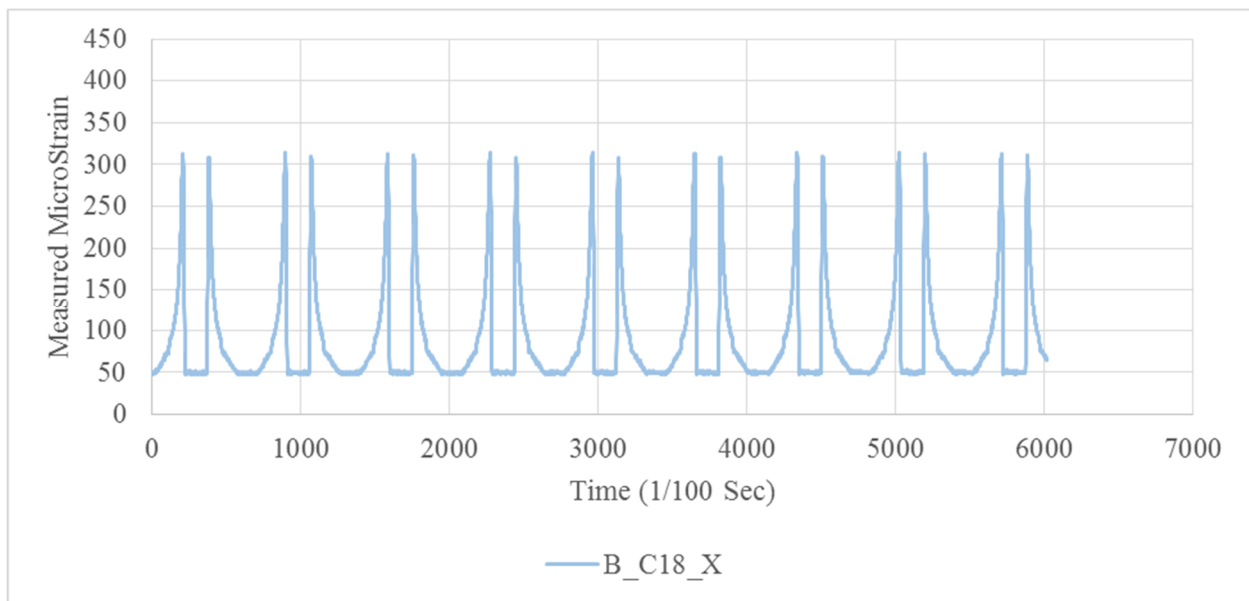


Figure 45: Recorded MicroStrain on 5/26/2016 at 1 AM for Gage B_C18_X

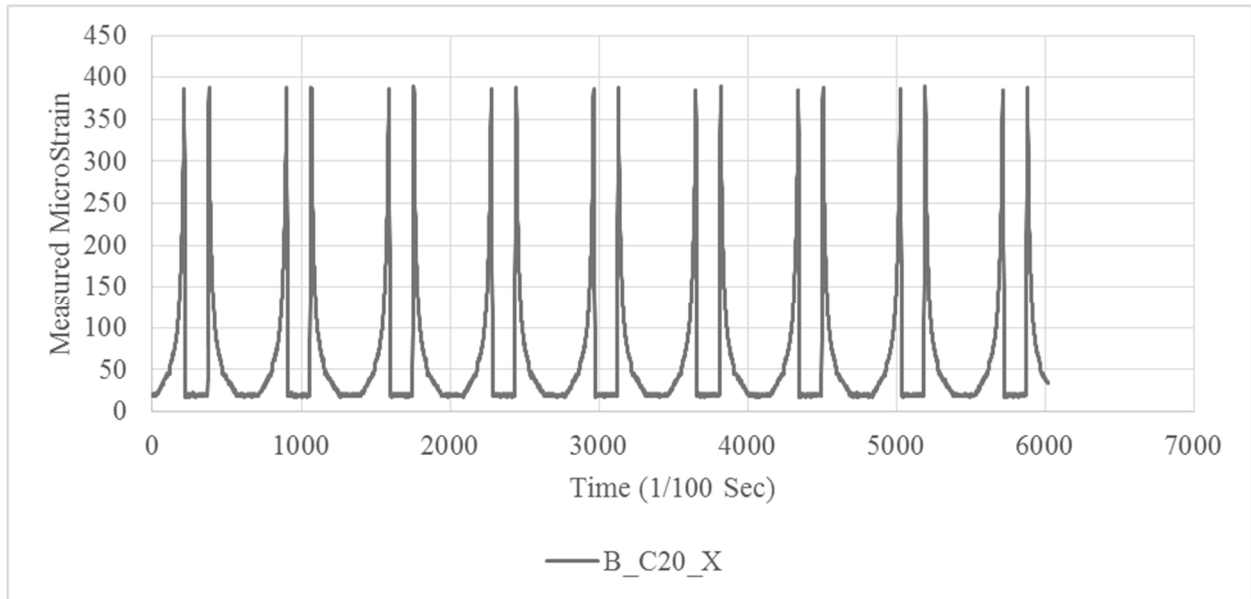


Figure 46: Recorded MicroStrain on 5/26/2016 at 1 AM for Gage B_C20_X

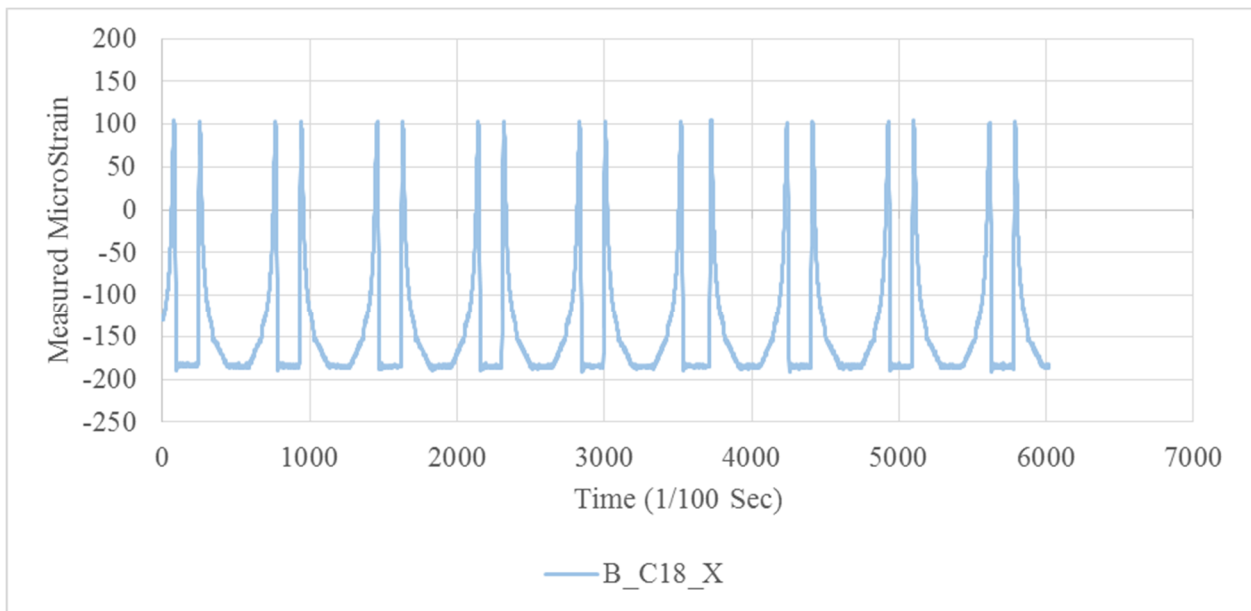


Figure 47: Recorded MicroStrain on 6/18/2016 at 1 AM for Gage B_C18_X

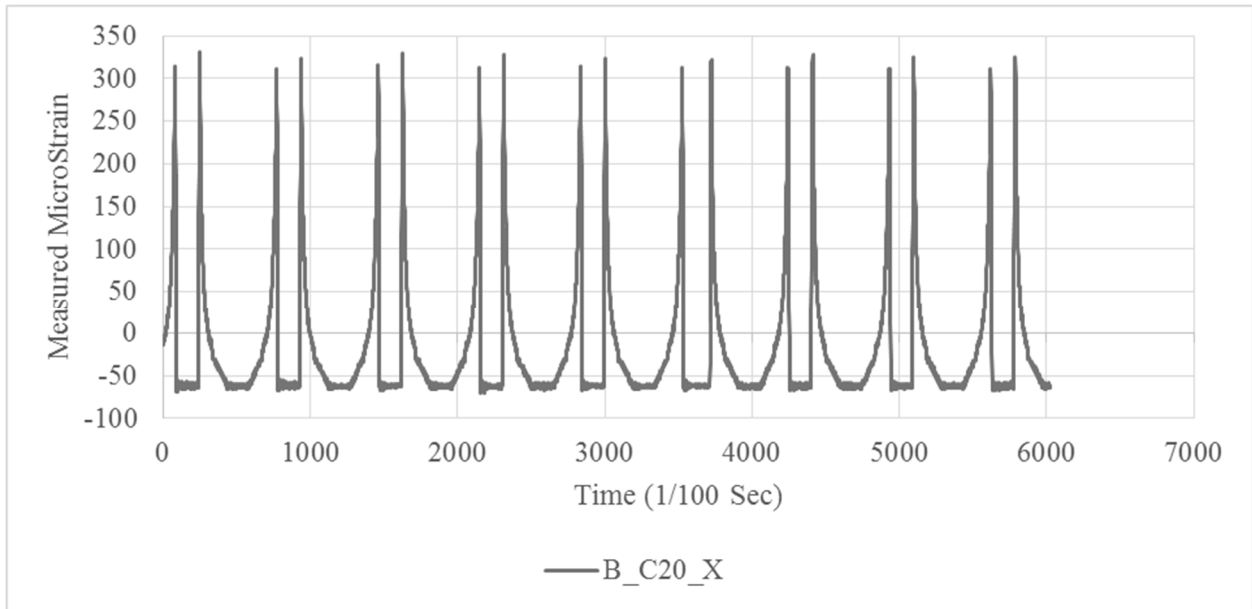


Figure 48: Recorded MicroStrain on 6/18/2016 at 1 AM for Gage B_C20_X

Due to the moving nature of the Heavy Vehicle Simulator load, stress reversal occurs for strain in the travel direction of the tire load. The maximum level of strain reversal was observed at gage B_C16_Y, in the generation I panel. The measured strain showing the stress reversal behavior is shown in Figure 49. Gage B_C16_Y had the highest recorded strain range for gages in the travel direction of the tire. Measurement at gage B_C2_Y is also included in Figure 49 as that gage had the highest recorded strain range for the generation II panel. Gage B_C10_Y is included as that gage is at a similar position in the generation II panel as gage B_C16_Y for the generation I panel.

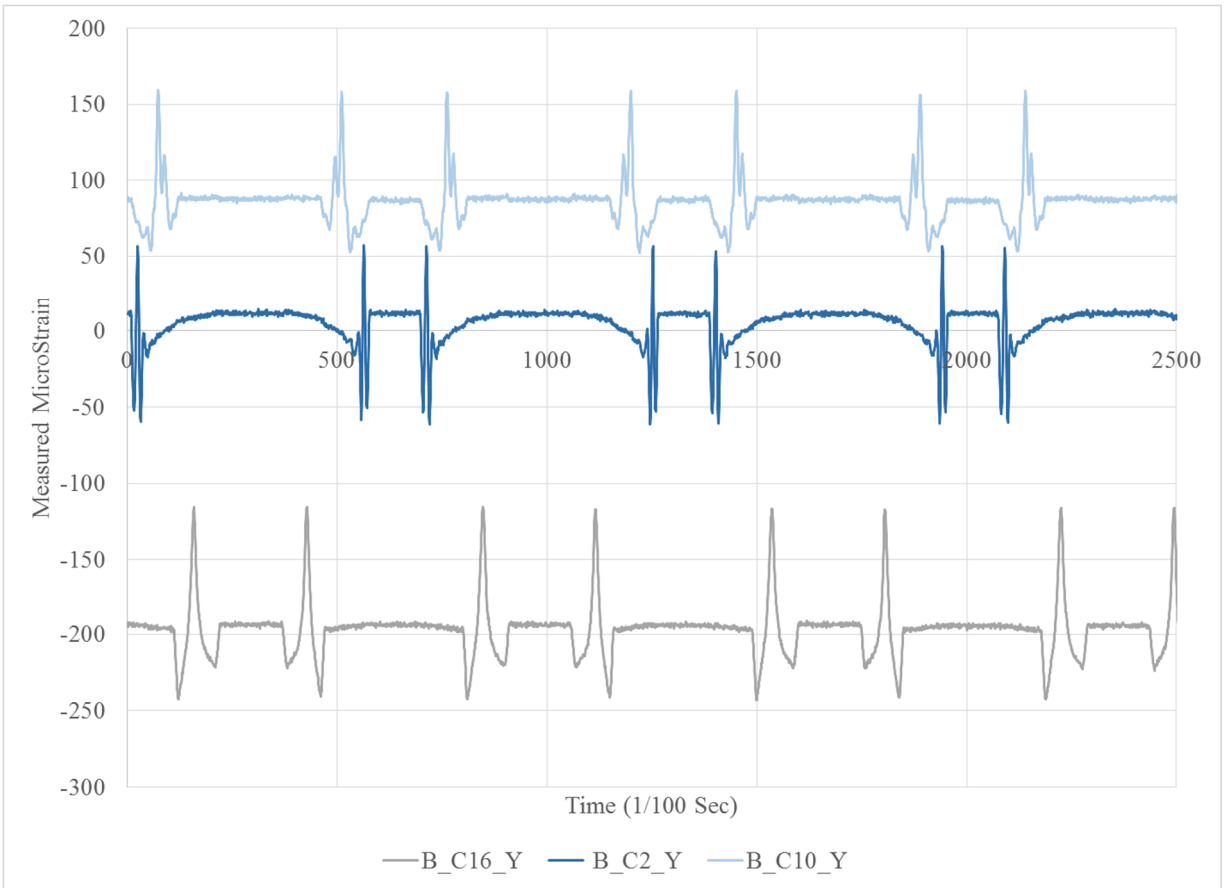


Figure 49: Recorded MicroStrain on 5/26/2016 at 1 AM for Gages B_C16_Y and B_C2_Y

Fatigue Results

Although the Heavy Vehicle Simulation test was different than the cyclic testing in both load magnitude and configuration, the results of the HVS test validate the conclusions made based on cyclic testing. The average strain range measured at gage B_C16_Y was 132 microstrain and the growth in strain range from the beginning to the end of the test was approximately 6 microstrain. The load applied during HVS testing was 11.1 kips, which is less than the design fatigue load at a single wheel, 13.8 kips, per AASHTO LRFD Article 3.6.1.4. [7] The ratio of design fatigue load (13.8) to applied load (11.1) is 1.24. The loading pattern applied is also different than the fatigue load. The fatigue load pattern includes four loading points, as previously described in the Structural Testing section. Structural testing included both a single loading point for test 1, similar to the loading pattern used for HVS, and a four point load pattern for tests 5 through 8, matching fatigue loading. The ratio of maximum measured tensile strain during test 5 and tensile strain during test 1, also accounting for the difference in applied load, is 1.03. That ratio accounts for the change in loading pattern. The estimated strain range at the fatigue load is predicted to be 176 microstrain, based on the measured strain range multiplied by the 1.24 and 1.03 ratios. That value is within 3% of the measured strain during cyclic structural testing and approximately 1 percent below the Factored Category E Constant Amplitude Fatigue Threshold, previously discussed in the Structural Testing section.

Deflection Results

Figure 50 through Figure 52 show the maximum deflection readings for the generation I panel at the beginning and end of the HVS testing and the maximum deflection reading for the generation II panel at the beginning of testing. Deflection of the generation II panel (Gage D_C9) is not shown at the end of testing because the gage became faulty. The data shown in Figure 50 through Figure 52 was post-processed. Support deflection was subtracted from the readings for each gage. The result shown is panel and stringer deflection only.

Deflection readings varied significantly over the duration of the test. Unadjusted deflection measurements for properly working gages were 0.12 inches or less over the duration of the test. The change in deflection readings over the duration of the test was as high as 0.04 inches. The rate of change over the duration of the test compared to the magnitude of the deflection readings is high, with a maximum ratio of 0.33. The deflection at gage D_C9 was approximately 0.04 inches at the beginning of HVS testing and increased to approximately 0.06 inches, a substantial increase. However, the measured deflection value is low. 6 of 13 deflection gages (GD_1, GD_2, D_C9, D_C14, D_F2, D_F14) became faulty during the test, particularly while water was applied to the deck. Due to the high number of faulty gages and low deflection movement, deflection readings taken during HVS testing are not a valuable measure of structural performance and therefore the growth in deflection readings is not an indicator of significant degradation.

Recorded deflection during HVS testing was lower than static structural testing. The deflection due to a single static load was 0.14 inches for static test 1, measured at gage D_C1. For that test, a 33.2 kip load was applied at the edge of the deck at line C. The transverse position is the same for test 1 and the HVS testing. The longitudinal location is not the same, since the heavy vehicle simulator load moves. For HVS testing, the closest gage to D_C1 was gage D_C3, which had a post-processed measurement of 0.036 inches at the beginning of testing and 0.037 inches at the end of testing. The processing removes support deflection and because the gage is at the edge of the panel, the result is panel deflection only. Assuming linear behavior, the deflection was 20% lower during HVS testing than during static testing.

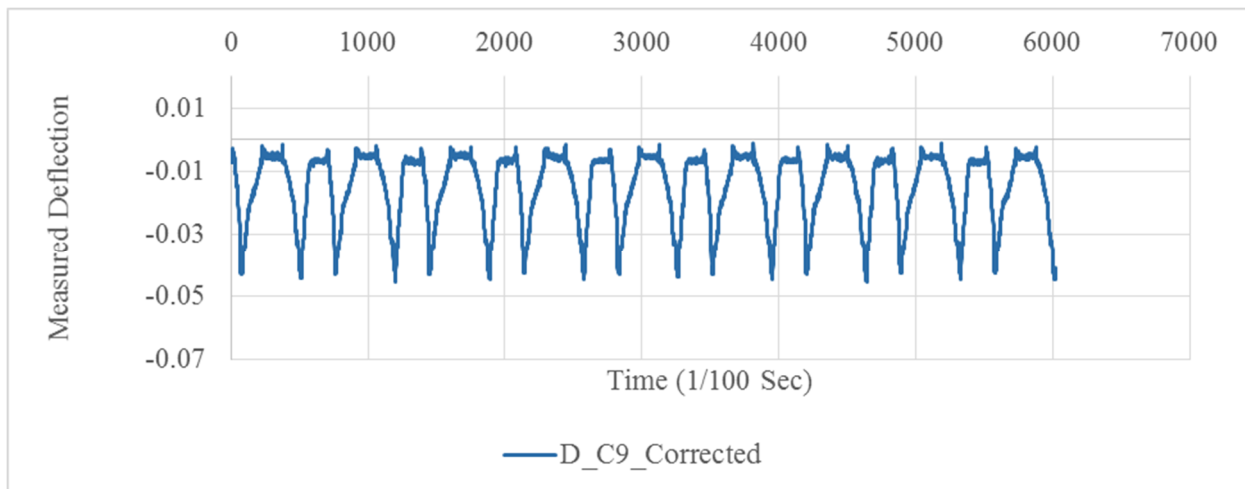


Figure 50: Deflection at Gage D_C9 on 5/26/2016 at 1 AM (Generation II Panel)

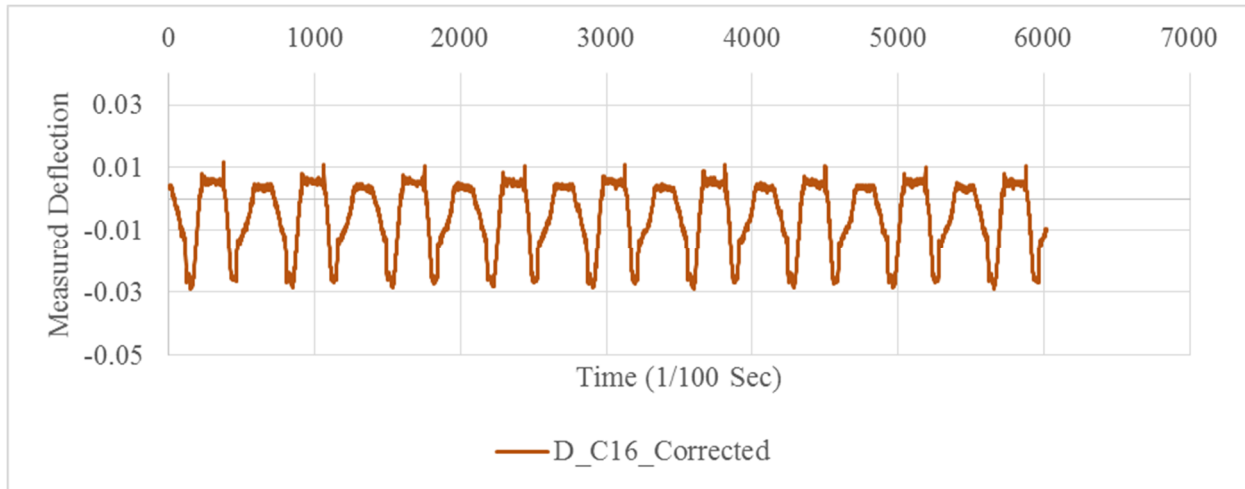


Figure 51: Deflection at Gage D_C16 on 5/26/2016 at 1 AM (Generation I Panel)

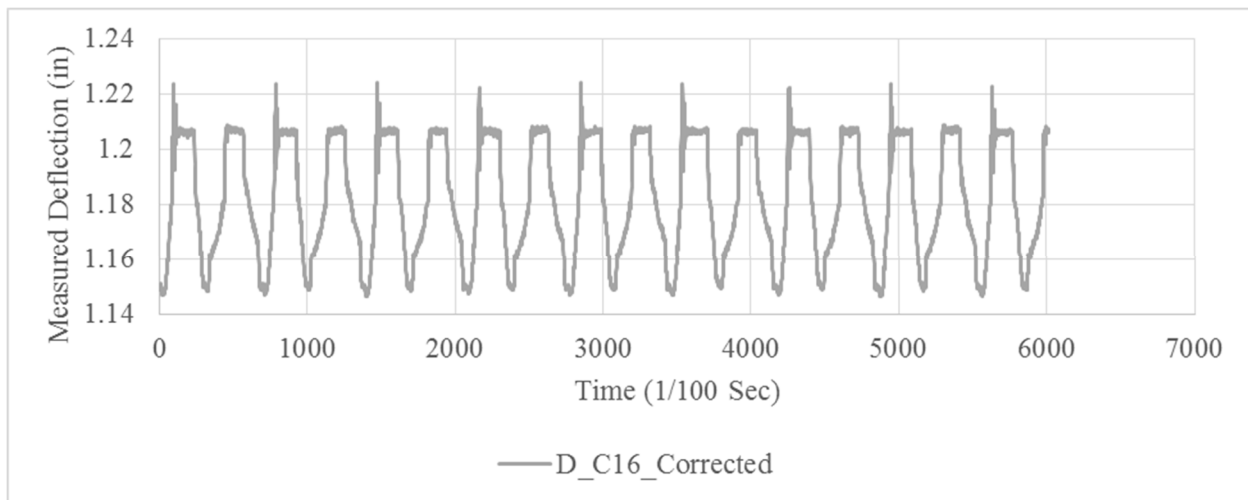


Figure 52: Deflection at Gage D_C16 on 6/18/2016 at 1 AM (Generation I Panel)

Slip Deflection Results

Two slip deflection gages were attached to the underside of the aluminum deck at each end of stringer two. The gages referenced the top flange of stringer two, measuring horizontal slip between the deck and steel stringer. Figure 53 presents the recorded slip range during testing. Gage A was installed on the generation I panel, while slip gage B was installed on the generation II panel.

The recorded slip range magnitude is very low, with an approximate maximum of 0.0007 inches. The small magnitude of the measurement is within the error of the gage and could also be due to local effects. The deck was designed to slip due to thermal load. Per the Research Program Notes, the difference in thermal coefficients between the steel and aluminum materials used is $6.3 \times 10^{-6} /F$. [4] Per section 2.7.1 of the FDOT Structures Design Guidelines, the design thermal range is 90 degrees F with a 1.2 design factor. [9] Based on that information, for the longer panel length of 8'-3", the design thermal movement is approximately 0.07 inches. Although the design intent was for the aluminum panel to slip in relation to the

steel beam during thermal cycles, the maximum recorded slip is approximately one hundred times less than the design thermal movement. Although referred to as “slip” for the purpose of discussion, due to the relatively small movement as compared to the design movement, the behavior cannot be considered to be the type of slip intended to be resisted by the faying surface and slip-critical bolted connection.

For most of the Figures presented in this report, the data was post-processed so that the data recorded while the heavy vehicle simulator was stopped is not included in the Figures. However, Figure 53 includes all data recorded. At the beginning of the test, while the heavy vehicle simulator was being set up and was not running, slip range was measured as a value close to zero. At the mid-point of the test, the HVS was stopped to complete the heated phase of the test and to set up for the saturated wearing surface phase of the test. Again, the slip range was measured as a value close to zero. During the test, when the heavy vehicle simulator was stopped for maintenance, the slip range shows intermittent values close to zero. Slip between the steel stringer and aluminum deck was only recorded while the heavy vehicle simulator was running and the deck was loaded. The recorded slip range is close to zero when there is no vehicular load on the test specimen. Figure 54 shows evidence that slip is recorded only when the HVS tire is in contact with the deck. The spikes shown in Figure 54 occur when the wheel leaves the test specimen at each end.

Evident from Figure 53 is that slip readings for gage A, on the generation I panel are consistently higher than readings for gage B on the generation II panel. The average reading for gage A is approximately double the average reading for gage B. The gap between the panel and stringer is larger for the generation I panel than the generation II panel and may be the cause of higher slip readings.

The recorded slip is clearly a function of structural loadings since readings start and stop according to when the heavy vehicle simulator was running. The cause is unknown. The recorded measurement is potentially due to axial compression, bending in the test specimen, or a combination thereof. Slip readings are much lower than would be expected due to thermal loads, by a factor of 100. The panel may not be performing as designed since slip due to thermal loads was not observed during testing. Inherent conservatism in the design of the faying surface and slip-critical bolted connection is a likely reason that the panel does not slip due to thermal effects. The behavior does not appear to be detrimental to performance of the system and the lack of significant slip between the panel and stringer may be preferred so that the inorganic zinc coating does not wear off of the steel beam and result in corrosion between the dissimilar metals.

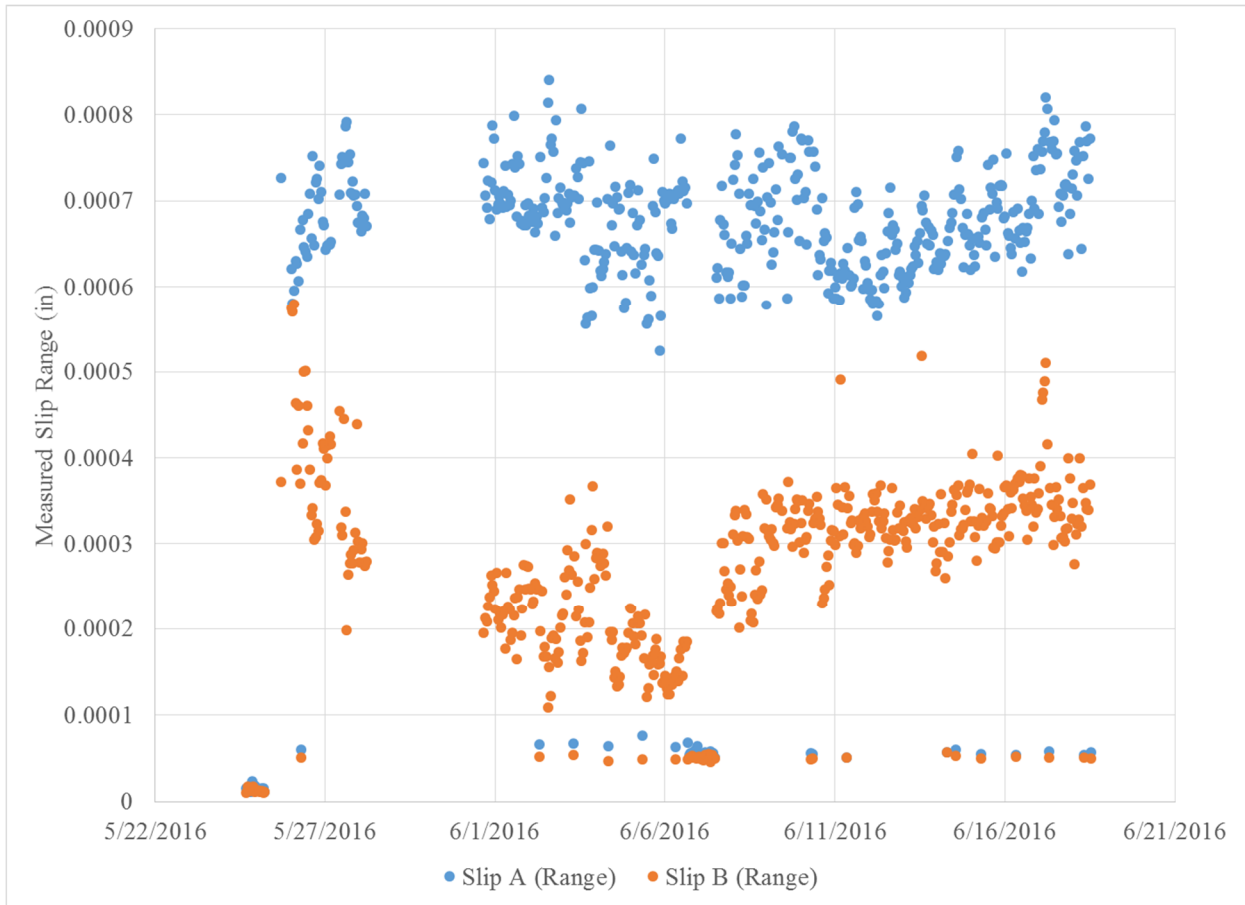


Figure 53: Slip Range Measurement vs. Time for Entire HVS Test

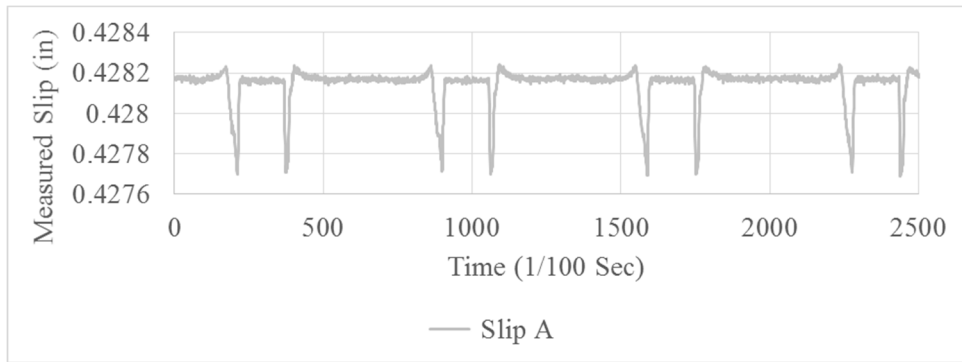


Figure 54: Slip Measurement vs. Time for 5/26/2016 at 1 AM

Wearing Surface Testing

Although not integral to the structural performance of the lightweight aluminum deck, a satisfactory wearing surface is essential to provide safe driving conditions for the public. Performance of the wearing surface can affect usability of the aluminum deck system. The wearing surface installed on this test specimen is the Euclid Flexolith product, installed in a two coat, ¼ inch thickness. A minimum bond strength of 250 psi is required. [4]

Bond Testing

Bond testing was performed prior to testing to establish a baseline for the wearing surface bond condition and to determine the controlling failure mode and corresponding strength for the overlay material bonded to the lightweight aluminum deck panel. Seventeen locations on the lightweight aluminum deck test specimen were tested. Ten locations were tested on a smaller aluminum deck sample. Personnel from the Corrosion Research Laboratory of the FDOT State Materials Office performed all tests and provided the information included in this section. Tests on the full size deck, before HVS loading, were performed at the FDOT Structures Research Center in Tallahassee. Tests on the smaller deck sample and on the test specimen after HVS loading were performed at the FDOT Corrosion Research Laboratory in Gainesville.

The bond test equipment used was a PosiTest AT Adhesion Tester. The surface was prepared by drilling a 2” O.D. core to the top of the aluminum surface. The overlay was cleaned with Acetone, roughened with a wire brush, and cleaned with pressurized air. Bond tests were performed in accordance with ASTM C1583.

The first round of tests was conducted on February 10, 2016 on the full size specimen. The weather was cold (40 degrees) and dry. A custom developed quick curing Pilgrim epoxy was used to bond the dollies to the overlay surface. Table 3 shows the bond locations tested and the results. All tests resulted in failure of the epoxy utilized to adhere the test dolly to the wearing surface. The results are inconclusive with respect to the overlay bond strength because, in most cases, the epoxy used to bond the test dolly to the wearing surface failed before the required strength for the overlay was reached.

Table 3: Tabulation of Results for Bond Test 1A

Location Per Plan in Appendix A: Structural Testing Procedure	Bond Strength (psi)	Failure Mode
A-2	268	Epoxy failure within height of epoxy used to bond the test dolly to the wearing surface
H-2	446	Dolly was not seated and jammed (invalid)
A-9	140	Epoxy failure within height of epoxy used to bond the test dolly to the wearing surface
H-9	223	Epoxy failure within height of epoxy used to bond the test dolly to the wearing surface
C-13	182	Epoxy failure within height of epoxy used to bond the test dolly to the wearing surface
E-17	110	Epoxy failure at bond to dolly
F-17	41	Epoxy failure at bond to dolly
G-17	313	Epoxy failure at bond to dolly
F-19	233	Epoxy failure at bond to dolly

The second bond test was performed on February 15, 2016 on the full size specimen. The weather during epoxy bonding of the dolly (on February 12th) to the wearing surface was warm (72 degrees) and dry and the aluminum material was heated for several hours before epoxy bonding. Dural Fast Set Epoxy Gel was used to bond the dollies to the overlay. Table 4 shows the bond locations tested and the results. All test results show failure in the epoxy used to bond the test dolly to the wearing surface, but for test 6, some aggregate was removed. The bond strength for all tests was higher than the 250 psi required by the designer.

Table 4: Tabulation of Results for Bond Test 1B

Location Per Bond Test 1B Plan in Appendix F: Bond Test Location Plan and Photo Inventory	Bond Strength (psi)	Failure Mode
1	464	Epoxy failure within height of epoxy used to bond the test dolly to the wearing surface
2	543	Dolly was not seated and jammed (test result not valid)
3	375	Epoxy failure within height of epoxy used to bond the test dolly to the wearing surface, some divets in dolly
4	376	Epoxy failure within height of epoxy used to bond the test dolly to the wearing surface
5	319	Epoxy failure within height of epoxy used to bond the test dolly to the wearing surface, some debonding from dolly
6	546	Epoxy failure within height of epoxy used to bond the test dolly to the wearing surface, some aggregate removed
7	407	Epoxy failure within height of epoxy used to bond the test dolly to the wearing surface
8	544	Epoxy failure within height of epoxy used to bond the test dolly to the wearing surface

The third bond test was performed on February 23, 2016 on the reduced sample. Weather was not a factor in the test performance as it was conducted within the FDOT Corrosion Research Laboratory. Ten locations were tested. The first five were tested at room temperature. Results were similar to the previous tests, with one location reaching the limit of the tester without breaking. For the remaining five tests, the deck section with dollies affixed was placed in an environmental chamber at 120 F for 2 hours. Tests on the remaining locations were conducted immediately upon removal, recording the psi, temperature, and characteristics of the failures. Failure modes were noticeably different than previously recorded at ambient temperature. Failures occurred at the bond to the aluminum and within the overlay. Failures were more ductile as well.

The results of the laboratory tests are presented in Table 5. Odd numbered locations were tested under laboratory temperature after allowing the epoxy adhesive to cure for about 1.5 hours, while even numbered locations were tested after an additional 2 hours of placement in a heated chamber. The bond strength at Location 9a exceeded the capacity of the tester at lab temperature. Location 9 was retested at elevated temperature since the dolly was still affixed and the results are presented as location 9b. The temperature of each location was measured with an IR thermometer immediately after each test. Figure 55 and Figure

56 show the two extreme failure modes of the bond test. Photos of all bond test locations are included in Appendix F: Bond Test Location Plan and Photo Inventory.

Table 5: Tabulation of Results for Bond Test 1C

Location	Bond Strength (psi)	Failure Mode	Temperature (°F)
1	396	~75% epoxy/dolly, ~25% intra-epoxy	75.5
2	288	~85% overlay/Al, ~15% intra-overlay	114.5
3	232	~75% epoxy/dolly, ~25% intra-epoxy	75.5
4	294	~30% overlay/Al, ~50% overlay fail, ~20% epoxy/dolly	115.5
5	220	~100% epoxy/dolly w/neg. epoxy failure	75.5
6	256	~20% epoxy/dolly, ~80% intra-overlay	114.5
7	542	~90% intra-epoxy w/Agg pull out, ~10% epoxy/dolly	75.0
8	405	~30% epoxy/overlay w/agg pullout, ~70% intra-epoxy	110.5
9a	548	Reached the maximum capacity of tester without breaking	75.5
9b	324	~20% overlay/Al, ~80% intra-overlay	110.5
10	373	~30% intra-epoxy, ~70% intra-overlay	108.5

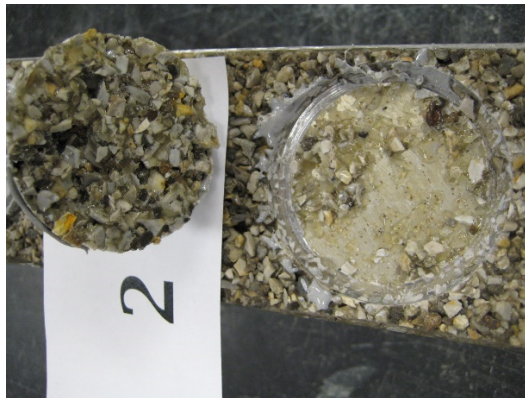


Figure 55: Bond Test 1C, Location 2

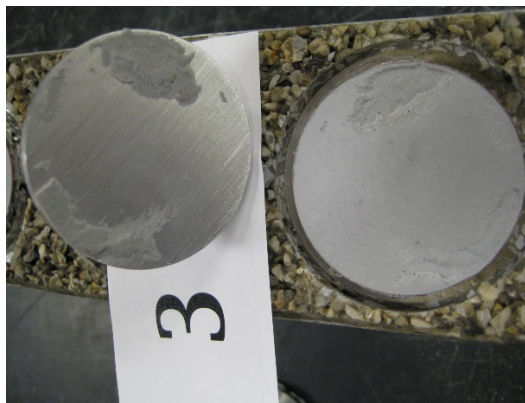


Figure 56: Bond Test 1C, Location 3

The final bond test was conducted on September 30, 2016 on the full size specimen, after heavy vehicle simulation (HVS) testing. Eight locations were tested, with four locations on each panel. Three of the locations tested were within the heavy vehicle simulator tire path. Except where there was significant failure of the bond to the dolly, all the tests were greater than 300 psi, higher than the required 250 psi bond strength.

Table 6: Tabulation of Results for Bond Test 2

Location	Bond Strength (psi)	Failure Mode
1 (Panel A)	264	~85% epoxy-dolly, ~15% intra-epoxy
2 (Panel A)	201	~100% epoxy/dolly
3 (Panel A)	323	~20% epoxy/dolly, ~75% intra-epoxy, ~5% intra-overlay
4 (Panel A)	321	~40-45% epoxy/dolly, ~55-60% intra-epoxy
5 (Panel B)	348	<5% epoxy/dolly, ~60% intra-epoxy, >40% intra-overlay
6 (Panel B)	399	100% intra-overlay
7 (Panel B)	33	~100% epoxy/dolly
8 (Panel B)	436	~5% epoxy/dolly, ~90% intra-epoxy, ~5% intra-overlay

Considering only the results of bond tests 1B and 1C, since the results of test 1A were inconclusive, there were two test locations with a bond strength less than the required 250 psi. Those tests were locations 3 and 5 for test 1C. For both of those tests, the failure mode was within the epoxy used to bond the steel dolly to the overlay or at the bond surface between that epoxy and the steel dolly. Per ASTM C1583, section 11.4, results should be discarded if that failure mode occurs. Therefore, the bond test indicates the wearing surface applied to the lightweight aluminum full size test specimen and smaller sample has an acceptable bond strength of greater than 250 psi.

Bond tests 1A, 1B and 1C were performed prior to HVS testing. Due to the bond test results, the HVS testing was modified to include heated conditions, as discussed in the previous section. Although wear is apparent at the tire path of the HVS, degradation of the bond between the wearing surface and aluminum substrate, which may be apparent as rutting or peeling, was not observed. In addition, the bond strength remained above the required 250 psi strength after HVS testing. Further inspection and observation should be conducted when the test specimen is placed in service. However, test results indicate the bond between the aluminum panel and epoxy overlay will perform well in field conditions.

Friction Testing

Friction testing was performed at the FDOT State Materials Office under the direction of Charles Holzschuher, State Pavement Performance Engineer. Three test methods were used based on ASTM E 1911, ASTM E 2157 and ISO 13473. Measurements collected include the coefficient of friction and the macrotexture Mean Profile Depth (MPD) in a discrete and continuous way. Testing was conducted before the HVS testing, after 300,000 HVS passes and after 600,000 HVS passes.

Results of friction testing show the coefficient of friction dropped about 20% after 600,000 HVS passes, but remains above the developmental specification 403 requirements. After 600,000 HVS passes, the results of both Mean Profile Depth (MPD) measurements show the MPD has dropped about 9% on

average, however the results exceed newer in-service longitudinal diamond grinding (LGD) concrete pavement and longitudinal grind and transverse grooved bridge decks. More detailed information is provided in the test report, in Appendix G: Friction Testing Report.

Discussion

The lightweight aluminum deck panel was subjected to 600,000 passes using the heavy vehicle simulator (HVS) at the FDOT State Materials Office. The thorough testing regimen was to verify the adequacy of the wearing surface before the test specimen is placed in service along with other fatigue and structural parameters. Material testing of the wearing surface shows the wearing surface maintained good bond before and after testing. Although bond strengths are reduced when heat is applied, the strength is above the 250 psi required by the designer. The friction of the wearing surface was also satisfactory after the testing regimen. After the heavy vehicle simulator testing, the friction readings were better than expected for a newly constructed concrete bridge deck.

Verification of structural capacity was not the primary intent of heavy vehicle simulation but the structural readings from the test are interesting. No significant structural degradation occurred during the test. The stress reversal documented during HVS testing was not observed in static testing as the behavior only occurs due to the moving load. The exact fatigue loading pattern cannot be replicated during heavy vehicle simulation testing due to limitations in the testing facility. However, results from HVS and static testing were used together to estimate the weld fatigue life. The result is slightly higher, but within 3% of the constant amplitude fatigue threshold. Therefore, the results found by previously conducted structural testing are confirmed by HVS testing. Dimensional differences for a newly constructed panel and/or support system could increase the strain range and result in a stress range at the weld that is higher than the infinite life fatigue limit.

Corrosion Testing

The potential for corrosion for the test specimen is higher than similar deck systems due to contact between the dissimilar aluminum and steel metals. This section presents the work and conclusions of the FDOT State Materials Office Corrosion Research Laboratory, provided to the authors by Laboratory Specialist Adrian Steele. Experimental work to determine the corrosion life of the lightweight aluminum deck test specimen is ongoing at the time of this report. Preliminary results are presented with more information to follow after publication of this report.

The accelerated corrosion testing plan consists of measuring the current flowing through wires between steel fasteners and a sample of the aluminum extrusion. Refer to Figure 57 and Figure 58. The ends of the extrusion are partially capped and Hollo-Bolt fasteners are suspended in the saltwater filling the chambers without directly contacting the aluminum. The Hollo-Bolts are meant to be used to replace the original fasteners as needed to maintain the structure. No testing was conducted with the original fasteners. Prior to testing, the Hollo-Bolts were disassembled, and the manufacturer's grease was removed mechanically and by solvent. They were re-assembled, and suspended in the saltwater in the extrusion cavities without directly contacting the aluminum. The fasteners were not plastically deformed as they would be if they were torqued to manufacturer's specification. When used as intended, the threaded wedge causes the tangs on the fastener's outer sleeve to bend outward creating some plastic deformation in the aluminum deck as well. The galvanic corrosion circuit was completed via wiring through shunt resistors, measuring current flowing through the wires between the fasteners and the extrusion.

The corrosion test specimens show a dark discoloration of the aluminum surface. The testing indicates the aluminum is slightly anodic with respect to the fasteners (positive current) as an examination of the galvanic series in seawater would concur. That is, the aluminum is presently providing a small measure of cathodic protection to the galvanized fasteners. The oxidation on the fasteners shows there is still some consumption of the zinc. As the zinc is consumed, the corrosion current will likely increase since iron and aluminum are farther apart on the galvanic series. The net current measured to date is shown in Figure 59. It is unlikely the corrosion will be as severe in actual service given the exposure will probably be limited to light salt spray or mist rather than full, long-term immersion.



Figure 57: Aluminum Extrusion Sample

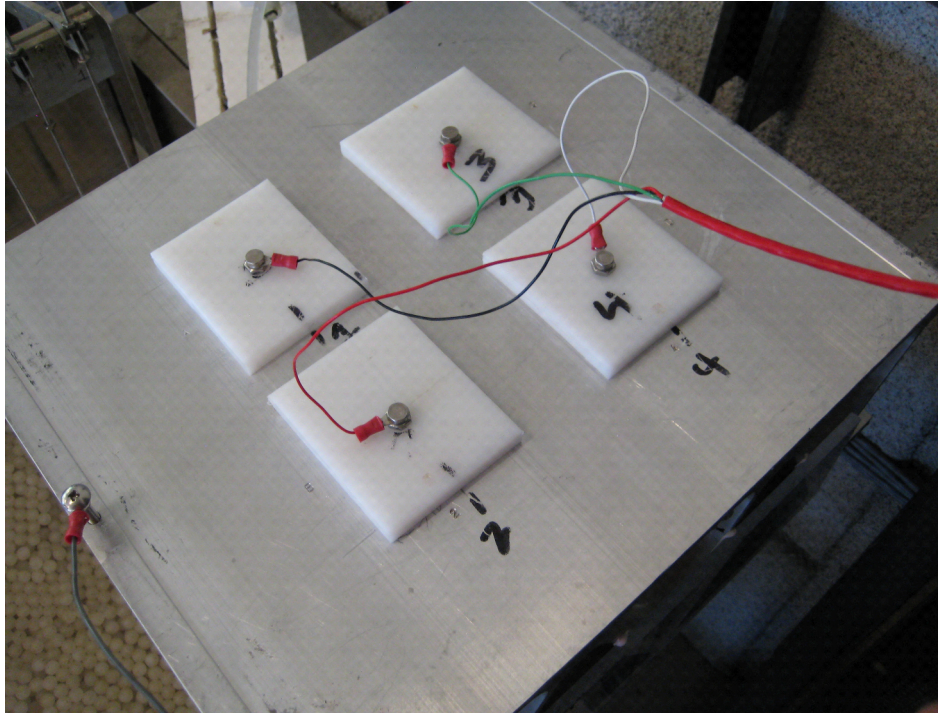


Figure 58: Corrosion Testing Assembly

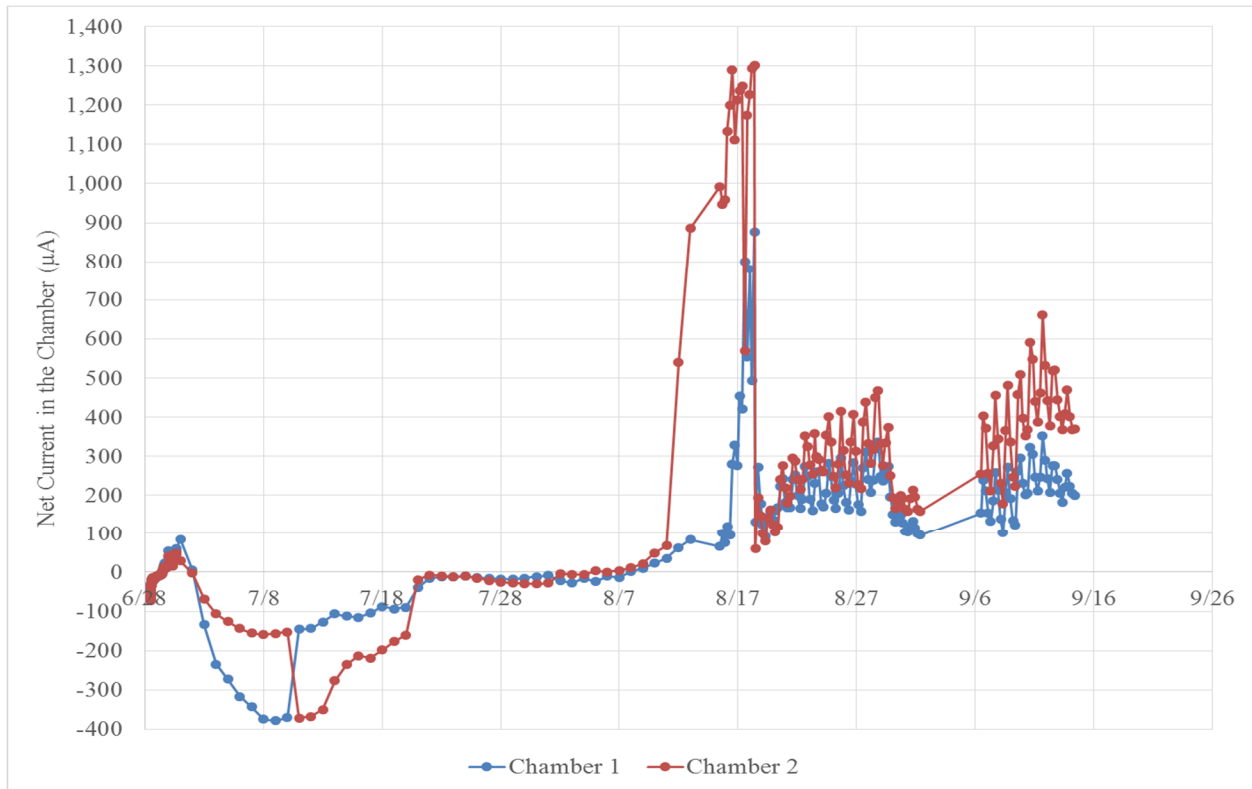


Figure 59: Net Current between Hollo-Bolts and Aluminum Deck

Further testing qualitatively evaluated corrosion of plastically deformed fasteners. Two Hollo-Bolt fasteners were used to attach steel plate coupons to a section of a Generation I deck specimen, as shown in Figure 60. The bolts were torqued to manufacturer's specification. The intent of the test was to qualitatively gauge how severe the corrosion might get as well as look into possible crevice and stress related corrosion effects.



Figure 60: Fastener Used for Corrosion Testing

The black discoloration previously noted in the visual inspection section was inspected due to corrosion concerns. The discoloration appearing in the abrasive blasted faying surface of the deck does not seem to be of serious concern. Examined at 60x magnification, Figure 61, the metal has not been attacked.



Figure 61: Discoloration Photograph, 60x Magnification

Conclusions

The Florida Department of Transportation has completed a comprehensive evaluation of a lightweight aluminum deck panel test specimen, provided by AlumaBridge, LLC. The evaluation included detailed inspection, structural testing, heavy vehicle simulation and wearing surface evaluation. Corrosion testing was included and is still ongoing.

Structurally, the test specimen performed well. The maximum demand to capacity ratio for strain measurements was 0.7. Deflection measurements were very close to the design limit, exceeding the Span/800 limit by less than 1/32". Fatigue is a potential design concern for the panel, as the stress range is predicted to be approximately equal to the constant amplitude fatigue threshold. Generally, infinite life fatigue details are preferred over finite life details. Testing of the panel indicates the weld between aluminum extrusions has a stress range below the infinite life limit based on the strain range measured in the panel. If the geometry of the panel or support system is changed for future projects, designers should ensure the stress range remains acceptable for the fatigue detail. To better understand fatigue resistance of friction stir welding associated with the planned joint types, a further fatigue studies could be performed.

The wearing surface proved to be an effective friction surface after rigorous testing. It is expected to perform well in-service, although frequent inspections during the trial period are appropriate since this deck system is a new technology. Corrosion continues to be a concern for this deck system due to the dissimilar metals used. Corrosion testing is ongoing, but the limited results are not an impediment to in-service trial of this deck system and the inorganic zinc coating on the steel stringers appears to be effective at limiting galvanic corrosion. Field inspections and corrosion testing conclusions will determine the service life which can be expected from this deck system. Proper controls need to be set up for fabrication and construction to ensure the aluminum panels do not have contact with dissimilar metals. Corrosion that occurs during the fabrication process and prior to placement on a bridge could limit the potential service life and should be avoided.

One key difference between the aluminum lightweight deck and open grid steel deck systems is the aluminum lightweight deck provides a solid driving surface. The solid surface is preferred because it protects the main structural system of the bascule bridge. However, solid deck systems will affect the way water drains from the bridge and may increase wind load on foundations of bascule bridges. Both of those design considerations need to be addressed before any solid surface deck is used to replace an open grid deck. If a complete deck replacement is planned, these design considerations can be addressed on a case-by-case basis for each bridge considered for deck replacement.

Thorough testing and evaluation of the AlumaBridge, LLC lightweight deck panel system conducted by the Florida Department of Transportation has been completed. Results from testing show the test specimen can safely be placed in service for a trial period for further evaluation. The research results show the aluminum deck panel design is controlled primarily by fatigue, although deflection is also close to recommended limits. Corrosion is a concern due to dissimilar metallic reactions. Further work will determine how the potential corrosion problem affects service life of the panel.

Bibliography

- [1] A. Mirmiran, K. Mackie, M. A. Saleem and J. Xia, "Alternatives to Steel Grid Decks," Florida Department of Transportation, 2009.
- [2] A. Mirmiran, K. Mackie, M. A. Saleem, J. Xia, P. Zohrevand and Y. Xiao, "Alternatives to Steel Grid Decks - Phase II," Florida Department of Transportation, 2012.
- [3] URS Corporation, Inc., "Bascule Bridge Lightweight Solid Deck Retrofit Research Project Deck Alternative Screening Report," 2015.
- [4] Hardesty & Hanover, LLC, "Bascule Bridge Lightweight Solid Deck Retrofit Research Project Aluminum Orthotropic Deck Research Program Notes," 2015.
- [5] Portland Bolt & Manufacturing Company, Inc., "Bolt Torque Chart," [Online]. Available: <http://www.portlandbolt.com/technical/bolt-torque-chart/>. [Accessed 11 November 2016].
- [6] SC Fastening Systems, LLC, "Torque ASTM A325," [Online]. Available: http://scfastening.com/wp-content/uploads/2015/02/Torque_A325.pdf. [Accessed 11 November 2016].
- [7] AASHTO, LRFD Bridge Design Specifications, Seventh Edition, Washington, DC: AASHTO, 2014 with 2015 Interims.
- [8] A. Miranda, A. P. Gerlich and S. Walbridge, "Aluminum Friction Stir Welds: Review of Fatigue Parameter Data and Probabilistic Fracture Mechanics Analysis," *Engineering Fracture Mechanics*, vol. 147, no. October 2015, pp. 243-260, 2015.
- [9] Florida Department of Transportation, FDOT Structures Manual, 2016.

Appendix A: Structural Testing Procedure

Load Test Procedure

For Static and Cyclic Tests of Full-Scale Lightweight Aluminum Deck Panel Test Specimen

Objectives

1. Verify Generation I and II Aluminum deck panels can support Truck and Tandem design loads.
2. Apply cyclic loading to Generation II Aluminum deck panel and measure fatigue indicators.
3. Verify results from FEA.

Gage Count

Item	Quantity
Deflection Gage	20
Rosette Bi-Axial 5mm Gage	92

Instrumentation

Instrumentation consists of bi-axial strain gages and deflection gages. When placed on the top and bottom surface of the deck panel, the strain gages measure strain in the aluminum deck panel in the longitudinal and transverse directions. When placed on the face of the deck panel (lines 1 and 20), they measure strain in the transverse and vertical directions. The deflection gages measure deflection of either the deck panel or steel beam, depending on placement.

Load Tests

- Test 1: Generation 2 Panel, Truck Positive Moment Proof Load
 - A. Service II Load Level
 - B. Strength I Load Level
 - C. Strength II Load Level
- Test 2: Generation 2 Panel, Tandem Positive Moment Proof Load
 - A. Service II Load Level
 - B. Strength I Load Level
- Test 3: Generation 2 Panel, Truck Negative Moment Proof Load
 - A. Service II Load Level
 - B. Strength I Load Level
 - C. Strength II Load Level
- Test 4: Generation 2 Panel, Truck Negative Moment Proof Load (Bearing Pad)
 - A. Service II Load Level
 - B. Strength I Load Level
 - C. Strength II Load Level
- Test 5: Generation 2 Panel, Tandem Negative Moment Proof Load
 - A. Service II Load Level
 - B. Strength I Load Level
- Test 6: Generation 2 Panel, Tandem Negative Moment Proof Load (Bearing Pad)
 - A. Service II Load Level
 - B. Strength I Load Level
- Test 7: Fatigue Truck Cyclic Load (Bearing Pad)
 - A. Fatigue I Load Level
- Test 8: Generation 1 Panel, Tandem Negative Moment Proof Load (Bearing Pad)
 - A. Service II Load Level
 - B. Strength I Load Level
- Test 9: Generation 1 Panel, Truck Negative Moment Proof Load (Bearing Pad)
 - A. Service II Load Level
 - B. Strength I Load Level
 - C. Strength II Load Level

Loading

The table below shows a summary of loading. Refer to Appendix B (Fabrication and Loading Plans) for more details.

Test	Cyclic/Static	# of Load Application Points	Load at Each Point (kip)	Total Actuator Load (kip)	
1	A	Static	1	33.2	33.2
	B			44.69	44.69
	C			57.46	57.46
2	A	Static	2 (longitudinal)	25.94	51.88
	B			34.91	69.82
3	A	Static	2 (transverse)	33.2	66.4
	B			44.69	89.38
	C			57.46	114.92
4	A	Static	2 (transverse)	33.2	66.4
	B			44.69	89.38
	C			57.46	114.92
5	A	Static	4	25.94	103.76
	B			34.91	139.64
6	A	Static	4	25.94	103.76
	B			34.91	139.64
7	A	Cyclic	4	1.25 to 15.05	5 to 60.2
8	A	Static	4	25.94	103.76
	B			34.91	139.64
9	A	Static	2 (transverse)	33.2	66.4
	B			44.69	89.38
	C			57.46	114.92

Gage Identification

The gage name designation is Location/Type (T for Top Rosette, B for Bottom Rosette, or D for Deflection), Transverse Location (Alphabetical Mark), Longitudinal Location (Numerical Mark). So, gage T_F11 is a rosette located on the top of the panel, at transverse grid location F and longitudinal grid location 11. Designation 'D' deflection gages located at lines 'C' and 'J' and the gages located at F1 and F20 are attached to the bottom of the panel. Designation 'D' deflection gages located at line 'F' (except F1 and F20) are attached to the bottom of the steel beam. Gage Z is a deflection gage located on the actuator head.

An 'X' in the table below indicates that the gage is hooked up for the indicated test.

Gage Name	Tests 1-2	Tests 3-7	Tests 8-9
Z	X	X	X
T_A1	X		
B_A1	X		
T_B1	X		
B_B1	X		
T_C1	X	X	
B_C1	X	X	
D_C1	X	X	X
T_D1	X	X	
B_D1	X	X	
T_E1	X	X	
B_E1	X	X	
T_F1		X	
B_F1		X	
D_F1	X	X	X
T_G1		X	
B_G1		X	
T_H1		X	
B_H1		X	
T_J1		X	
B_J1		X	
D_J1	X	X	X
T_A2	X		
B_A2	X		
T_B2	X		
B_B2	X		
B_C2	X	X	
T_D2	X	X	
B_D2	X	X	
T_E2	X	X	
B_E2	X	X	
T_F2		X	
T_G2		X	
B_G2		X	

T_H2		X	
B_H2		X	
B_J2		X	
T_C3	X		
B_C3	X		
T_F3		X	
T_C4	X		
B_C4	X		
T_F4		X	
T_C5	X		
B_C5	X		
T_F5		X	
T_C6	X		
B_C6	X		
T_F6		X	
T_C7	X		
T_F7		X	
B_C8	X		
T_A9	X		
T_B9	X		
D_C9	X	X	X
T_D9	X	X	
T_E9	X	X	
T_F9		X	
D_F9	X	X	X
T_G9		X	
T_H9		X	
D_J9	X	X	X
B_A10	X		
B_B10	X		
B_C10	X	X	
B_D10	X	X	
B_E10	X	X	
B_G10		X	
B_H10		X	
B_J10		X	
T_C11	X		
T_F11		X	
B_C12	X		
T_C13	X		
T_F13		X	
D_C14	X	X	X
D_F14	X	X	X
D_J14	X	X	X
D_C15	X	X	X
D_J15	X	X	X

B_G16			X
B_H16			X
B_C16			X
D_C16	X	X	X
B_D16			X
B_E16			X
B_J16			X
D_J16	X	X	X
T_E17			X
T_F17			X
T_G17			X
B_G18			X
B_H18			X
B_C18			X
B_D18			X
B_E18			X
B_J18			X
T_F19			X
T_C20			X
B_C20			X
D_C20	X	X	X
T_F20			X
B_F20			X
D_F20	X	X	X
T_J20			X
B_J20			X
D_J20	X	X	X

Test Procedure

1. Test Preparation (order of these steps is not important):
 - a. Pour grout pads and install W14 support beams level. Place test specimen per plan for test 1.
 - b. Inspect weld gap using feeler gages and record opening sizes.
 - c. Remove wearing surface at indicated locations. Perform Bond Test 1 on wearing surface per location indicated on Instrumentation Plan.
 - d. Locate gages.
 - e. Visually inspect welds.
2. Instrumentation:
 - a. Install rosette and deflection gages per instrumentation plan.
 - b. Hook up gages for tests 1-2.
3. Prepare for and perform tests 1 and 2. Stop at each load level increment (A, B, C) and record gage readings.
4. Hook up gages for tests 3-7.
5. Prepare for and perform tests 3 thru 7. Stop at each load level increment (A, B, C) and record gage readings.
6. Hook up gages for tests 8-9.
7. Prepare for and perform tests 8 and 9. Stop at each load level increment (A, B, C) and record gage readings.
8. Intermediate Testing Evaluation:
 - a. Inspect weld gap using feeler gages and record opening sizes.
 - b. Visually inspect wearing surface.
 - c. Visually inspect welds.
9. Transport specimen to State Materials Office for Heavy Vehicle Simulation Testing. See separate test procedure and details.
10. Post Testing Evaluation:
 - a. Inspect weld gap using feeler gages and record opening sizes.
 - b. Perform Bond Test 2 on wearing surface per location indicated.
 - c. Visually inspect welds.

Material Strengths

The Research Program Notes provided to FDOT by Hardesty & Hanover note that the Aluminum material is ASTM B221 Alloy 6063-T6. Table 7.4.1-1 in the AASHTO LRFD Bridge Design Specifications 7th Edition (2014) notes the following properties for Aluminum extrusions:

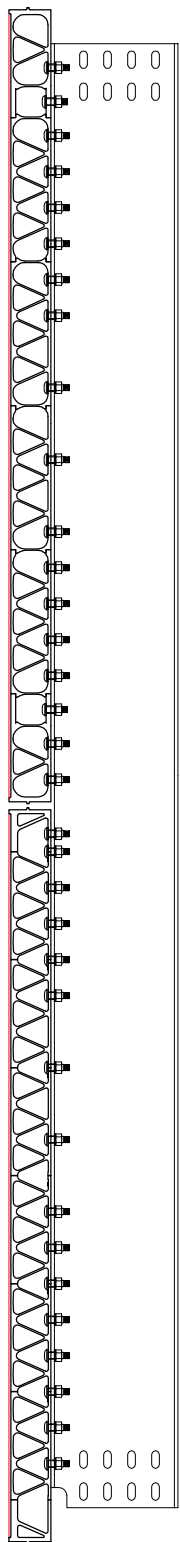
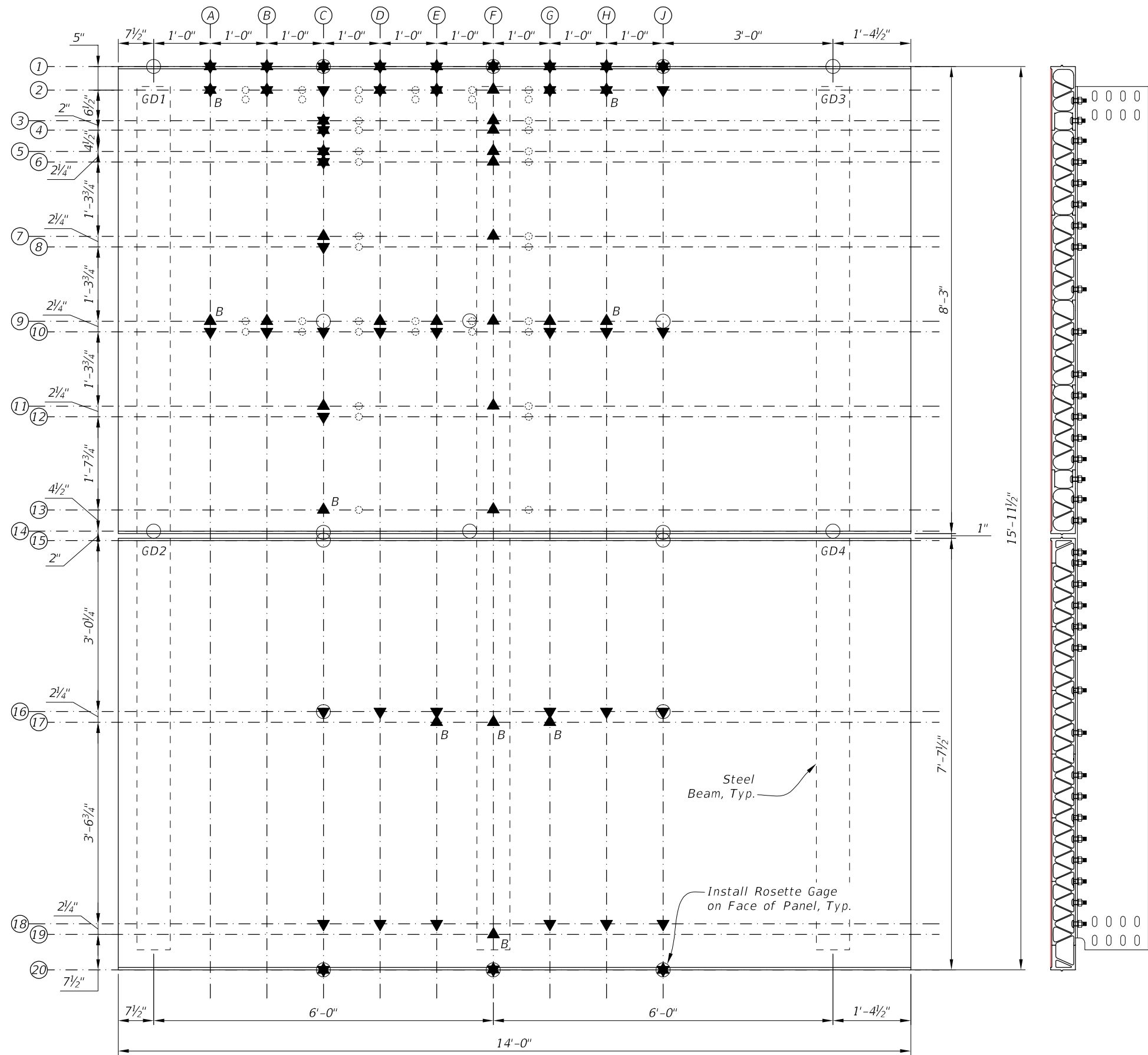
ASTM Specification	B221
Alloy-Temper	6063-T6
Thickness t (in)	All
Ftu (ksi)	30
Fty (ksi)	25
Ftuw (ksi)	17
Ftyw (ksi)	8
Unwelded Ct	189
Welded Ct	715

Table 7.4.1-3 (AASHTO LRFD) notes the following Aluminum Properties:

Modulus of elasticity	E	10,100 ksi
Shear modulus of elasticity	G	3800 ksi
Poisson's ratio	v	0.33
Thermal coefficient of expansion	α	13 x 10 ⁻⁶ in./in./°F
Compressive yield strength for unwelded tempers beginning with H	Fcy	0.9Fty
Compressive yield strength for all other material	Fcy	Fty
Shear yield strength	Fsy	0.6Fty
Shear ultimate strength	Fsu	0.6Ftu

The stringer beam which the aluminum deck panels are attached to was specified as a W16x50 beam. Per the AISC Steel Construction Manual, 13th edition, the common ASTM designation for a W shape is A992, which has a minimum yield strength (Fy) of 50 ksi and an ultimate tensile strength (Fu) of 65 ksi.

Appendix A: Instrumentation Plan



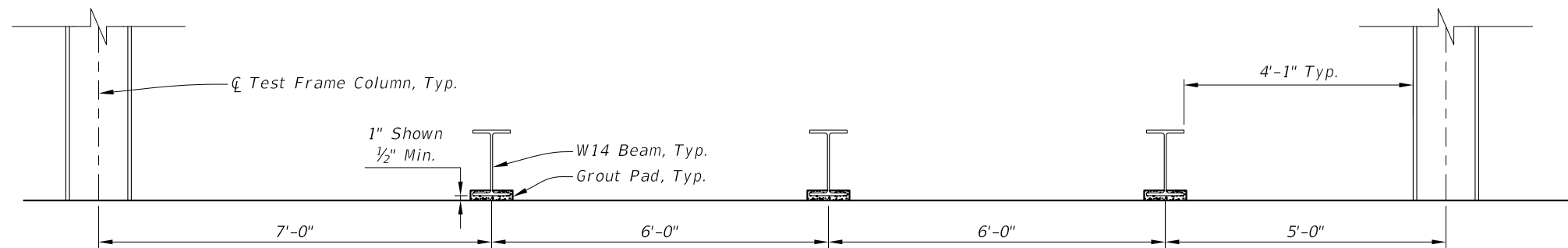
LEGEND

- ★ denotes Strain Gauge location on Top & Bott. of Panel
- ▲ denotes Strain Gauge location on Top of Panel
- ▼ denotes Strain Gauge location on Bott. of Panel
- denotes 1" Dia. Omitted Wearing Surface Improperly Located
- denotes Deflection Gauge location on Bottom of Panel or Beam
- B denotes Bond Test 1 location on Top of Panel

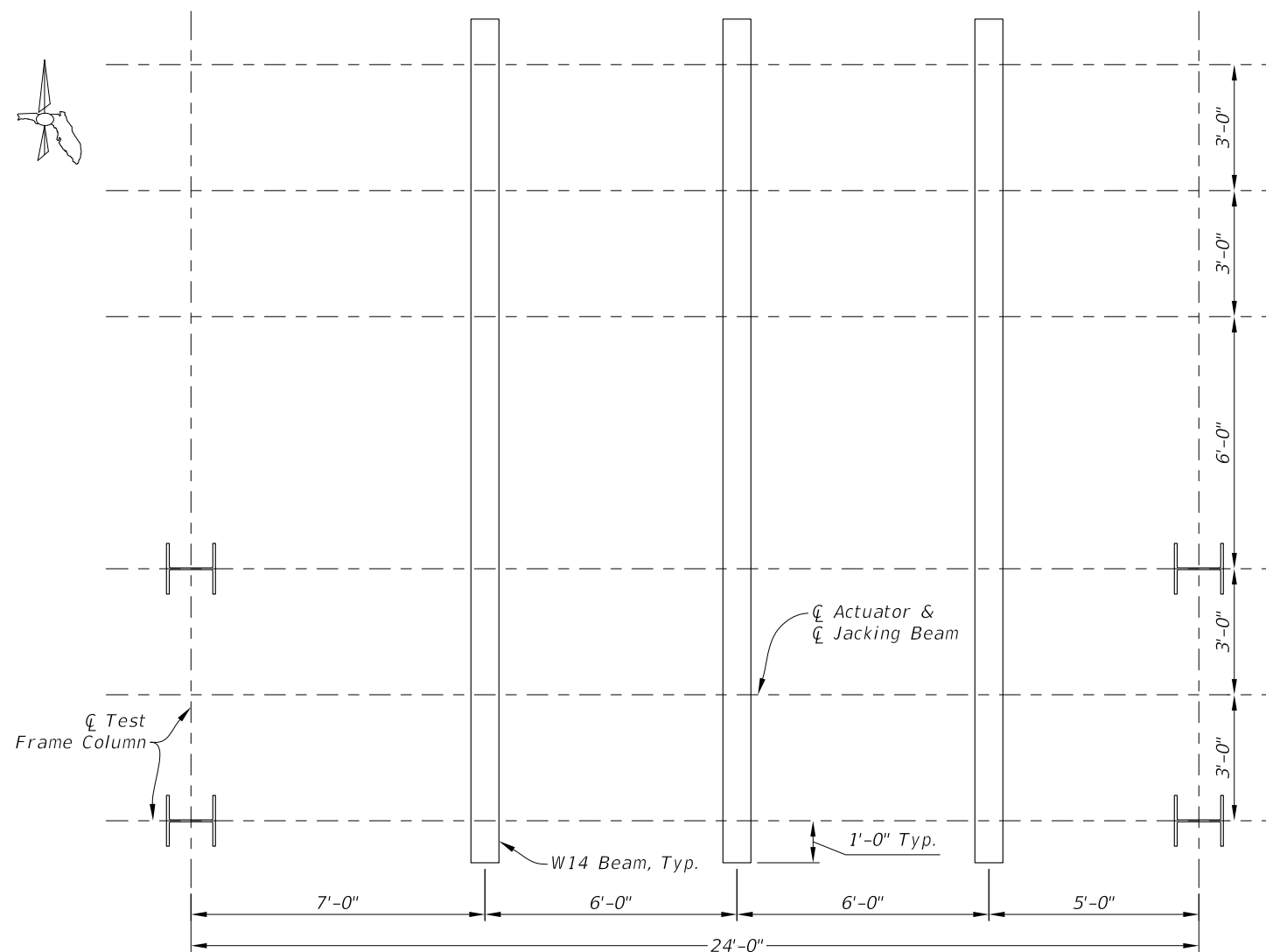
PLAN

REVISIONS						DRAWN BY: CJF 12-15	STATE OF FLORIDA DEPARTMENT OF TRANSPORTATION			SHEET TITLE: Instrumentation Plan - Overall	REF. DWG. NO.
DATE	BY	DESCRIPTION	DATE	BY	DESCRIPTION		ROAD NO.	COUNTY	FINANCIAL PROJECT ID.		
							RD #	COUNTY	FPID #	Lightweight Aluminum Deck Testing	D-1

Appendix B: Fabrication and Loading Plans

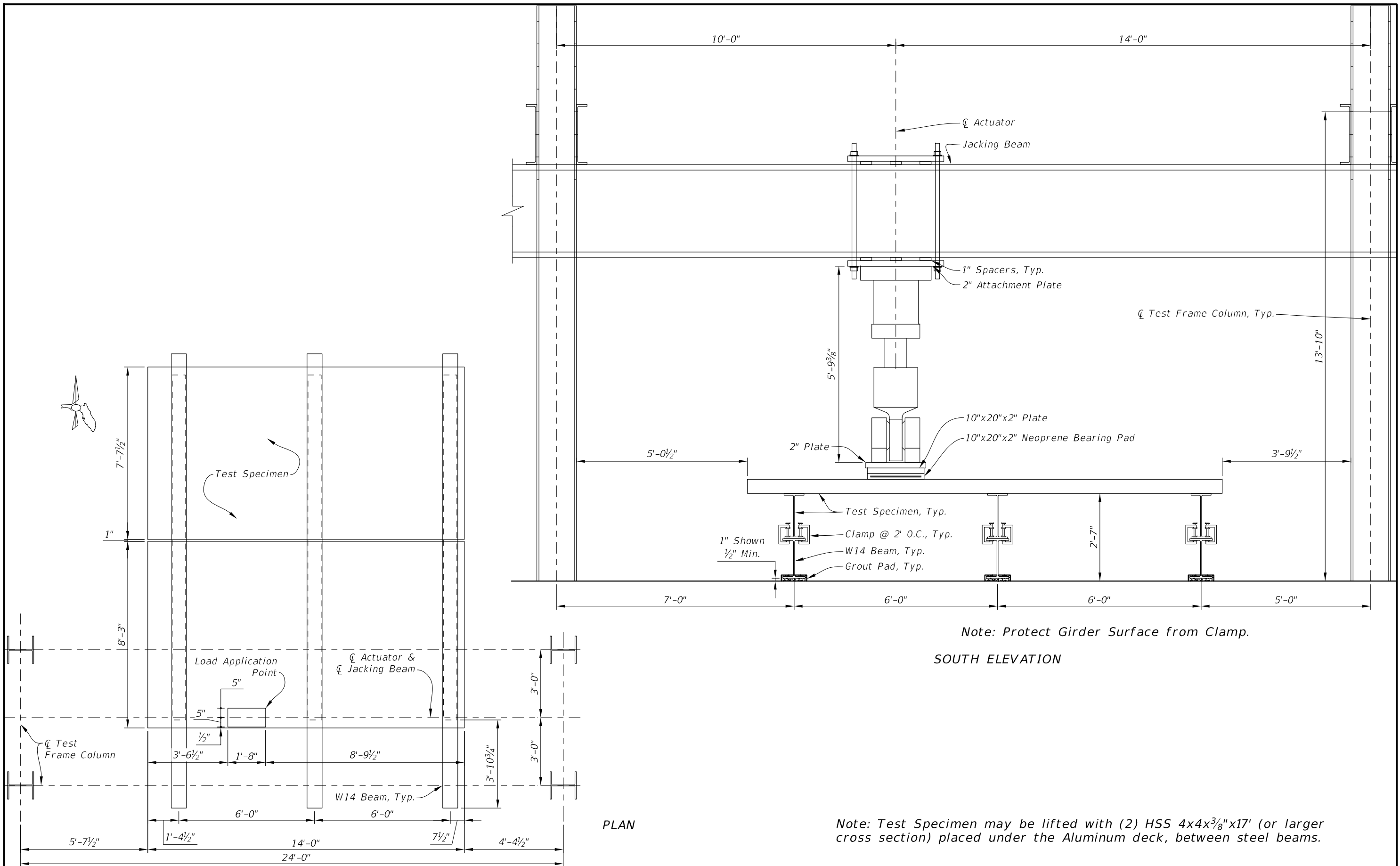


SOUTH ELEVATION



PLAN

REVISIONS						DRAWN BY: CJF 12-15	STATE OF FLORIDA DEPARTMENT OF TRANSPORTATION			SHEET TITLE: Support Fabrication	REF. DWG. NO.
DATE	BY	DESCRIPTION	DATE	BY	DESCRIPTION		ROAD NO.	COUNTY	FINANCIAL PROJECT ID.		
----	----	----	----	----	----	??			PROJECT NAME:		
----	----	----	----	----	----	DESIGNED BY: CJF 12-15	RD #	COUNTY	FPID #	Lightweight Aluminum Deck Testing	SHEET NO.
----	----	----	----	----	----	CHECKED BY: ??					1

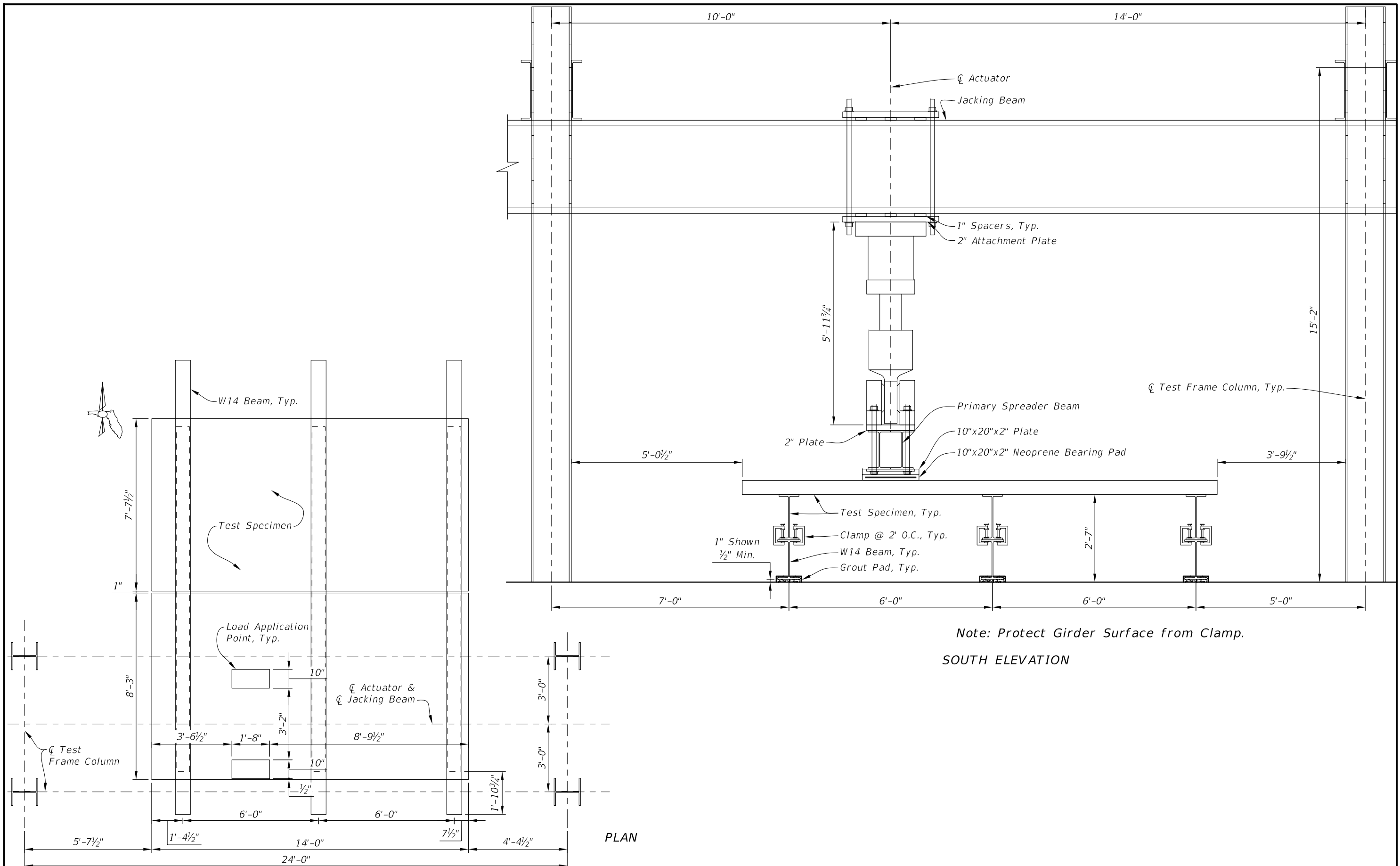


Note: Protect Girder Surface from Clamp.
SOUTH ELEVATION

Note: Test Specimen may be lifted with (2) HSS 4x4x3/8"x17' (or larger cross section) placed under the Aluminum deck, between steel beams.

REVISIONS					
DATE	BY	DESCRIPTION	DATE	BY	DESCRIPTION

DRAWN BY: CJF 12-15			STATE OF FLORIDA DEPARTMENT OF TRANSPORTATION			SHEET TITLE: Test 1: Generation 2 Panel, Truck M+ Proof Load		REF. DWG. NO.
CHECKED BY: ??						PROJECT NAME: Lightweight Aluminum Deck Testing		SHEET NO. 2
DESIGNED BY: CJF 12-15			ROAD NO.	COUNTY	FINANCIAL PROJECT ID.	PROJECT NAME:		
CHECKED BY: ??			RD #	COUNTY	FPID #	PROJECT NAME:		



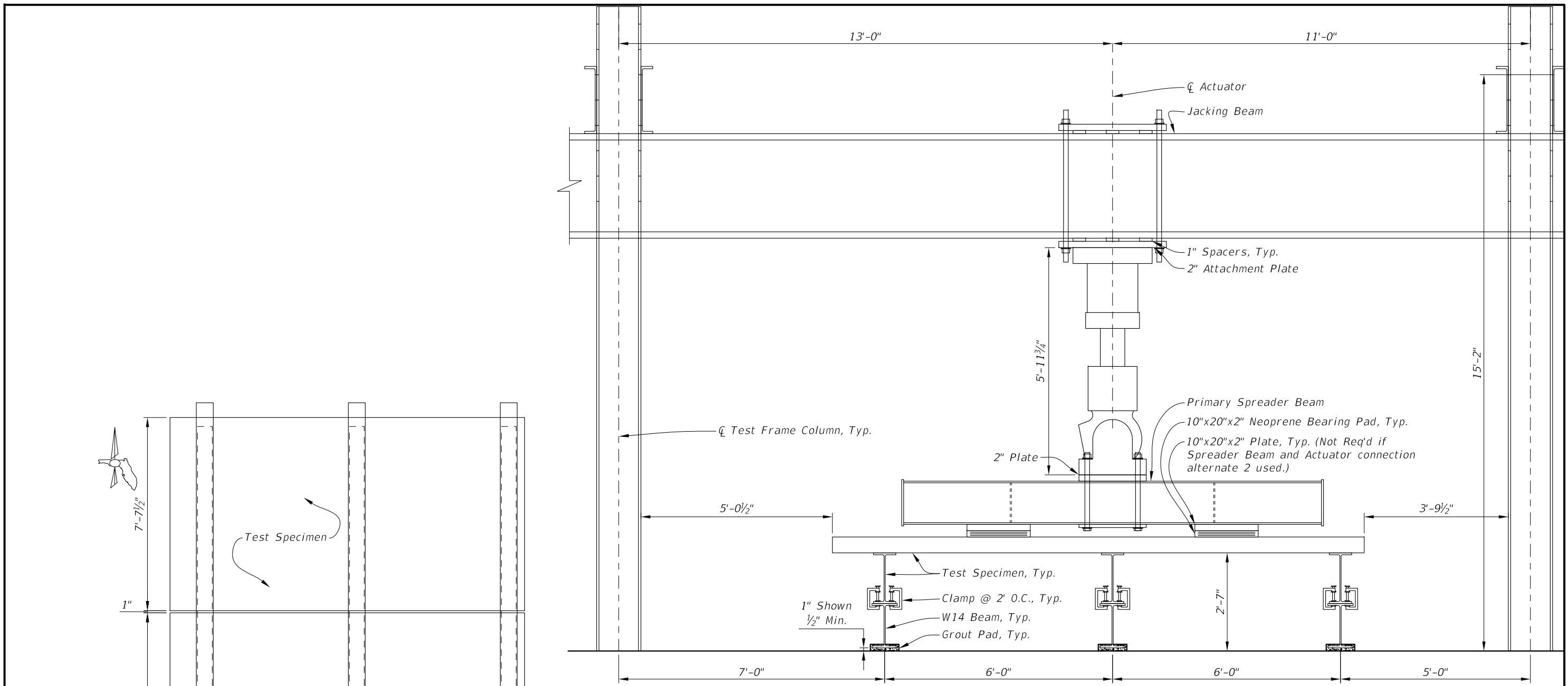
Note: Protect Girder Surface from Clamp.
SOUTH ELEVATION

PLAN

REVISIONS					
DATE	BY	DESCRIPTION	DATE	BY	DESCRIPTION

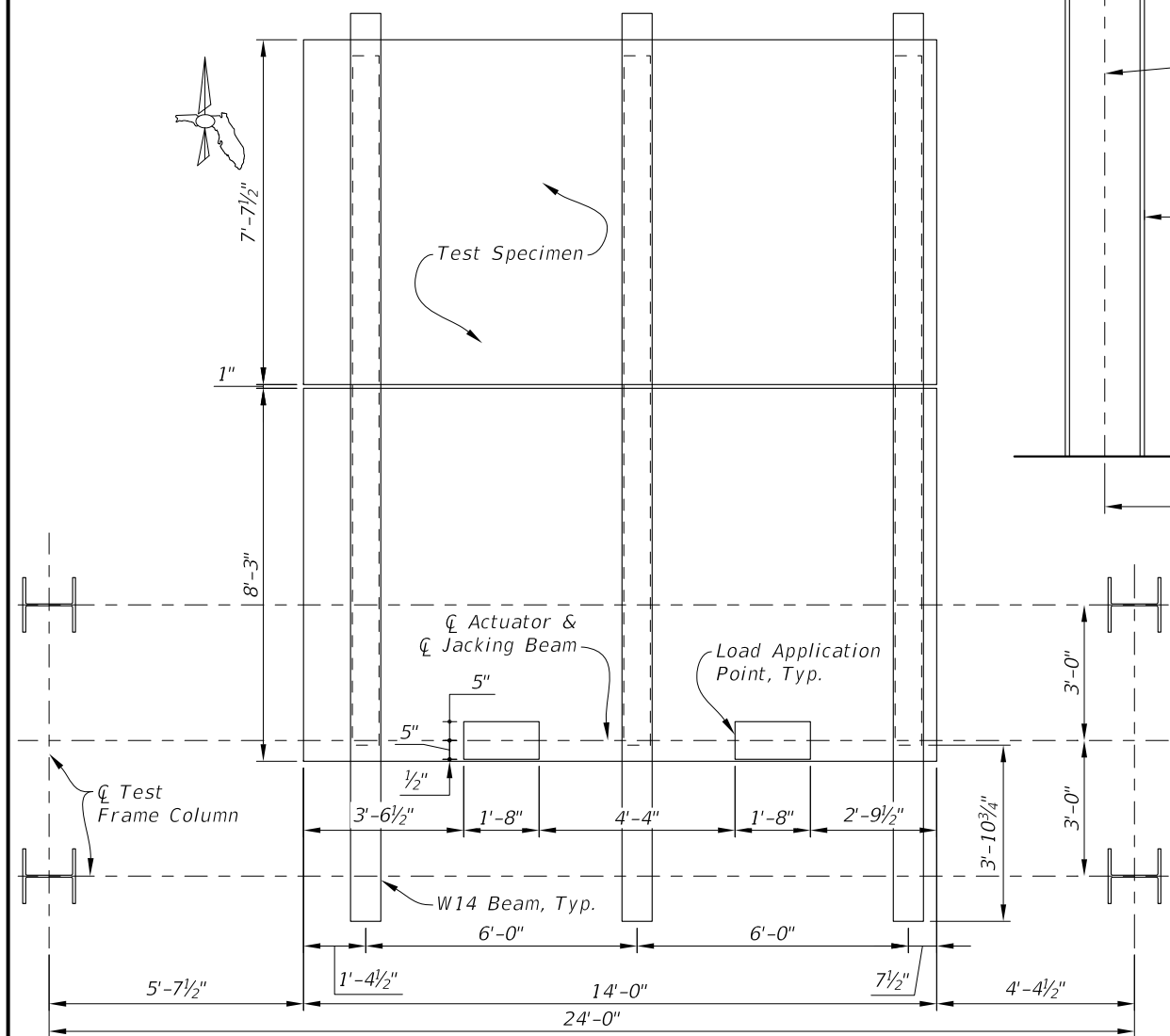
DRAWN BY: CJF 12-15 CHECKED BY: ?? DESIGNED BY: CJF 12-15 CHECKED BY: ??	STATE OF FLORIDA DEPARTMENT OF TRANSPORTATION	SHEET TITLE: Test 2: Generation 2 Panel, Tandem M+ Proof Load	REF. DWG. NO.
ROAD NO. RD #	COUNTY	FINANCIAL PROJECT ID. FPID #	PROJECT NAME: Lightweight Aluminum Deck Testing
SHEET NO.			3

DRAWN BY: CJF 12-15 CHECKED BY: ?? DESIGNED BY: CJF 12-15 CHECKED BY: ??	STATE OF FLORIDA DEPARTMENT OF TRANSPORTATION	SHEET TITLE: Test 2: Generation 2 Panel, Tandem M+ Proof Load	REF. DWG. NO.
ROAD NO. RD #	COUNTY	FINANCIAL PROJECT ID. FPID #	PROJECT NAME: Lightweight Aluminum Deck Testing
SHEET NO.			3



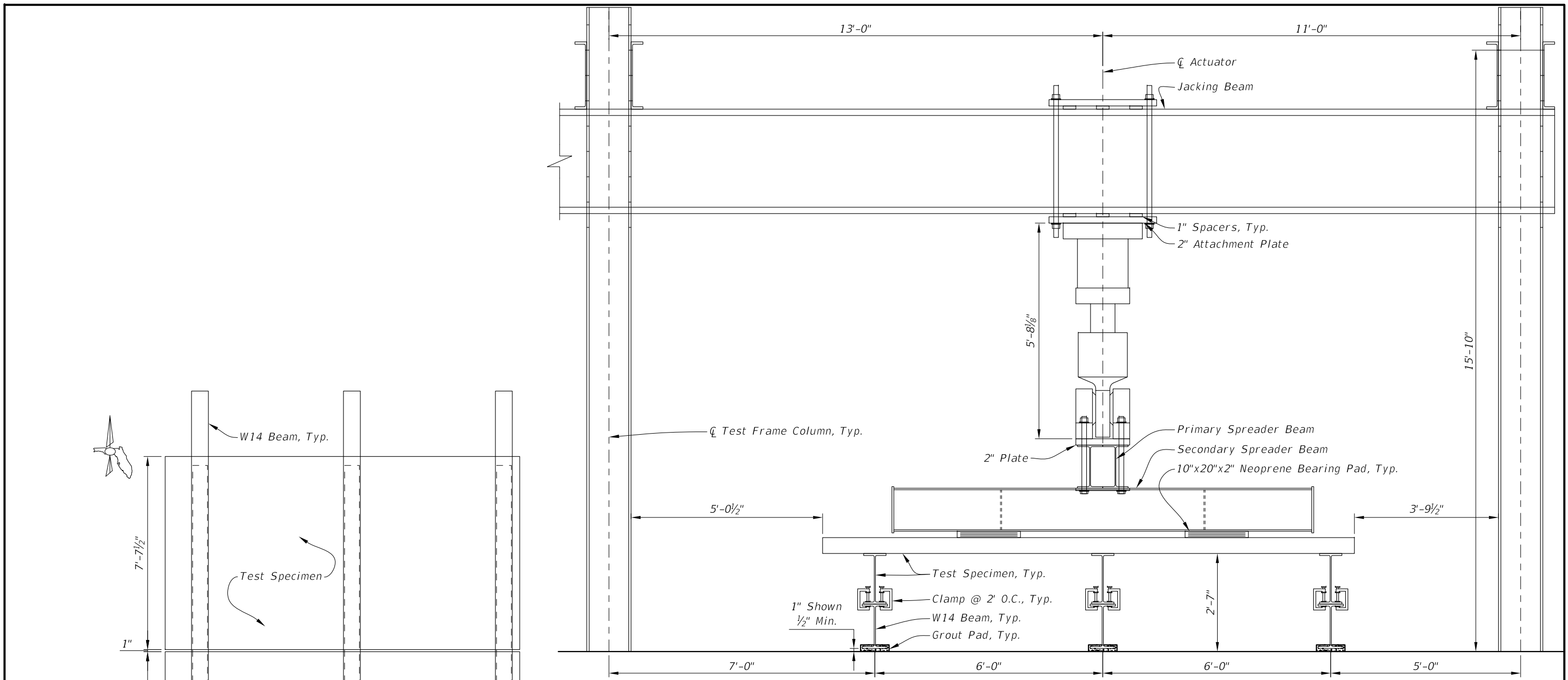
Note: Protect Girder Surface from Clamp.

SOUTH ELEVATION



PLAN

REVISIONS						DRAWN BY: CJF 12-15	STATE OF FLORIDA DEPARTMENT OF TRANSPORTATION			SHEET TITLE: Test 3: Generation 2 Panel, Truck M- Proof Load	REF. DWG. NO.
DATE	BY	DESCRIPTION	DATE	BY	DESCRIPTION		ROAD NO.	COUNTY	FINANCIAL PROJECT ID.		
						DESIGNED BY: CJF 12-15	RD #	COUNTY	FPID #	PROJECT NAME: Lightweight Aluminum Deck Testing	SHEET NO. 4
						CHECKED BY: ??					



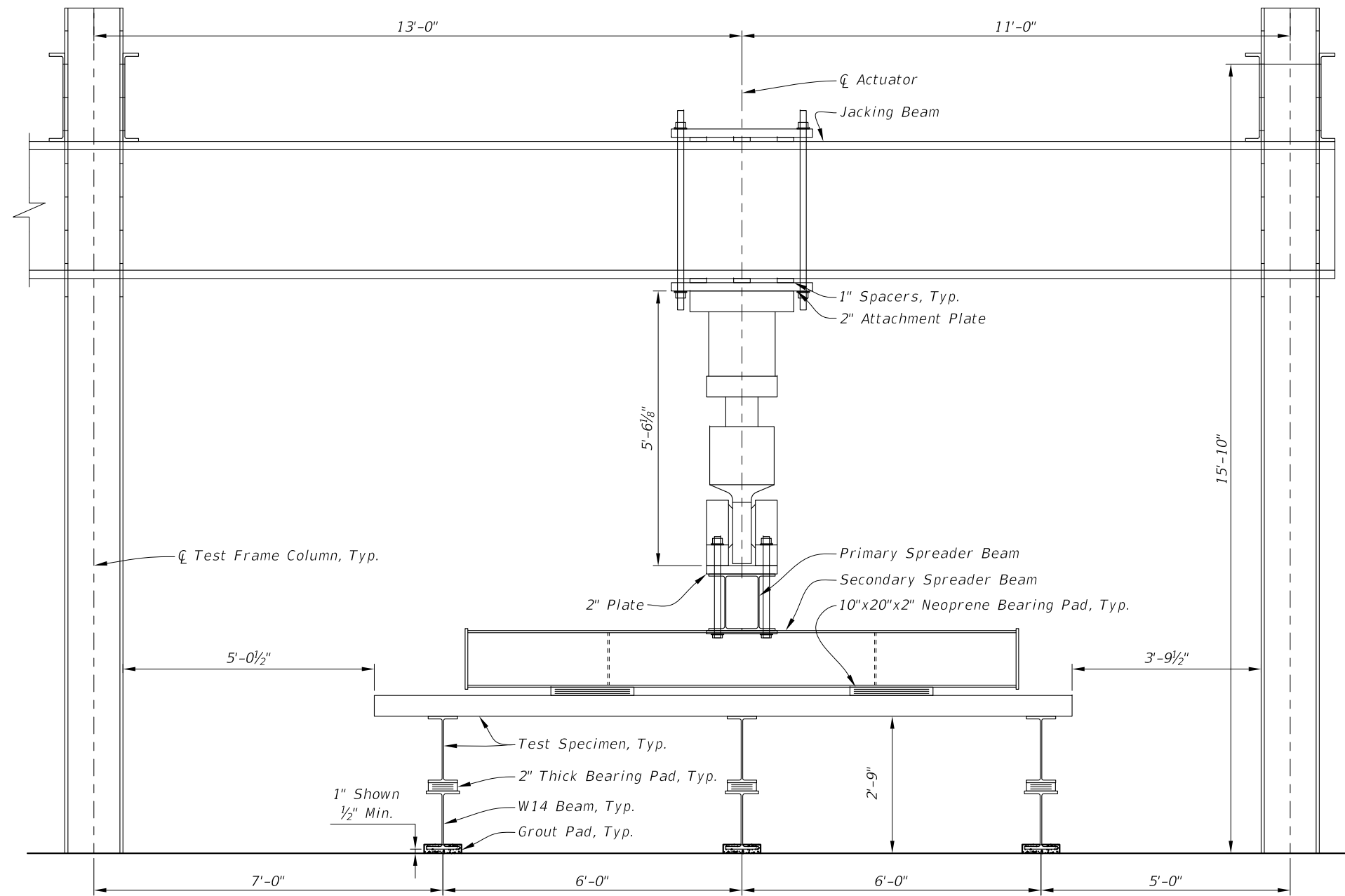
Note: Protect Girder Surface from Clamp.

SOUTH ELEVATION

PLAN

REVISIONS					
DATE	BY	DESCRIPTION	DATE	BY	DESCRIPTION

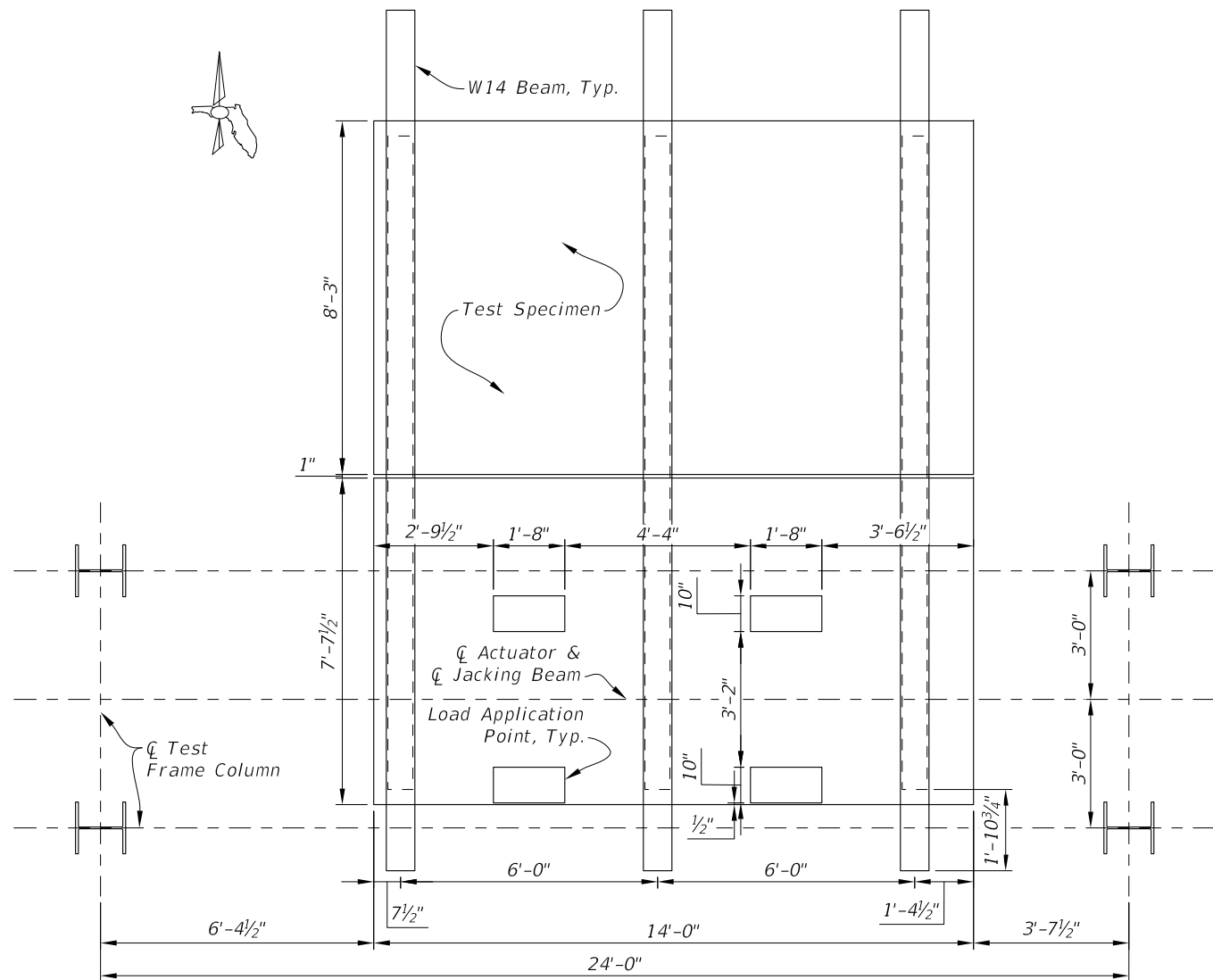
DRAWN BY: CJF 12-15 CHECKED BY: ?? DESIGNED BY: CJF 12-15 CHECKED BY: ??	STATE OF FLORIDA DEPARTMENT OF TRANSPORTATION			SHEET TITLE: <i>Test 5: Generation 2 Panel, Tandem M- Proof Load</i>	REF. DWG. NO.
ROAD NO. RD #	COUNTY	FINANCIAL PROJECT ID. FPID #	PROJECT NAME: <i>Lightweight Aluminum Deck Testing</i>	SHEET NO.	6



SOUTH ELEVATION

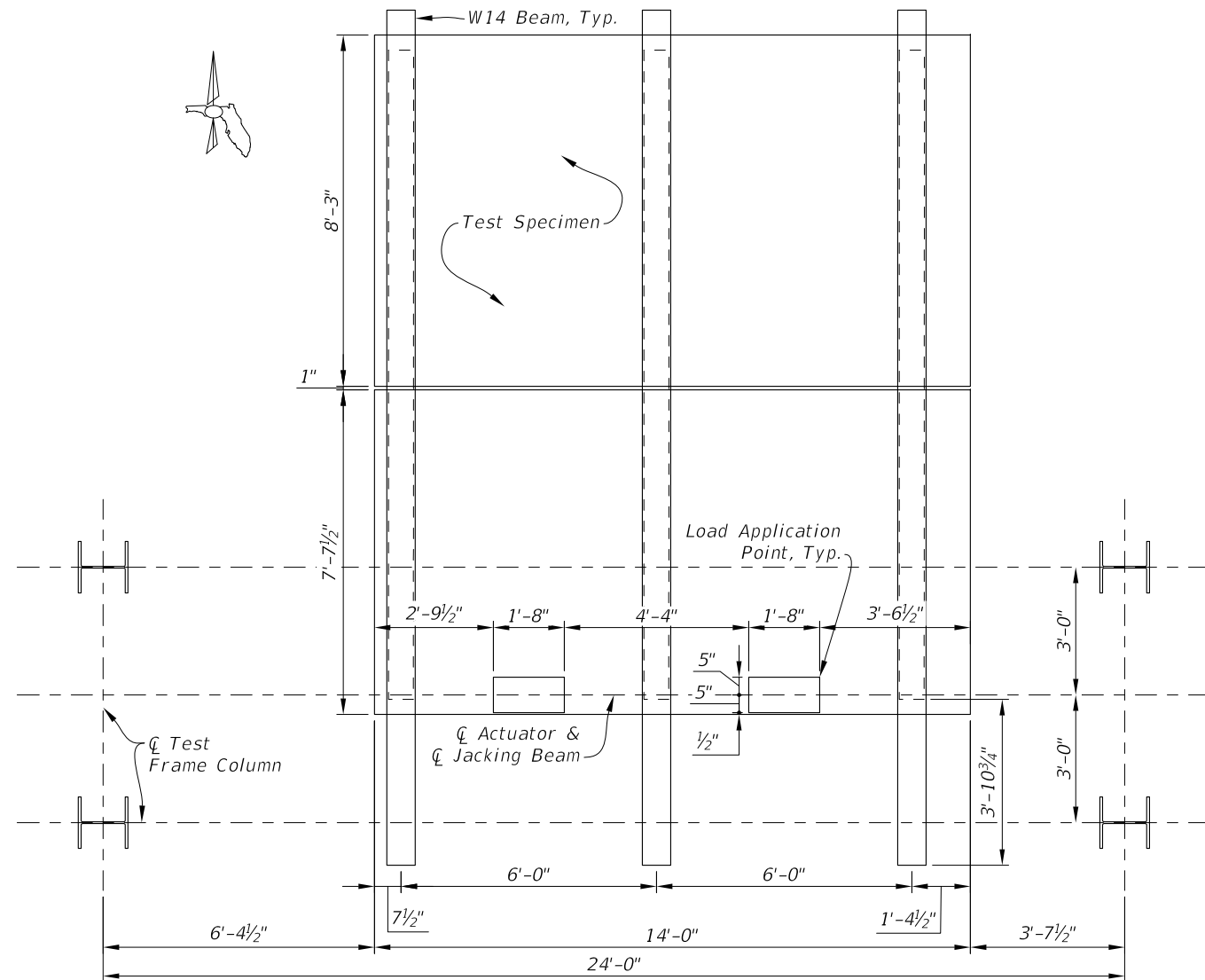
NOTE: See Test 5 for Plan view.

REVISIONS						DRAWN BY: CJF 12-15 CHECKED BY: ?? DESIGNED BY: CJF 12-15 CHECKED BY: ??	STATE OF FLORIDA DEPARTMENT OF TRANSPORTATION			SHEET TITLE: Test 6: Generation 2 Panel, Tandem M- Proof Load (Bearing Pad) and Test 7: Fatigue Truck Cyclic Load	REF. DWG. NO.
DATE	BY	DESCRIPTION	DATE	BY	DESCRIPTION		ROAD NO.	COUNTY	FINANCIAL PROJECT ID.		
							RD #	COUNTY	FPID #	PROJECT NAME: Lightweight Aluminum Deck Testing	SHEET NO. 7



PLAN: TEST 8

NOTE: See Test 6 for similar Elevation view.



PLAN: TEST 9

NOTE: See Test 4 for similar Elevation view.

REVISIONS						DRAWN BY: CJF 12-15	STATE OF FLORIDA DEPARTMENT OF TRANSPORTATION			SHEET TITLE: Generation 1 Panel, Test 8: Tandem Proof Load and Test 9: Truck Proof Load	REF. DWG. NO.
DATE	BY	DESCRIPTION	DATE	BY	DESCRIPTION		ROAD NO.	COUNTY	FINANCIAL PROJECT ID.		
---	---	---	---	---	---	RD #	COUNTY	FPID #	Lightweight Aluminum Deck Testing	SHEET NO.	
---	---	---	---	---	---					8	

Appendix B: Heavy Vehicle Simulator Testing Procedure

HVS Test Procedure

Moving Load Test of Full-Scale Lightweight Aluminum Deck Panel Test Specimen

Objectives

- 1. Simulate real-world loading conditions.
- 2. Verify adequacy of wearing surface when heat and water are applied along with a simulated moving load.
- 3. Verify structural behavior is similar to static tests completed at SRC with higher load level.

Gage Count

Item	Quantity
Deflection Gage	13
Rosette Bi-Axial 5mm Gage	34
Slip Deflection Gages	2

Instrumentation

Instrumentation consists of bi-axial strain gages, deflection gages and slip deflection gages. When placed on the top and bottom surface of the deck panel, the strain gages measure strain in the aluminum deck panel in the longitudinal and transverse directions. When placed on the face of the deck panel (lines 1 and 20), they measure strain in the transverse and vertical directions. The deflection gages measure deflection of either the deck panel or steel beam, depending on placement.

Loading

Details of the target HVS loading conditions are listed below. Loading will be along line C, shown on the Instrumentation Plan.

Constant Load Level: 11 kips

Wander: No

Applied Temperature: 120° F or 50° C for First 300,000 Bi-Directional Passes

Applied Water: Saturate Aggregate for Second 300,000 Bi-Directional Passes or until June 20, 2016 (whichever occurs first)

Total Number of Load Passes: 600,000 (1 Month)

Test Supplies

Instrumentation supplies installed on the test specimen prior to shipment are not included in this list.

Provided By SRC:

Item	Quantity
AlumaBridge Test Specimen	1
Soaker Hose	2
Concrete Grinder	1
13.75" Tall Double Acting Hollo Cylinder and Pumps	2
6" long 2x6 Dunnage	16
1/4" Concrete Mechanical Anchors	4
Tall Deflection Stand	1
Drill and 1/4" Chuck, Wrenches	2
Extension Cord	2
Hillman Roller Assembly with HSS Tube	2
Deflection Offset weight	1

Provided By or Located at SMO:

Item	Quantity
Spacer Blocks	2
Open Grid Steel Deck Panels	2 (C and D)
Water Pump	3
HVS Bridge	2 pieces
1"x6"x23' Plate	2
Forklift	1

Gage Identification

The gage name designation is Location/Type (T for Top Rosette, B for Bottom Rosette and D for Deflection), Transverse Location (Alphabetical Mark), Longitudinal Location (Numerical Mark). So, gage T_F11 is a rosette located on the top of the panel, at transverse grid location F and longitudinal grid location 11.

The gages listed in the table below are hooked up for the HVS test.

Displacement Gages	Strain Gages on Generation 2 Panel	Strain Gages on Generation 1 Panel
GD_1	T_C1	B_C16
GD_2	B_C1	B_D16
GD_5_Bm	T_F1	B_E16
GD_5_Pnl	B_F1	T_E17
D_C3	B_A2	T_F17
D_C9	B_B2	T_G17
D_C14	B_C2	B_C18
D_C16	B_D2	B_D18
D_C18	T_E2	B_E18
D_F2	B_E2	T_F19
D_F14	T_F2	T_C20
D_F19_Bm	T_G2	B_C20
D_F19_Pnl	T_E9	T_F20
Slip_A	T_F9	B_F20
Slip_B	T_G9	
	T_F7	
	B_C8	
	B_A10	
	B_B10	
	B_C10	
	B_D10	
	B_E10	
	T_F11	
	B_C12	

Test Procedure

1. Place HVS Bridge.
2. Place HVS in testing area.
3. Remove HVS bridge.
4. Place 1"x6"x23' Plates with Hilman Roller Assemblies. (See Installation Sequence)
5. Place test specimen on Hilman Roller Assemblies to West of Test Pit. Install with 7.5 inch overhang towards pit opening. (See Installation Sequence)
6. Verify deflection gages are undamaged after transport. Repair as necessary.
7. Roll test specimen into place.
8. Place Forklift at west side of deck. Place each Holo Cylinder on (2) 2x6 Dunnage under NE and SE corners of deck. Lift deck simultaneously using forklift and holo cylinders. Remove Hilman Roller assemblies. Place (2) 2x6 Dunnage under each beam. Lower simultaneously to dunnage. Remove dunnage under cylinder and place on ground. Lift deck using cylinders and forklift. Remove dunnage under beams. Lower simultaneously to 1" plates.
9. Run texture test at HVS wheel path.
10. Hook up instrumentation and check gages.
11. Run dry HVS loading as detailed in loading section.
12. Run texture test at HVS wheel path.
13. Set up soaker hose. Set up and test pump.
14. Run wet HVS loading as detailed in loading section.
15. Remove test specimen from testing area. Remove instrumentation and gages.
16. Place HVS Bridge
17. Remove HVS from testing area.
18. Post Testing Evaluation:
 - a. Inspect weld gap using feeler gages and record opening sizes.
 - b. Perform Bond Test 2 on wearing surface at HVS loading path.
 - c. Visually inspect welds.
 - d. Visually inspect wearing surface.
 - e. Run texture test at HVS wheel path.
19. Repair wearing surface.
20. Perform any required corrosion tests – refer to SMO Corrosion Lab.

Material Strengths

The Research Program Notes provided to FDOT by Hardesty & Hanover note that the Aluminum material is ASTM B221 Alloy 6063-T6. Table 7.4.1-1 in the AASHTO LRFD Bridge Design Specifications 7th Edition (2014) notes the following properties for Aluminum extrusions:

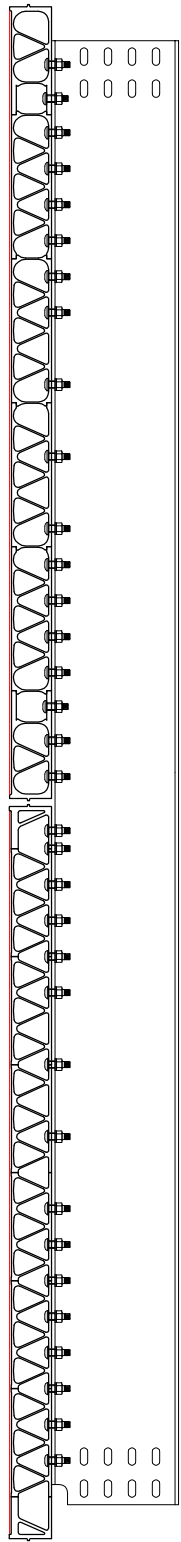
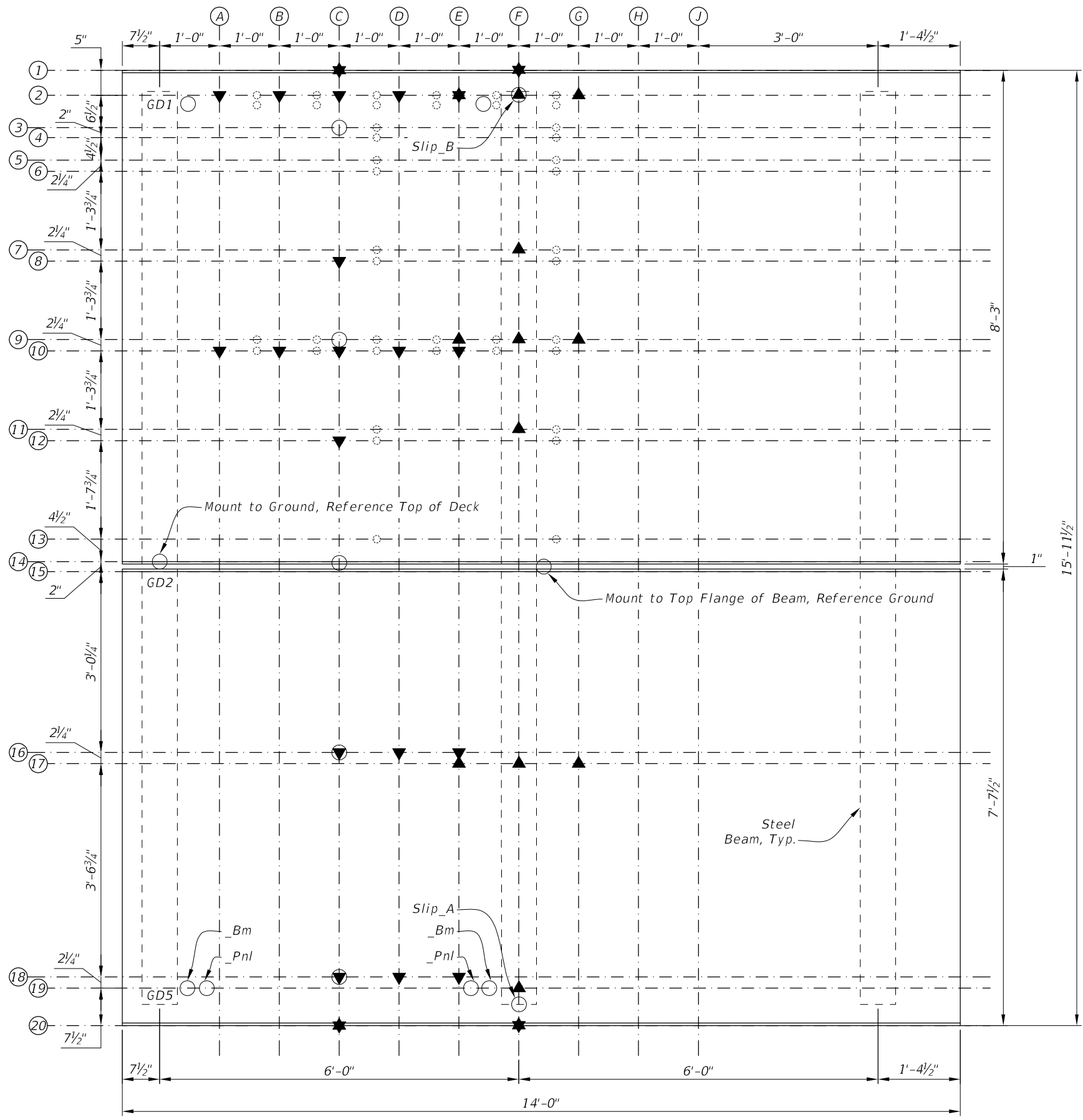
ASTM Specification	B221
Alloy-Temper	6063-T6
Thickness t (in)	All
F _{tu} (ksi)	30
F _{ty} (ksi)	25
F _{tuw} (ksi)	17
F _{tyw} (ksi)	8
Unwelded C _t	189
Welded C _t	715

Table 7.4.1-3 (AASHTO LRFD) notes the following Aluminum Properties:

Modulus of elasticity	E	10,100 ksi
Shear modulus of elasticity	G	3800 ksi
Poisson's ratio	ν	0.33
Thermal coefficient of expansion	α	13 x 10 ⁻⁶ in./in./°F
Compressive yield strength for unwelded tempers beginning with H	F _{cy}	0.9F _{ty}
Compressive yield strength for all other material	F _{cy}	F _{ty}
Shear yield strength	F _{sy}	0.6F _{ty}
Shear ultimate strength	F _{su}	0.6F _{tu}

The stringer beam which the aluminum deck panels are attached to was specified as a W16x50 beam. Per the AISC Steel Construction Manual, 13th edition, the common ASTM designation for a W shape is A992, which has a minimum yield strength (F_y) of 50 ksi and an ultimate tensile strength (F_u) of 65 ksi.

Appendix A: Instrumentation Plan



- LEGEND**
- ★ denotes Strain Gauge location on Top & Bott. of Panel
 - ▲ denotes Strain Gauge location on Top of Panel
 - ▼ denotes Strain Gauge location on Bott. of Panel
 - denotes 1" Dia. Omitted Wearing Surface Improperly Located
 - denotes Deflection Gauge location on Bottom of Panel or Beam

PLAN

REVISIONS						DRAWN BY: CJF 12-15	STATE OF FLORIDA DEPARTMENT OF TRANSPORTATION			SHEET TITLE: Instrumentation Plan - HVS Testing	REF. DWG. NO.
DATE	BY	DESCRIPTION	DATE	BY	DESCRIPTION		ROAD NO.	COUNTY	FINANCIAL PROJECT ID.		
						CHECKED BY: ??				PROJECT NAME: Lightweight Aluminum Deck Testing	SHEET NO.
						DESIGNED BY: CJF 12-15	RD #	COUNTY	FPID #		D-1
						CHECKED BY: ??					

Appendix C: Material and Weld Certifications

Freeman, Christina

From: Greg Osberg <gregosberg@alumabridge.com>
Sent: Wednesday, March 09, 2016 4:31 PM
To: Freeman, Christina
Cc: mriley@lbfoster.com
Subject: FW: Test report.
Attachments: 14218certs215571-160309.pdf; 14217certs215561-160309.pdf;
14216certs215551-160309.pdf

Christina,

Revised certs are attached.

Greg

From: Anthony Langley [mailto:alangley@taberextrusions.com]
Sent: Wednesday, March 09, 2016 4:24 PM
To: Greg Osberg
Subject: RE: Test report.

Greg,
The certs have been corrected to include the actual results.

Regards,
Anthony Langley
Inside Sales Representative
Taber Extrusion, LLC
Russellville, AR
alangley@taberextrusions.com
479-968-1021 ext:261

From: Greg Osberg [mailto:gregosberg@alumabridge.com]
Sent: Tuesday, March 08, 2016 2:41 PM
To: Anthony Langley
Subject: FW: Test report.

Anthony,

Can you answers Christina's question?

Thanks,

Greg

Greg Osberg
AlumaBridge, LLC
Mobile: 612.518.0398
gregosberg@alumabridge.com



ISO 9001 * AS 9100
CERTIFIED QUALITY



Taber Extrusions, LLC

Made in the USA

915 South Elmira Avenue
Russellville, AR 72802
Phone: (479)968-1021 * Fax:(479)890-4666

CERTIFIED INSPECTION REPORT

Certificate of Conformance

We certify that the material was inspected in accordance with, and has been found to meet the applicable requirements described herein, including specifications forming a part of the description. If the product is outside the scope of the specifications or if exception to the specification have been taken by TABER EXTRUSIONS, (Russellville, AR) the product conforms to the additional requirements or exceptions. Testing records will be on file and available at TABER EXTRUSIONS, for a period of ten years to demonstrate compliance.

Chemical Composition Limits (percent by weight)

	Al	Mg	Mn	Zn	Zr	Si	Fe	Cu	Ni	Cr	Ti	V	B	Others		
														Each	Total	
Min.		0.45				0.20										
Max.	Rem.	0.90	0.10	0.10		0.60	0.35	0.10		0.10	0.10				0.05	0.15

Actual Mechanical Properties Test Results (*1000 PSI)

LotNum	*UTS		*TYS		El, in 2", %		Cond, %IACS		Test Type
	Min.	Max.	Min.	Max.	Min.	Max.	Min.	Max.	
35598	34.7		29.5		10.0				L

Actual Chemical Composition (percent by weight)

Heat Number	Al	Si	Fe	Cu	Mn	Mg	Cr	Zn	Ti	Zr	Supplier
39790-1	Rem.	0.49	0.25	0.03	0.02	0.56	0.01	0.02	0.02	0.00	Taber Extrusions, LLC, Gulfport, MS, USA
39791-1	Rem.	0.46	0.23	0.03	0.02	0.56	0.01	0.03	0.02	0.00	Taber Extrusions, LLC, Gulfport, MS, USA
39798-2	Rem.	0.45	0.21	0.06	0.04	0.56	0.02	0.02	0.02	0.00	Taber Extrusions, LLC, Gulfport, MS, USA
39799-1	Rem.	0.46	0.22	0.05	0.04	0.58	0.02	0.02	0.02	0.00	Taber Extrusions, LLC, Gulfport, MS, USA
39799-3	Rem.	0.48	0.23	0.05	0.04	0.59	0.02	0.02	0.02	0.00	Taber Extrusions, LLC, Gulfport, MS, USA

Remarks:

Die Number: TM-14216 Alloy: 6063 - T6 Specification(s): ASTM B221 -14
 Number Of Bundles: 3
 Total Net Weight (Lbs): 3,399 Total Number Of Pieces: 9
 Sold To: AlumaBridge, LLC Ship To: HFW
 Customer Order Number: 1013
 Sales Order Number: 21555
 Customer Part Number(s):

Description: Female Generation II Length (inches): 180.00
 Tickets: 119923, 119924, 119925

Date: September 02, 2015

Quality Control



ISO 9001 * AS 9100
CERTIFIED QUALITY



Taber Extrusions, LLC

Made in the USA

915 South Elmira Avenue
Russellville, AR 72802
Phone: (479)968-1021 * Fax:(479)890-4666

CERTIFIED INSPECTION REPORT

Certificate of Conformance

We certify that the material was inspected in accordance with, and has been found to meet the applicable requirements described herein, including specifications forming a part of the description. If the product is outside the scope of the specifications or if exception to the specification have been taken by TABER EXTRUSIONS, (Russellville, AR) the product conforms to the additional requirements or exceptions. Testing records will be on file and available at TABER EXTRUSIONS, for a period of ten years to demonstrate compliance.

Chemical Composition Limits (percent by weight)

	Al	Mg	Mn	Zn	Zr	Si	Fe	Cu	Ni	Cr	Ti	V	B	Others		
														Each	Total	
Min.		0.45				0.20										
Max.	Rem.	0.90	0.10	0.10		0.60	0.35	0.10		0.10	0.10				0.05	0.15

Actual Mechanical Properties Test Results (*1000 PSI)

LotNum	*UTS		*TYS		El, in 2", %		Cond, %IACS		Test Type
	Min.	Max.	Min.	Max.	Min.	Max.	Min.	Max.	
35597	39.0		35.3		10.0				L

Actual Chemical Composition (percent by weight)

Heat Number	Al	Si	Fe	Cu	Mn	Mg	Cr	Zn	Ti	Zr	Supplier
39791-1	Rem.	0.46	0.23	0.03	0.02	0.56	0.01	0.03	0.02	0.00	Taber Extrusions, LLC, Gulfport, MS, USA
39799-3	Rem.	0.48	0.23	0.05	0.04	0.59	0.02	0.02	0.02	0.00	Taber Extrusions, LLC, Gulfport, MS, USA

Remarks:

Die Number: TM-14217 Alloy: 6063 - T6 Specification(s): ASTM B221 -14
 Number Of Bundles: 1
 Total Net Weight (Lbs): 1,572 Total Number Of Pieces: 4
 Sold To: AlumaBridge, LLC Ship To: HFW
 Customer Order Number: 1013
 Sales Order Number: 21556
 Customer Part Number(s):

Description: Male Generation II Length (inches): 180.00
 Tickets: 119926

Date: September 02, 2015

Quality Control



ISO 9001 * AS 9100
CERTIFIED QUALITY



Taber Extrusions, LLC

Made in the USA

915 South Elmira Avenue
Russellville, AR 72802
Phone: (479)968-1021 * Fax:(479)890-4666

CERTIFIED INSPECTION REPORT

Certificate of Conformance

We certify that the material was inspected in accordance with, and has been found to meet the applicable requirements described herein, including specifications forming a part of the description. If the product is outside the scope of the specifications or if exception to the specification have been taken by TABER EXTRUSIONS, (Russellville, AR) the product conforms to the additional requirements or exceptions. Testing records will be on file and available at TABER EXTRUSIONS, for a period of ten years to demonstrate compliance.

Chemical Composition Limits (percent by weight)

	Al	Mg	Mn	Zn	Zr	Si	Fe	Cu	Ni	Cr	Ti	V	B	Others	
														Each	Total
Min.		0.45				0.20									
Max.	Rem.	0.90	0.10	0.10		0.60	0.35	0.10		0.10	0.10			0.05	0.15

Actual Mechanical Properties Test Results (*1000 PSI)

LotNum	*UTS		*TYS		El, in 2", %		Cond, %IACS		Test Type
	Min.	Max.	Min.	Max.	Min.	Max.	Min.	Max.	
35620	45.0		40.4		13.0				L

Actual Chemical Composition (percent by weight)

Heat Number	Al	Si	Fe	Cu	Mn	Mg	Cr	Zn	Ti	Zr	Supplier
39790-3	Rem.	0.50	0.25	0.03	0.02	0.57	0.01	0.02	0.02	0.00	Taber Extrusions, LLC, Gulfport, MS, USA
39791-1	Rem.	0.46	0.23	0.03	0.02	0.56	0.01	0.03	0.02	0.00	Taber Extrusions, LLC, Gulfport, MS, USA
39798-1	Rem.	0.45	0.21	0.06	0.04	0.56	0.02	0.02	0.02	0.00	Taber Extrusions, LLC, Gulfport, MS, USA
39798-2	Rem.	0.45	0.21	0.06	0.04	0.56	0.02	0.02	0.02	0.00	Taber Extrusions, LLC, Gulfport, MS, USA
39799-3	Rem.	0.48	0.23	0.05	0.04	0.59	0.02	0.02	0.02	0.00	Taber Extrusions, LLC, Gulfport, MS, USA
39876-1	Rem.	0.47	0.27	0.07	0.05	0.59	0.03	0.03	0.03	0.00	Taber Extrusions, LLC, Gulfport, MS, USA
39876-3	Rem.	0.47	0.27	0.07	0.05	0.59	0.03	0.03	0.03	0.00	Taber Extrusions, LLC, Gulfport, MS, USA

Remarks:

Die Number: TM-14218 Alloy: 6063 - T6

Specification(s): ASTM B221 -14

Number Of Bundles: 2

Total Number Of Pieces: 5

Total Net Weight (Lbs): 1,625

Sold To: AlumaBridge, LLC

Ship To: HFW

Customer Order Number: 1013

Sales Order Number: 21557

Customer Part Number(s):

Description: End Cap Ext.

Length (inches): 180.00

Tickets: 119927, 119928

Date: September 02, 2015

Quality Control

Freeman, Christina

From: gpatton@hardesty-hanover.com
Sent: Friday, January 15, 2016 9:47 AM
To: Freeman, Christina
Cc: Sardinias, Alberto O; Dockstader, Darryll; Potter, William; Robertson, Robert
Subject: RE: Aluminum deck research and aluminum deck testing
Attachments: Alumabridge Inspection Report 1-21-2015 Gen I.docx; Alumabridge Inspection Report 10-2-2015 Gen II.docx; FDOT-INS2-FDOT Weld Inspection Record Gen II.pdf; FDOT-INS3- PERFORMED PANEL Gen I.pdf; FDOT-INS3-FDOT Alumabridge Final Machining Gen II.pdf

Christina,

As requested, attached are the inspection records that we received from AlumaBridge for both the Gen I and Gen II Panels. HF Webster performed the weld inspection except for the UT Testing, which was performed by Western Inspection Services. The UT Testing was performed in accordance with the AWS D1.2 Structural Welding Code - Aluminum, 2014 Edition for Friction Stir Welding, page 108, Table 7.3 Cyclically Loaded Structures.

For your information, originally there were two Gen I panels fabricated and completed in January 2015. After the second of the two Gen I panels was friction stir welded into the panel, it was found that the aluminum alloy of one of the extrusions did not meet the material specifications. In lieu of cutting out the bad extrusion, it was decided to abandon the second Gen I panel. At this point, AlumaBridge, in consultation with HF Webster, decided to refine the 5-inch aluminum deck system, which led to development of the Gen II system. Following the engineering of the Gen II system, trail extrusions and trial friction stir welding was performed and then the Gen II test panel was fabricated and completed in October 2015.

George C. Patton, PE, MSCE
Movable Bridge Design Lead

email: gpatton@hardesty-hanover.com
address: 18302 Highwoods Preserve Parkway, Suite 114, Tampa, FL 33647
office: 813.304.2385
cell: 813.815.2564



From: "Freeman, Christina" <Christina.Freeman@dot.state.fl.us>
To: "gpatton@hardesty-hanover.com" <gpatton@hardesty-hanover.com>
Date: 01/15/2016 09:03 AM
Subject: RE: Aluminum deck research and aluminum deck testing

George,



NON - DESTRUCTIVE TESTING

Western Inspection Services, Inc.

PO Box 7249, Gillette, Wy 82717

Phone (307) 682-1192 Fax (307) 686-4019

1-21-2105

To: Greg Osberg- President/CEO

AlumaBridge LLC

Western inspection Services was requested by Greg Osberg to travel to Rapid City South Dakota and ultrasonically inspect two bridge panel components which were erected at HF Webster's newest facility. These inspections were performed on January 1-19-2015. The acceptance criteria were taken from the AWS D1.2 Aluminum 2014 Edition friction stir page 108 Table 7.3 Cyclically Loaded Structures.

1) Panel 1 –

All welds on this panel conformed to the friction weld acceptance criteria.

2) Panel 2

Upper welds numbers 5 and 7 100% failed full length. These rejectable discontinuities were located from .375-.625 inches in depth from the top plate.

At bottom side of panel weld #2 a rejectable discontinuity 4 feet long, .250 inches in depth @ inner toe-line was located.

Western Inspection Services

Craig Bush
A.S.M.E. Level 111
A.W.S.C.W.I.
Office-307-686-6184
Cell-307-660-9686



NON - DESTRUCTIVE TESTING

Western Inspection Services, Inc.

PO Box 7249, Gillette, Wy 82717

Phone (307) 682-1192 Fax (307) 686-4019

10-2-2015

To: Greg Osberg- President/CEO

AlumaBridge LLC

Western inspection Services was requested by Greg Osberg to travel to Rapid City South Dakota and ultrasonically inspect one bridge panel components at HF Webster's newest facility. These inspections were performed on October 1-2015. The acceptance criteria was taken from the AWS D1.2 Aluminum 2014 Edition friction stir page 108 Table 7.3 Cyclically Loaded Structures,

1) Panel 1 –All welds conformed to the friction weld acceptance criteria

Approximately 140 linear feet was ultrasonically inspected on the new bridge panel with no negative indications.

W.I.S. noticed that while doing the inspections the flaw detector screen was much clearer which indicates better grain structure in the new extrusions.

Upon completion of the inspections W.I.S. was shown a macro etch done by H.F.Webster. This test showed a much better weld grain and material grain structure compared to the previous extrusions which caused a re-rejection of one of the previous bridge panels.

Western Inspection Services

Craig Bush
A.S.M.E. Level 111
A.W.S.C.W.I.
Office-307-682-1192
Cell-307-660-9686



2430 Dyess Ave, Rapid City, SD 57701
 605-343-3260 (Office) 605-343-1801 (Fax)

Welding Testing Inspection Record

A-Code: **FDOT**

B-Code: **INS2**

C-Code:

Summary:

Product: FDOT Welded Panel	Drawing #: 5-inch Alum DeckTest Panels HF Webster	Serial No/PIT Code: Panel 1
----------------------------	---	-----------------------------

Inspection Criteria:

Test	Location	Sample Size
Visual inspection by FSW operator or FSW engineer	100% of welds	All Welds
Visual inspection of macro sections	Upper & Lower (See Below)	All Welds (Start and End)
Tensile Test per ATSM E8 (minimum of 17 KSI)	Upper & Lower (See Below)	All Welds (Start and End)

Inspection Summary:

Test	Test #	Sample ID	Location	Result	Pass/Fail
Surface Visual	Weld 1	-	Upper	-	Pass
	Weld 1	-	Lower	-	Pass
	Weld 2	-	Upper	-	Pass
	Weld 2	-	Lower	-	Pass
	Weld 3	-	Upper	-	Pass
	Weld 3	-	Lower	-	Pass
	Weld 4	-	Upper	-	Pass
	Weld 4	-	Lower	-	Pass
	Weld 5	-	Upper	-	Pass
	Weld 5	-	Lower	-	Pass

Test	Test #	Sample ID	Location	Result	Pass/Fail
Macro Visual	Weld 1	1S-L	Start	-	Pass
	Weld 1	1E-U	End	-	Pass
	Weld 2	2S-U	Start	-	Pass
	Weld 2	2E-L	End	-	Pass
	Weld 3	3S-L	Start	-	Pass
	Weld 3	3E-U	End	-	Pass
	Weld 4	4S-U	Start	-	Pass
	Weld 4	4E-L	End	-	Pass
	Weld 5	5S-L	Start	-	Pass
	Weld 5	5E-U	End	-	Pass



2430 Dyess Ave, Rapid City, SD 57701
 605-343-3260 (Office) 605-343-1801 (Fax)

Welding Testing Inspection Record

A-Code: **FDOT**

B-Code: **INS2**

C-Code:

Test	Test #	Sample ID	Location	Result (ksi)	Pass/Fail
Tensile	Weld 1	1S-U	Start	22.3	Pass
	Weld 1	1E-L	End	24.8	Pass
	Weld 2	2S-L	Start	24.2	Pass
	Weld 2	2E-U	End	22.8	Pass
	Weld 3	3S-U	Start	22.4	Pass
	Weld 3	3E-L	End	20.8	Pass
	Weld 4	4S-L	Start	23.9	Pass
	Weld 4	4E-U	End	23.5	Pass
	Weld 5	5S-U	Start	22.8	Pass
	Weld 5	5E-L	End	24.0	Pass

Surface Visual Approval:

Visual Inspected By: Chad Westendorf

Date: 10-1-15

Macro Visual Approval:

Visual Inspected By: Chad Westendorf

Date: 10-5-15

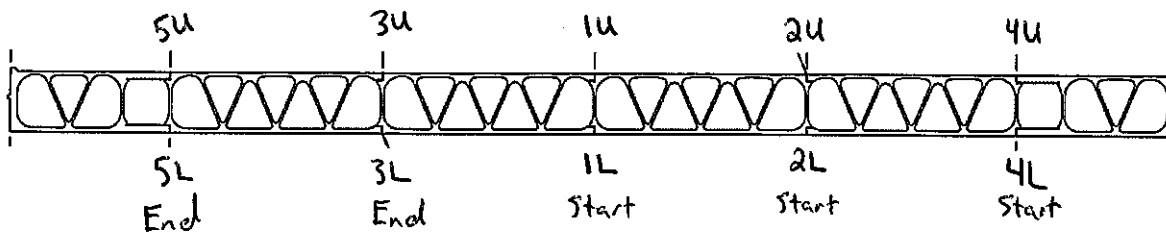
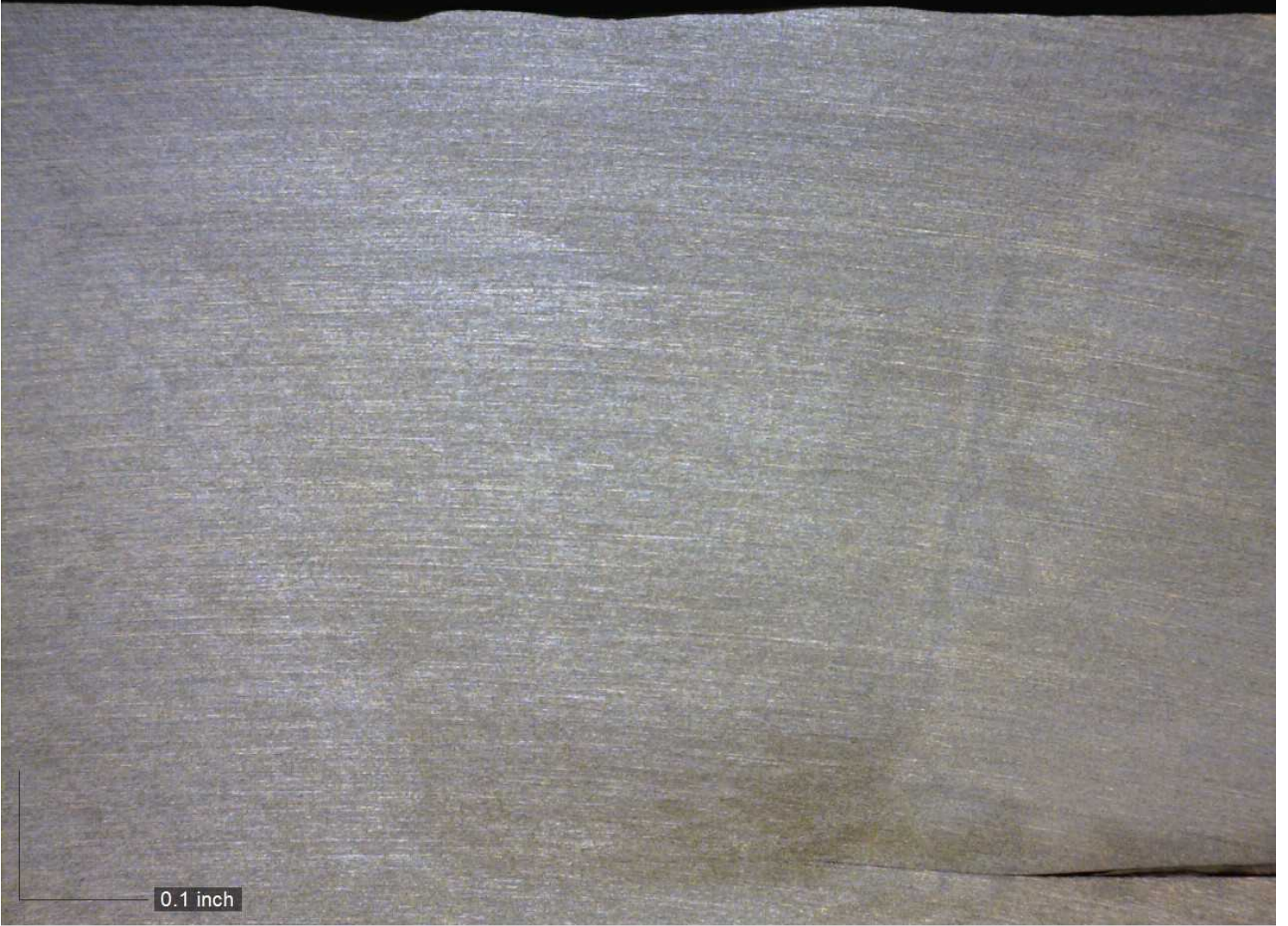
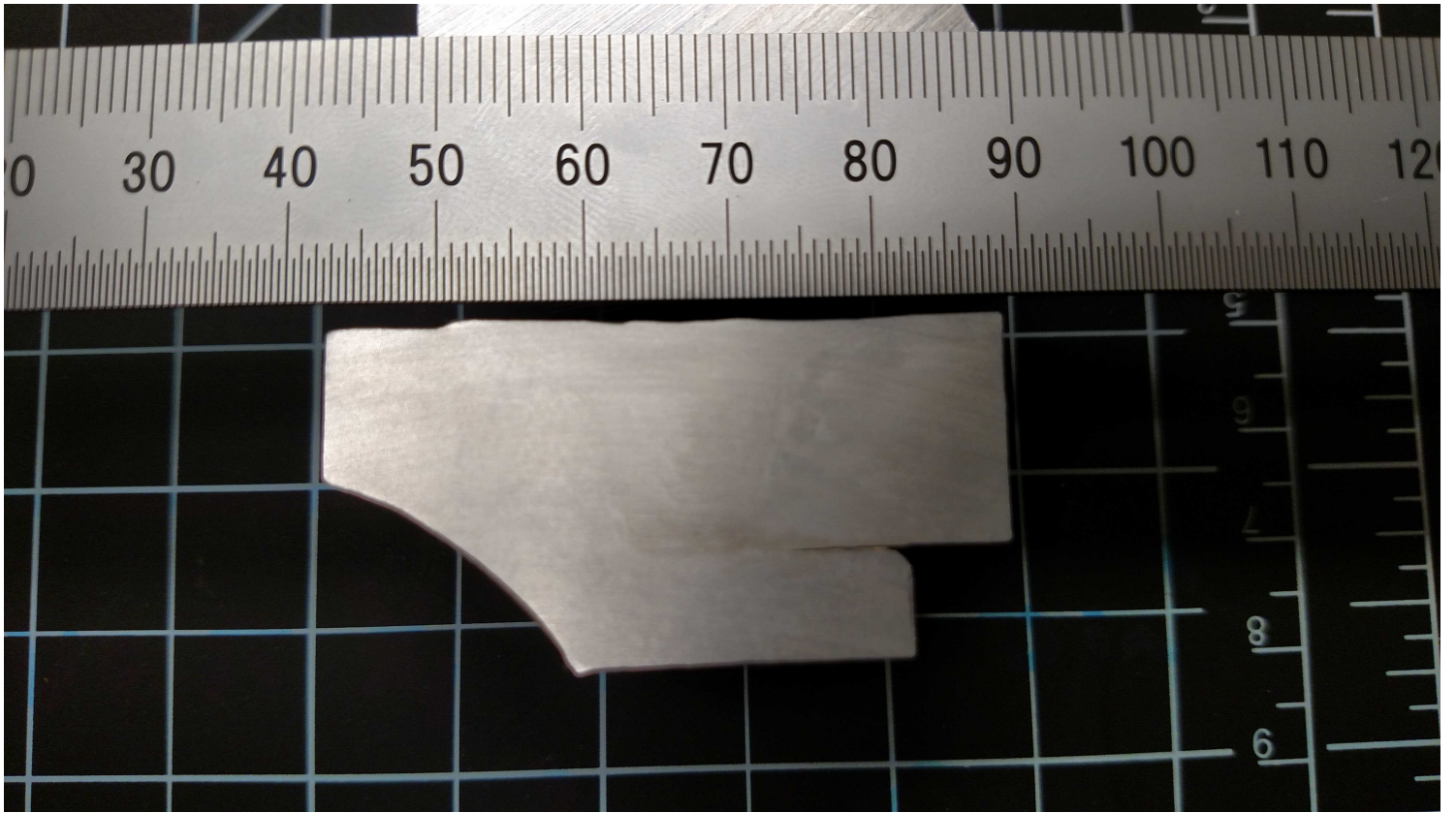


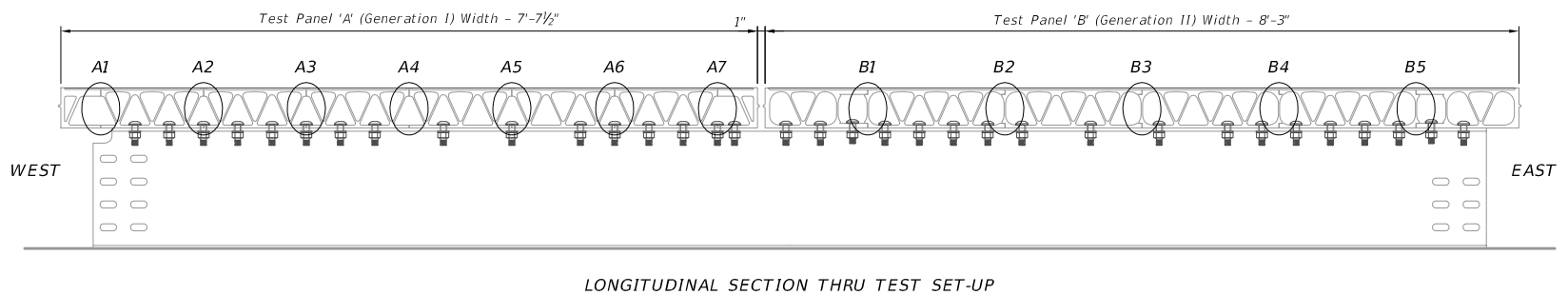
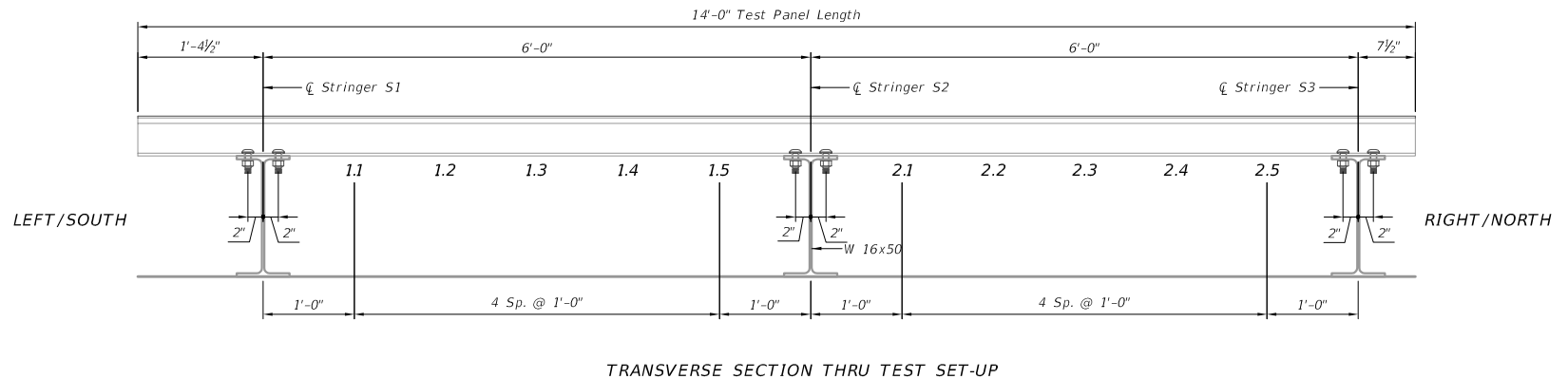
Figure 1: Panel 1 weld identification

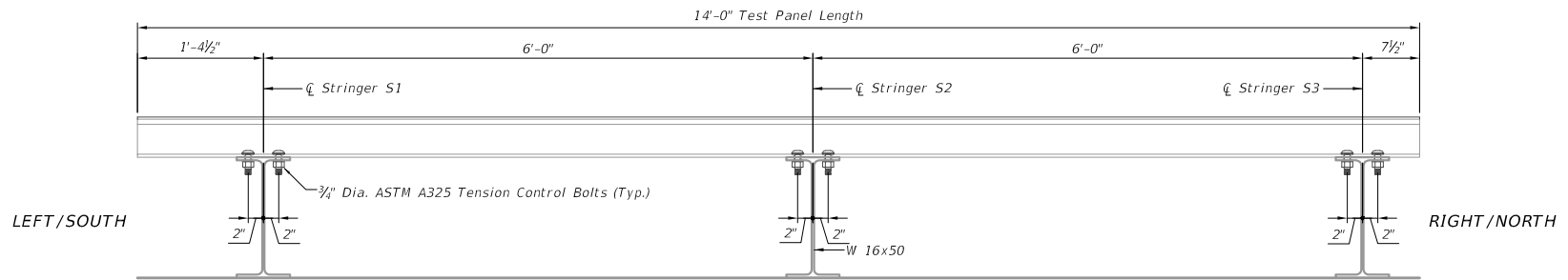
A116 1280x1024 2015/10/05 12:54:16 Unit: inch Magnification: 20x No Calibration



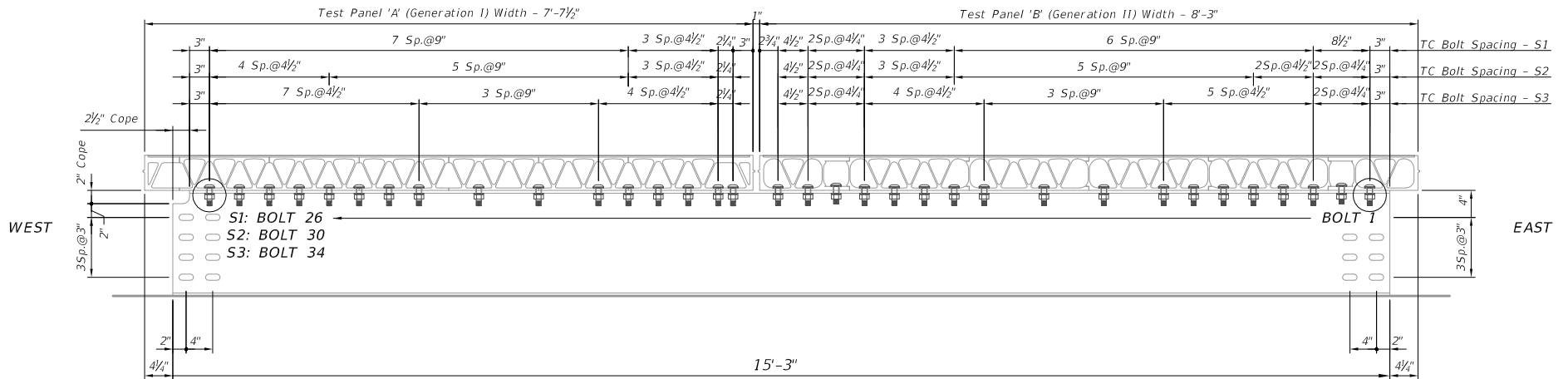


Appendix D: Visual Inspection Records





TRANSVERSE SECTION THRU TEST SET-UP



LONGITUDINAL SECTION THRU TEST SET-UP

Table 1: Generation II Panel Weld Gap

Preliminary Inspection performed by CJF on 2/4/2016. Weather was dry and 52 degrees F.

Intermediate Inspection performed by CJF on 5/16/2016. Weather was clear and 75 degrees F.

Final Inspection performed by JR on 8/26/2016. Weather was cloudy and 85 degrees F.

Weld Location		Inspection Stage	Width (Feeler Gage)							
			.0015"	.004"	.006"	.008"	.010"	.012"	.015"	.025"
B1	Left	Preliminary								
		Intermediate								
		Final								
	Bottom	Preliminary								
		Intermediate								
		Final								
Right	Preliminary									
	Intermediate									
	Final									
B2	Left	Preliminary								
		Intermediate								
		Final								
	Bottom	Preliminary								
		Intermediate								
		Final								
Right	Preliminary									
	Intermediate									
	Final									
B3	Left	Preliminary								
		Intermediate								
		Final								
	Bottom	Preliminary								
		Intermediate								
		Final								
Right	Preliminary									
	Intermediate									
	Final									

Table 2: Generation II Panel Visible Seam Length (1/64 inch)

Preliminary Inspection performed by CJF on 2/4/2016. Weather was dry and 52 degrees F.

Intermediate Inspection performed by CJF on 5/16/2016. Weather was clear and 75 degrees F.

Final Inspection performed by JR on 8/26/2016. Weather was cloudy and 85 degrees F.

WELD			PRELIMINARY	INTERMEDIATE	FINAL
B1	Left	Top	12	12	10
		Bottom	20	22	20
	Right	Top	36	4	38
		Bottom	32	18	34
B2	Left	Top	8	3	6
		Bottom	16	6	12
	Right	Top	28	2	31
		Bottom	14	3	20
B3	Left	Top	24	4	4
		Bottom	16	4	3
	Right	Top	28	2	32
		Bottom	26	3	29
B4	Left	Top	20	4	5
		Bottom	26	20	20
	Right	Top	36	4	38
		Bottom	32	4	24
B5	Left	Top	26	12	20
		Bottom	24	20	26
	Right	Top	36	8	29
		Bottom	28	6	29

Table 3: Panel to Beam Gap at Stringer 1 Left

Bolt #	Gap			Bolt #	Gap		
	Preliminary	Intermediate	Final		Preliminary	Intermediate	Final
East End	0.0015	NC	NC	22	-	NC	NC
1	0.0015	NC	0.018		0.014	NC	0.01
	0.008	0.014	0.009	23	0.0015	NC	NC
2	-	NC	NC		0.02	0.028	0.025
	0.018	NC	0.011	24	0.003	NC	0.001
3	-	NC	NC		0.06	NC	0.09
	0.008	NC	0.012	25	0.07	NC	0.032
4	-	NC	NC		0.16	NC	0.13
	0.012	NC	0.018	26	0.11	NC	0.06
5	-	NC	NC	West End	0.24	NC	0.24
	0.007	NC	0.02				
6	-	NC	NC				
	0.005	0.007	0.07				
7	-	NC	NC				
	0.013	NC	NC				
8	-	NC	NC				
	-	NC	NC				
9	-	NC	NC				
	-	NC	NC				
10	-	NC	NC				
	0.007	NC	NC				
11	-	NC	NC				
	0.016	NC	NC				
12	-	NC	NC				
	0.01	NC	0.018				
13	-	NC	NC				
	-	NC	NC				
14	-	NC	NC				
End of Panel B	-	NC	NC				
End of Panel A	0.11	NC	0.078				
15	0.0015	0.004	0.01				
	0.0015	0.003	NC				
16	0.0015	NC	0.05				
	0.06	NC	0.035				
17	-	NC	NC				
	0.014	NC	0.016				
18	-	NC	NC				
	0.006	NC	0.04				
19	0.03	NC	0.028				
	0.0016	0.016	0.022				
20	0.0015	NC	NC				
	0.01	NC	0.01				
21	-	NC	NC				
	0.0015	0.012	NC				

Inspection Dates:

Preliminary: 3/7/2016
 Intermediate: 5/18/2016
 Final: 8/26/2016

"-" indicates feeler gage cannot be inserted.
 "NM" indicates "Not Measured"
 "NC" indicates "No Change" from the previous inspection.

Table 4: Panel to Beam Gap at Stringer 1 Right

Bolt #	Gap			Bolt #	Gap		
	Preliminary	Intermediate	Final		Preliminary	Intermediate	Final
East End	NM	-	NC	22	NM	-	0.0015
1	NM	-	NC		NM	0.006	NC
	NM	-	0.006	23	NM	-	-
2	NM	-	NC		NM	0.016	NC
	NM	0.016	NC	24	NM	-	0.004
3	NM	-	NC		NM	0.035	NC
	NM	0.011	NC	25	NM	0.035	0.015
4	NM	-	NC		NM	0.13	0.125
	NM	-	NC	26	NM	0.1	0.0625
5	NM	-	NC	West End	NM	0.26	NC
	NM	0.012	NC				
6	NM	-	NC				
	NM	0.0015	NC				
7	NM	-	NC				
	NM	0.01	NC				
8	NM	-	NC				
	NM	-	NC				
9	NM	-	NC				
	NM	-	NC				
10	NM	-	NC				
	NM	-	NC				
11	NM	-	NC				
	NM	0.008	NC				
12	NM	-	NC				
	NM	0.007	NC				
13	NM	0.006	0				
	NM	-	NC				
14	NM	-	NC				
End of Panel B	NM	-	NC				
End of Panel A	NM	0.11	NC				
15	NM	0.011	NC				
	NM	-	NC				
16	NM	0.008	NC				
	NM	0.035	NC				
17	NM	0.004	NC				
	NM	0.014	NC				
18	NM	-	NC				
	NM	0.006	0.004				
19	NM	0.014	NC				
	NM	0.018	NC				
20	NM	-	NC				
	NM	0.01	NC				
21	NM	-	NC				
	NM	0.006	NC				

Inspection Dates:

Preliminary: 3/7/2016
 Intermediate: 5/18/2016
 Final: 8/26/2016

"-" indicates feeler gage cannot be inserted.
 "NM" indicates "Not Measured"
 "NC" indicates "No Change" from the previous inspection.

Table 5: Panel to Beam Gap at Stringer 2 Left

Bolt #	Gap			Bolt #	Gap		
	Preliminary	Intermediate	Final		Preliminary	Intermediate	Final
East End	NM	-	0.0015	22	NM	-	-
1	NM	-	-		NM	-	0.01
	NM	-	-	23	NM	-	-
2	NM	-	-		NM	-	-
	NM	-	-	24	NM	-	-
3	NM	-	-		NM	-	-
	NM	-	-	25	NM	-	-
4	NM	-	-		NM	0.012	0.008
	NM	-	-	26	NM	-	-
5	NM	-	-		NM	0.012	0.004
	NM	-	0.0015	27	NM	-	-
6	NM	-	-		NM	0.013	NC
	NM	0.008	NC	28	NM	-	-
7	NM	-	-		NM	0.01	0.012
	NM	0.007	NC	29	NM	-	0.0015
8	NM	-	-		NM	0.032	0.09375
	NM	-	-	30	NM	0.013	0.04
9	NM	-	-	West End	NM	0.16	0.125
	NM	0.01	0.08				
10	NM	-	-				
	NM	-	-				
11	NM	-	-				
	NM	-	-				
12	NM	-	-				
	NM	-	0.004				
13	NM	-	-				
	NM	0.01	NC				
14	NM	-	-				
	NM	0.007	-				
15	NM	-	-				
	NM	-	-				
16	NM	-	-				
End of Panel B	NM	-	-				
End of Panel A	NM	0.19	NC				
17	NM	0.011	0.015				
	NM	0.07	NC				
18	NM	0.09	0.015				
	NM	0.15	NC				
19	NM	0.011	NC				
	NM	0.12	0.062				
20	NM	0.01	NC				
	NM	0.018	NC				
21	NM	-	-				
	NM	0.01	0.015				

Inspection Dates:

Preliminary: 3/7/2016
 Intermediate: 5/18/2016
 Final: 8/26/2016

"-" indicates feeler gage cannot be inserted.
 "NM" indicates "Not Measured"
 "NC" indicates "No Change" from the previous inspection.

Table 6: Panel to Beam Gap at Stringer 2 Right

Bolt #	Gap			Bolt #	Gap		
	Preliminary	Intermediate	Final		Preliminary	Intermediate	Final
East End	NM	-	0.005	22	NM	-	-
1	NM	-	-		NM	0.012	-
	NM	0.01	0.01	23	NM	-	-
2	NM	-	-		NM	0.01	NC
	NM	0.0018	0.004	24	NM	-	-
3	NM	-	-		NM	0.0015	-
	NM	0.0018	NC	25	NM	-	-
4	NM	-	-		NM	0.006	NC
	NM	-	-	26	NM	-	-
5	NM	-	-		NM	0.008	NC
	NM	0.006	-	27	NM	-	-
6	NM	-	-		NM	0.018	NC
	NM	-	-	28	NM	-	-
7	NM	-	-		NM	0.015	NC
	NM	0.008	NC	29	NM	0.009	NC
8	NM	-	-		NM	0.07	0.035
	NM	-	-	30	NM	0.07	0.013
9	NM	-	-	West End	NM	0.15	0.09375
	NM	0.01	NC				
10	NM	-	-				
	NM	-	-				
11	NM	-	-				
	NM	-	-				
12	NM	-	-				
	NM	-	-				
13	NM	-	-				
	NM	0.008	NC				
14	NM	-	-				
	NM	-	0.007				
15	NM	-	-				
	NM	-	-				
16	NM	-	-				
End of Panel B	NM	-	-				
End of Panel A	NM	0.14	0.09375				
17	NM	0.012	NC				
	NM	0.006	NC				
18	NM	0.014	0.012				
	NM	0.09	0.0625				
19	NM	0.012	NC				
	NM	0.013	NC				
20	NM	-	-				
	NM	0.012	NC				
21	NM	-	-				
	NM	0.012	0.003				

Inspection Dates:

Preliminary: 3/7/2016
 Intermediate: 5/18/2016
 Final: 8/26/2016

"-" indicates feeler gage cannot be inserted.
 "NM" indicates "Not Measured"
 "NC" indicates "No Change" from the previous inspection.

Table 7: Panel to Beam Gap at Stringer 3 Left

Bolt #	Gap			Bolt #	Gap		
	Preliminary	Intermediate	Final		Preliminary	Intermediate	Final
East End	NM	-	NC	22	NM	-	-
1	NM	-	0.0015		NM	-	0.0015
	NM	0.01	0.008	23	NM	-	-
2	NM	-	NC		NM	0.008	0.012
	NM	-	0.0015	24	NM	-	-
3	NM	-	NC		NM	-	-
	NM	-	-	25	NM	-	-
4	NM	-	NC		NM	0.008	0.004
	NM	0.006	0.006	26	NM	-	-
5	NM	-	NC		NM	-	-
	NM	0.005	0.003	27	NM	-	-
6	NM	-	-		NM	-	-
	NM	0.007	NC	28	NM	-	-
7	NM	-	-		NM	0.01	0.008
	NM	-	-	29	NM	-	-
8	NM	-	-		NM	-	-
	NM	-	-	30	NM	-	-
9	NM	-	-		NM	-	-
	NM	0.012	-	31	NM	-	-
10	NM	-	-		NM	0.012	0.01
	NM	0.01	NC	32	NM	-	-
11	NM	-	-		NM	-	-
	NM	0.008	NC	33	NM	-	-
12	NM	-	-		NM	0.012	0.015
	NM	-	-	34	NM	0.006	NC
13	NM	-	-	West End	NM	0.09	0.09375
	NM	-	-				
14	NM	-	-				
	NM	-	-				
15	NM	-	-				
	NM	0.008	NC				
16	NM	-	-				
	NM	0.008	NC				
17	NM	-	-				
	NM	-	-				
18	NM	-	-				
End of Panel B	NM	-	-				
End of Panel A	NM	0.13	0.09375				
19	NM	0.008	0.01				
	NM	0.01	0.015				
20	NM	0.016	NC				
	NM	0.1	0.025				
21	NM	0.005	NC				
	NM	0.01	NC				

Inspection Dates:

Preliminary: 3/7/2016
 Intermediate: 5/18/2016
 Final: 8/26/2016

"-" indicates feeler gage cannot be inserted.
 "NM" indicates "Not Measured"
 "NC" indicates "No Change" from the previous inspection.

Table 8: Panel to Beam Gap at Stringer 3 Right

Bolt #	Gap			Bolt #	Gap		
	Preliminary	Intermediate	Final		Preliminary	Intermediate	Final
East End	0.0015	NC	0.01	22	-	NC	NC
1	0.004	NC	0.06		0.012	NC	0.013
	0.006	0.014	0.016	23	-	NC	NC
2	-	NC	NC		0.014	NC	0.015
	0.008	NC	0.003	24	-	NC	NC
3	-	NC	NC		-	NC	0.006
	0.0015	NC	-	25	-	NC	NC
4	-	NC	NC		0.012	NC	0.02
	-	NC	NC	26	-	NC	NC
5	-	NC	NC		0.011	0.015	0.018
	-	NC	NC	27	-	NC	NC
6	-	NC	NC		0.009	NC	NC
	0.012	NC	0.01	28	-	NC	NC
7	0.0015	NC	-		0.012	NC	0.016
	-	NC	NC	29	0.014	NC	0.011
8	-	NC	NC		0.008	NC	0.005
	-	NC	NC	30	-	NC	NC
9	-	NC	NC		0.007	NC	0.007
	0.015	NC	0.018	31	-	NC	NC
10	-	NC	NC		0.016	NC	0.022
	0.003	NC	-	32	-	NC	NC
11	0.004	NC	-		0.012	NC	NC
	0.01	NC	NC	33	-	NC	NC
12	-	NC	NC		0.024	NC	0.035
	0.0015	NC	-	34	0.012	NC	0.015
13	-	NC	NC	West End	0.09	NC	0.115
	-	NC	NC				
14	0.0015	NC	-				
	-	NC	NC				
15	0.0015	NC	-				
	0.011	NC	0.015				
16	-	NC	NC				
	0.004	0.011	-				
17	-	NC	NC				
	-	NC	NC				
18	-	NC	NC				
End of Panel B	-	NC	NC				
End of Panel A	0.08	NC	NC				
19	0.02	NC	NC				
	0.01	NC	0.005				
20	0.01	NC	NC				
	0.06	NC	0.035				
21	0.006	NC	NC				
	0.018	NC	0.02				

Inspection Dates:

Preliminary: 3/7/2016
 Intermediate: 5/18/2016
 Final: 8/26/2016

"-" indicates feeler gage cannot be inserted.
 "NM" indicates "Not Measured"
 "NC" indicates "No Change" from the previous inspection.

Appendix E: Visual Inspection Photo Inventory

Photo Inventory:

Preliminary Inspection



A1-1.1



A1-1.2



A1-1.3



A1-1.4



A1-1.5



A1-2.1



A1-2.2



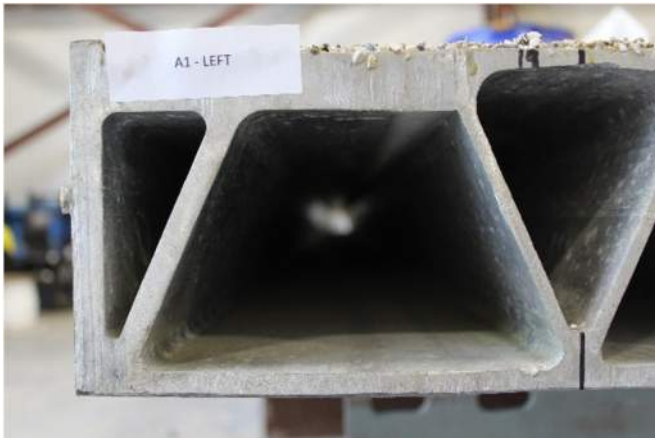
A1-2.3



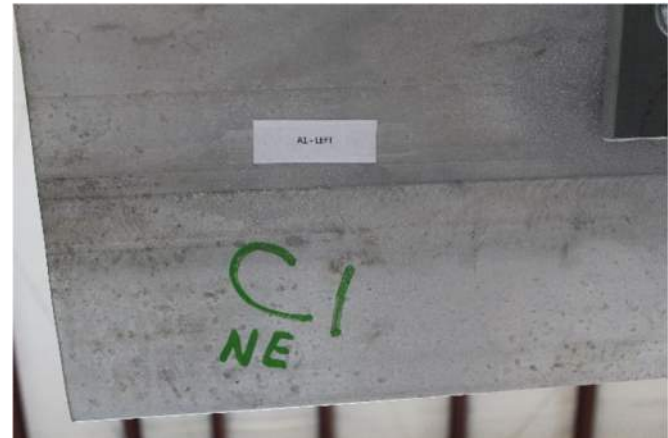
A1-2.4



A1-2.5



A1-LEFT



A1-LEFT-BOTTOM



A1-RIGHT



A1-RIGHT-BOTTOM



A2-1.1



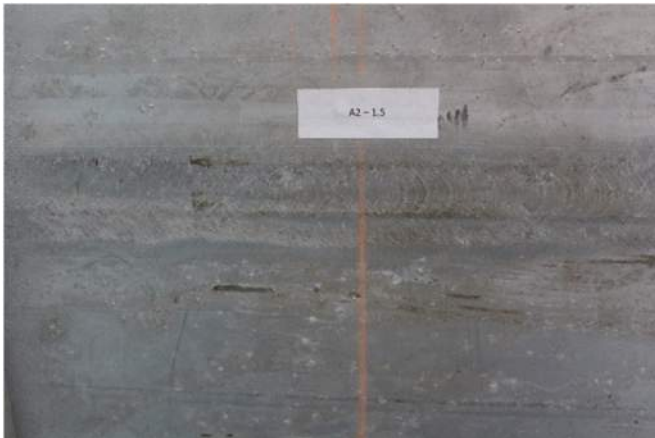
A2-1.2



A2-1.3



A2-1.4



A2-1.5



A2-2.1



A2-2.2



A2-2.3



A2-2.4



A2-2.5



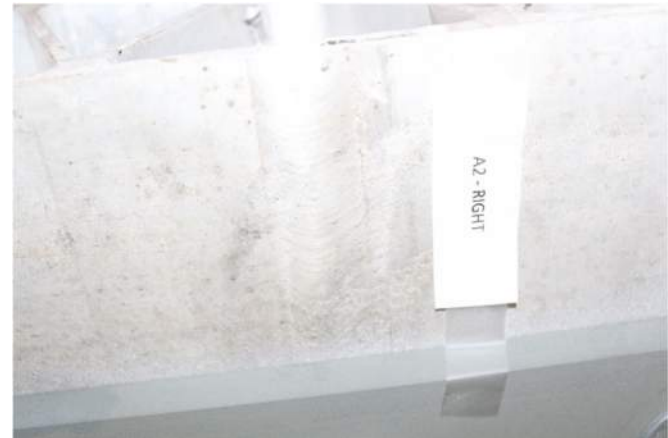
A2-LEFT



A2-LEFT-BOTTOM



A2-RIGHT



A2-RIGHT-BOTTOM



A3-1.1



A3-1.2



A3-1.3



A3-1.4



A3-1.5



A3-2.1



A3-2.2



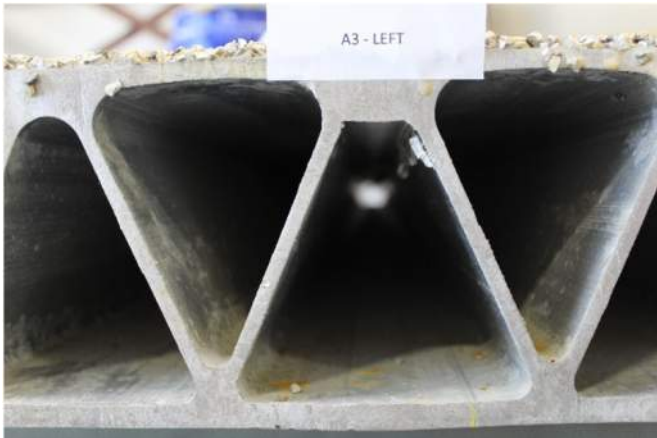
A3-2.3



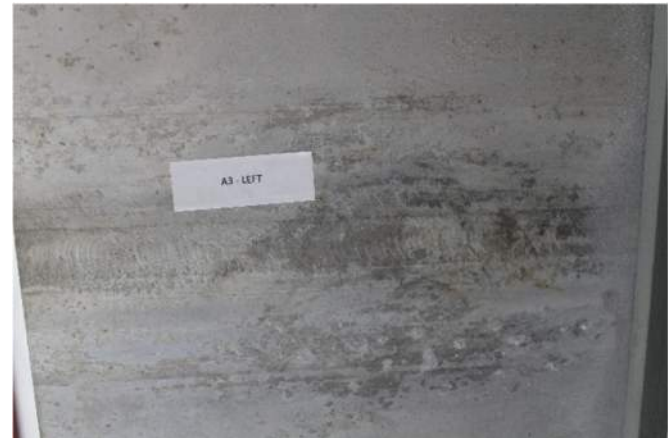
A3-2.4



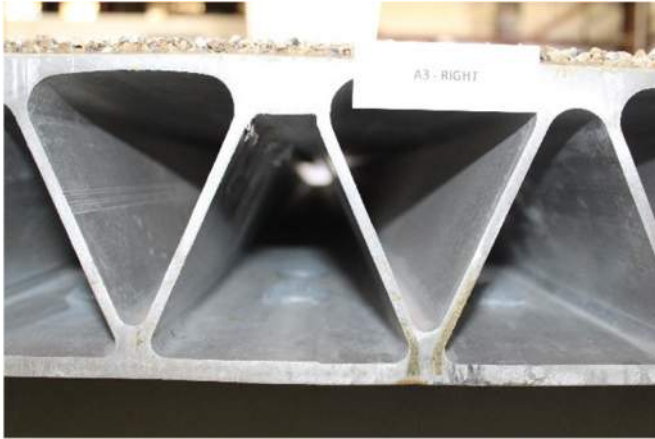
A3-2.5



A3-LEFT



A3-LEFT-BOTTOM



A3-RIGHT



A3-RIGHT-BOTTOM



A4-1.1



A4-1.2



A4-1.3



A4-1.3TO1.4



A4-1.4



A4-1.5



A4-2.1



A4-2.2



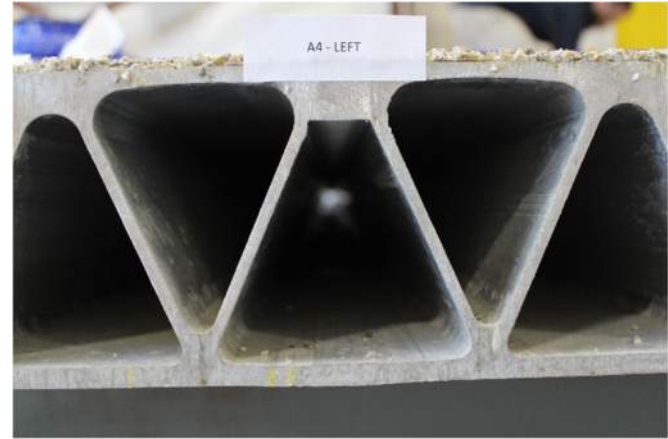
A4-2.3



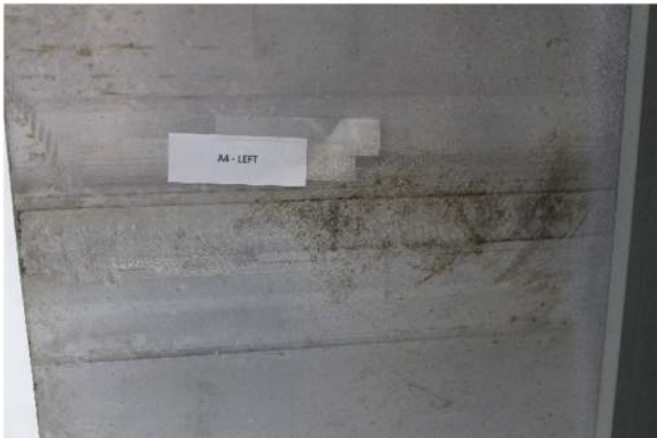
A4-2.4



A4-2.5



A4-LEFT



A4-LEFT-BOTTOM



A4-RIGHT



A4-RIGHT-BOTTOM



A5-1.1



A5-1.2



A5-1.3



A5-1.4



A5-1.5



A5-2.1



A5-2.2



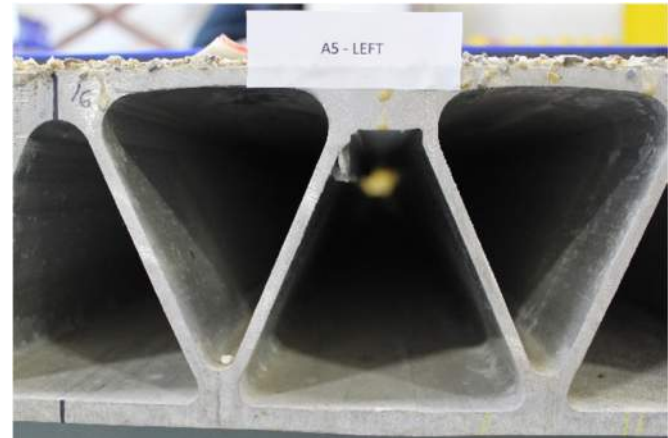
A5-2.3



A5-2.4



A5-2.5



A5-LEFT



A5-LEFT-BOTTOM



A5-RIGHT



A5-RIGHT-BOTTOM



A6-1.1



A6-1.2



A6-1.3



A6-1.4



A6-1.5



A6-2.1



A6-2.2



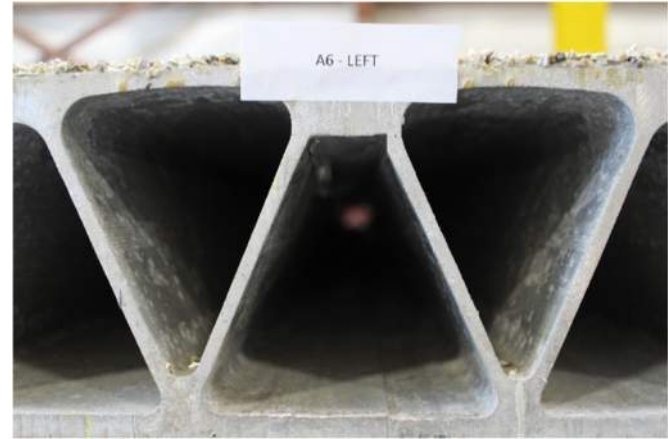
A6-2.3



A6-2.4



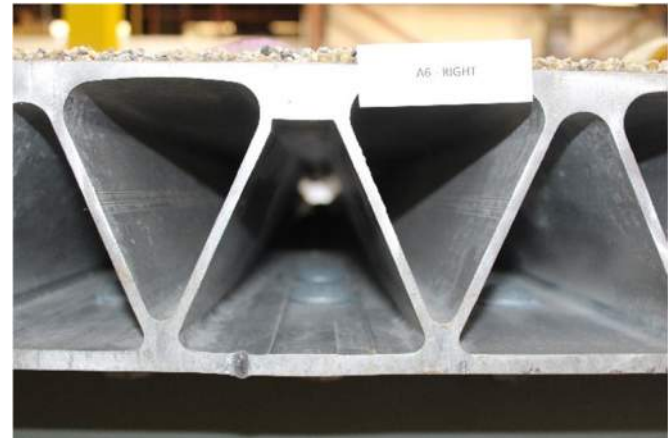
A6-2.5



A6-LEFT



A6-LEFT-BOTTOM



A6-RIGHT



A6-RIGHT-BOTTOM



A7-1.1



A7-1.2



A7-1.3



A7-1.4



A7-1.5



A7-2.1



A7-2.2



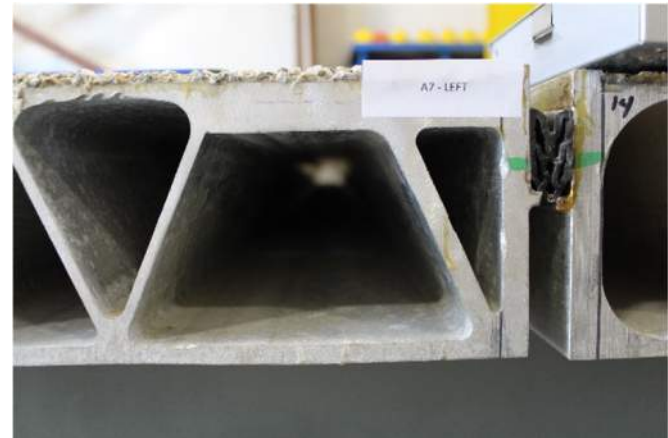
A7-2.3



A7-2.4



A7-2.5



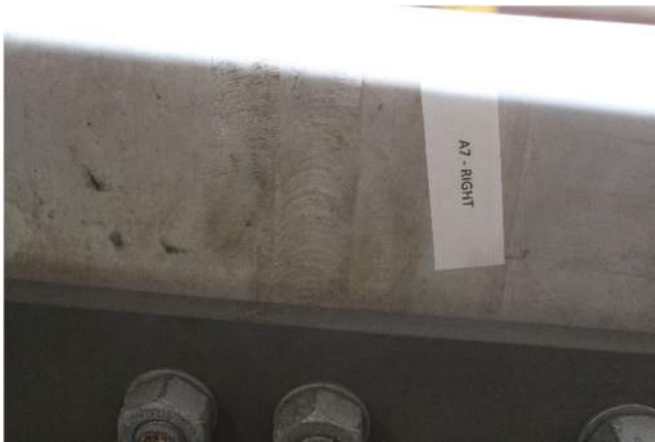
A7-LEFT



A7-LEFT-BOTTOM



A7-RIGHT



A7-RIGHT-BOTTOM



B1-1.1



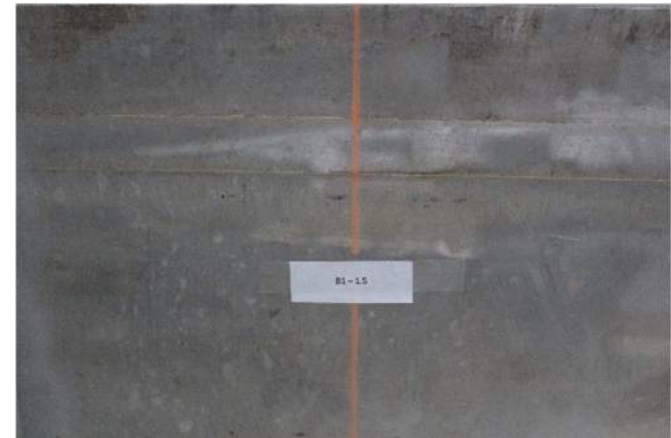
B1-1.2



B1-1.3



B1-1.4



B1-1.5



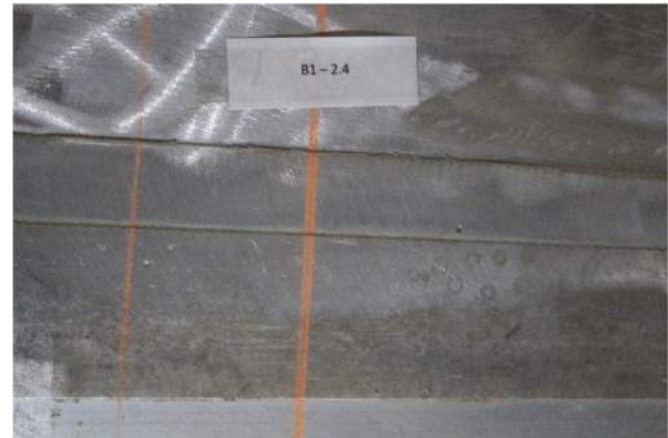
B1-2.1



B1-2.2



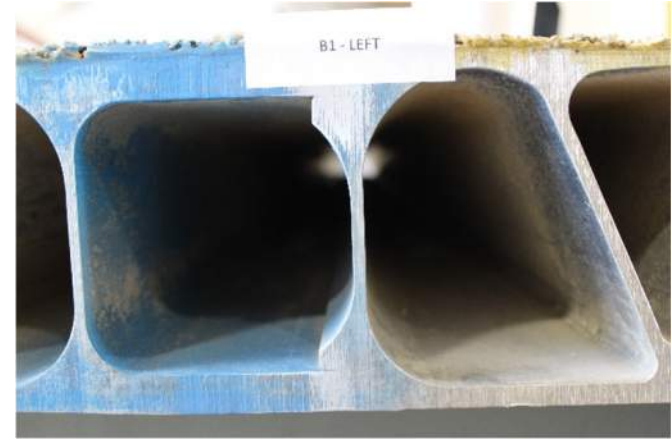
B1-2.3



B1-2.4



B1-2.5



B1-LEFT



B1-LEFT-BOTTOM3



B1-RIGHT



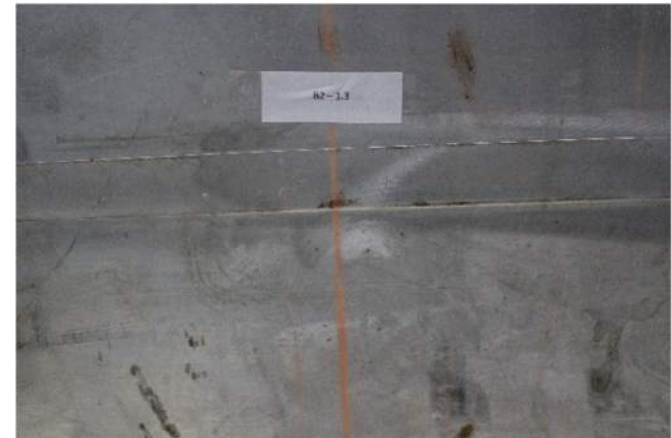
B1-RIGHT-BOTTOM



B2-1.1



B2-1.2



B2-1.3



B2-1.4



B2-1.5



B2-2.1



B2-2.2



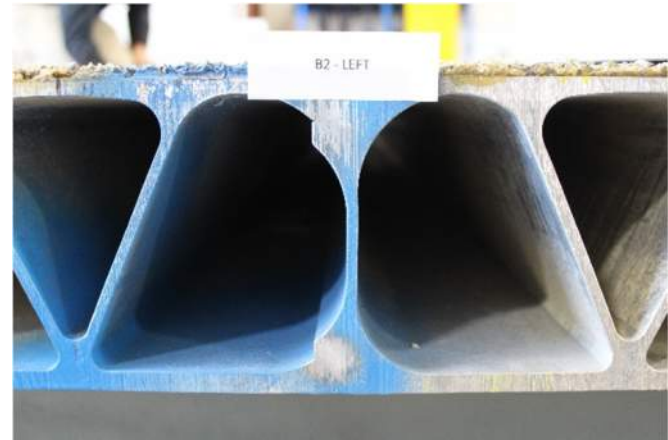
B2-2.3



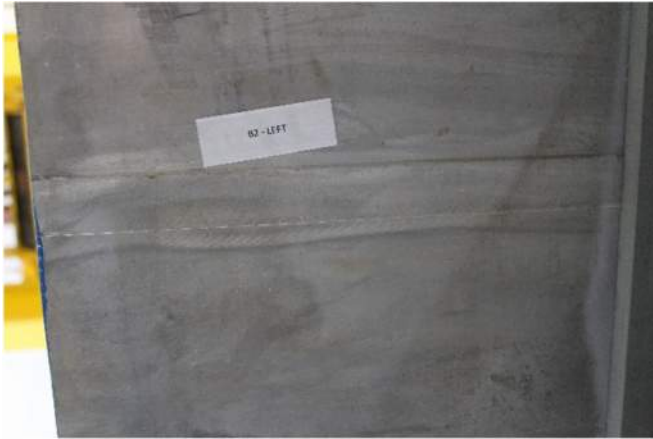
B2-2.4



B2-2.5



B2-LEFT



B2-LEFT-BOTTOM



B2-RIGHT



B2-RIGHT-BOTTOM



B3-1.1



B3-1.2



B3-1.3



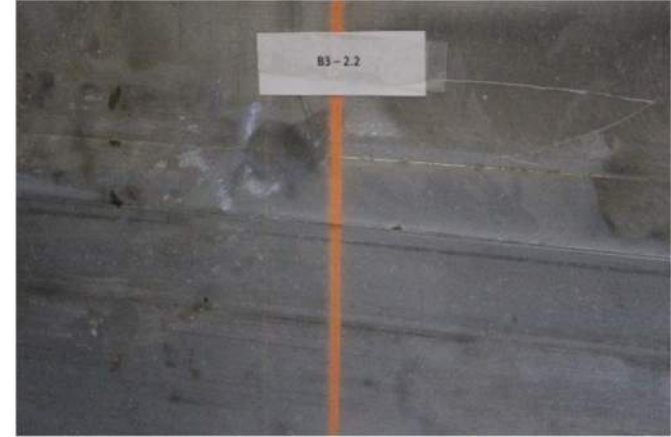
B3-1.4



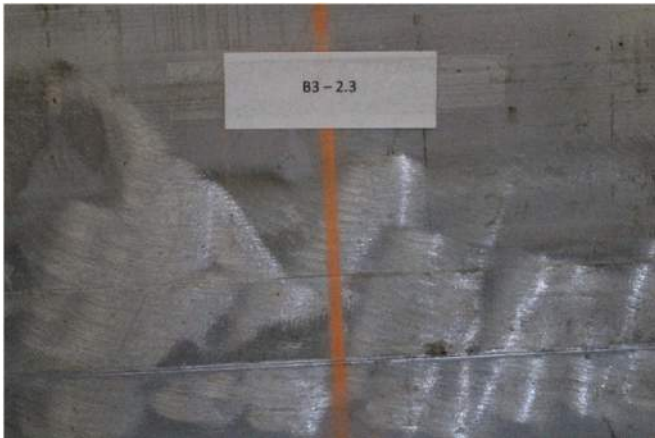
B3-1.5



B3-2.1



B3-2.2



B3-2.3



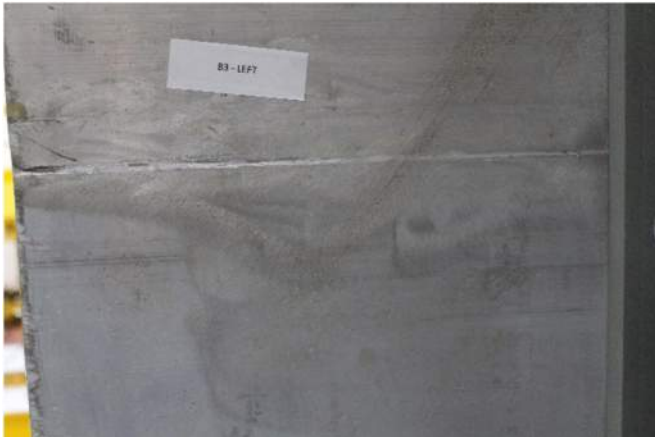
B3-2.4



B3-2.5



B3-LEFT



B3-LEFT-BOTTOM



B3-RIGHT



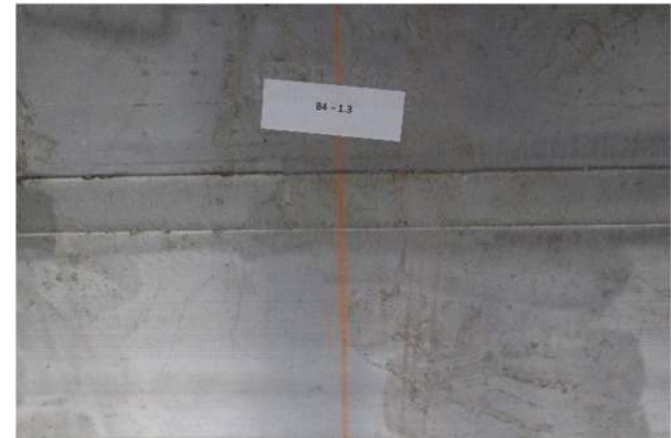
B3-RIGHT-BOTTOM



B4-1.1



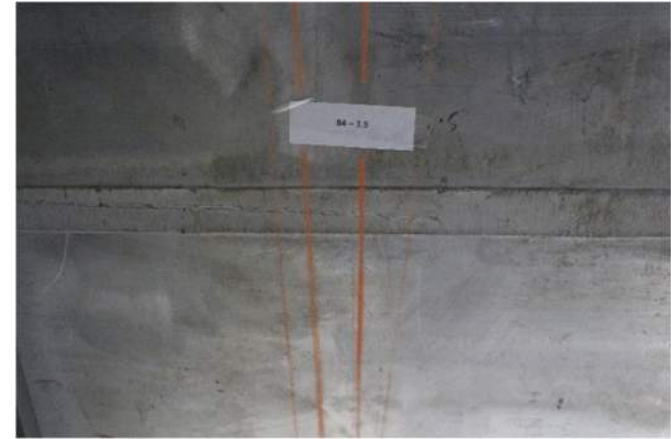
B4-1.2



B4-1.3



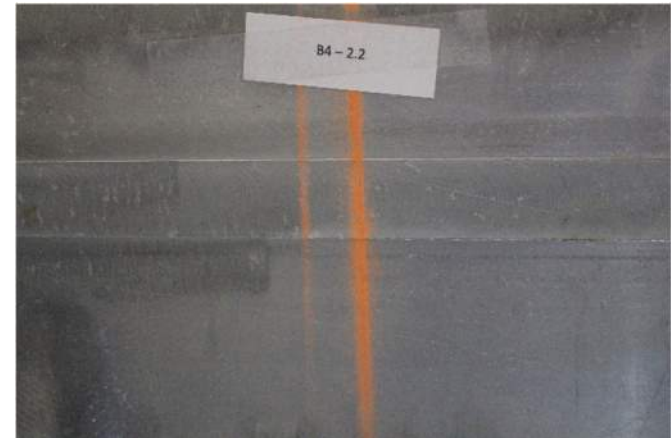
B4-1.4



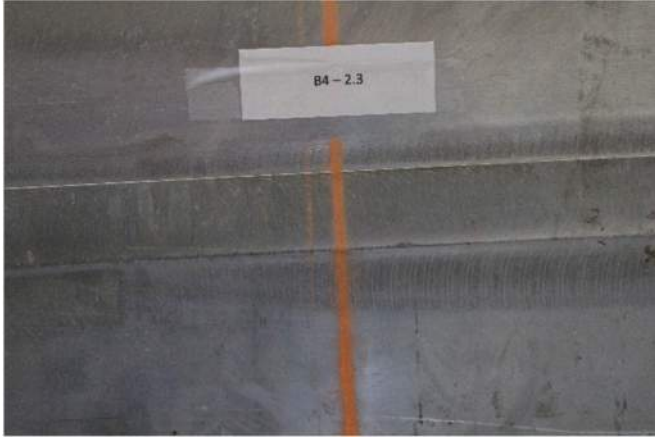
B4-1.5



B4-2.1



B4-2.2



B4-2.3



B4-2.4



B4-2.5



B4-LEFT



B4-LEFT-BOTTOM



B4-RIGHT



B4-RIGHT-BOTTOM



B5-1.1



B5-1.2



B5-1.3



B5-1.4



B5-1.5



B5-2.1



B5-2.2



B5-2.3



B5-2.4



B5-2.5



B5-LEFT



B5-LEFT-BOTTOM



B5-RIGHT



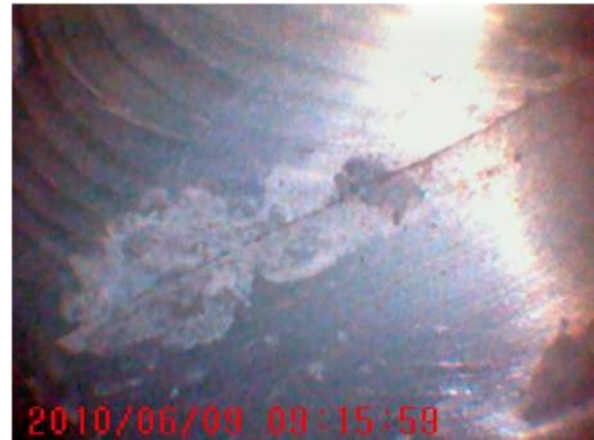
B5-RIGHT-BOTTOM



BORESCOPE (1)



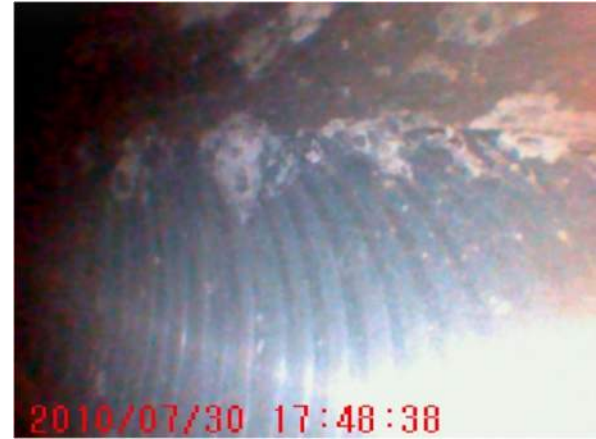
BORESCOPE (2)



BORESCOPE (3)



BORESCOPE (4)



BORESCOPE (5)



BORESCOPE (6)



BORESCOPE (7)



BORESCOPE (8)



BORESCOPE (9)



BORESCOPE (10)



BORESCOPE (11)



BORESCOPE (12)



BORESCOPE (13)



BORESCOPE (14)



BORESCOPE (15)



BORESCOPE (16)



SUPPORT STAIN

Photo Inventory:

Intermediate Inspection



A1-1.1



A1-1.2



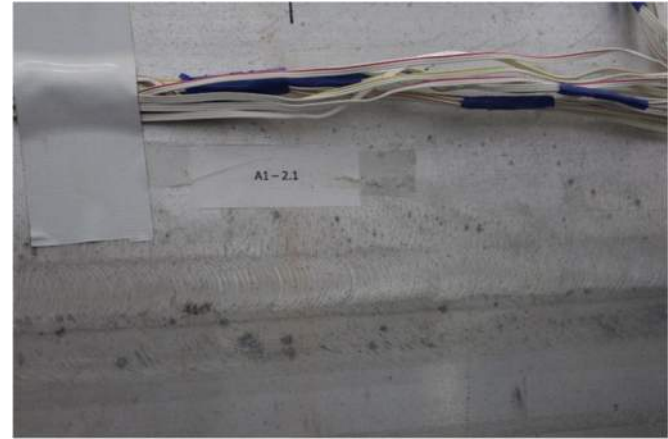
A1-1.3



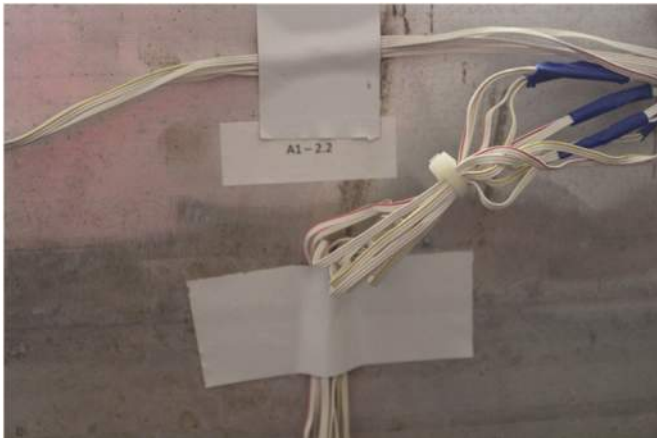
A1-1.4



A1-1.5



A1-2.1



A1-2.2



A1-2.3



A1-2.4



A1-2.5



A1-LEFT



A1-LEFT-BOTTOM



A1-RIGHT



A1-RIGHT-BOTTOM



A2-1.1



A2-1.2



A2-1.3



A2-1.4



A2-1.5



A2-2.1



A2-2.2



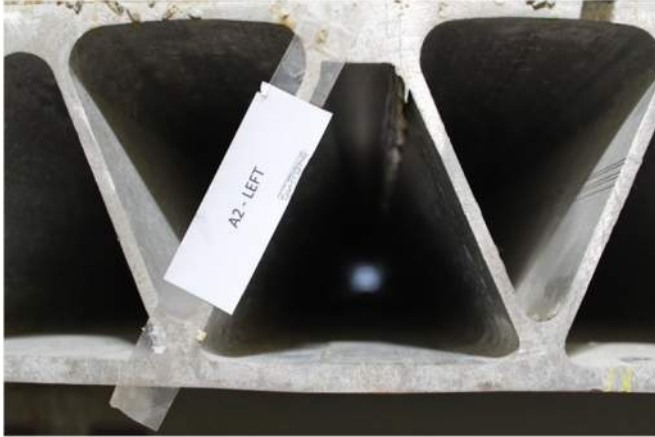
A2-2.3



A2-2.4



A2-2.5



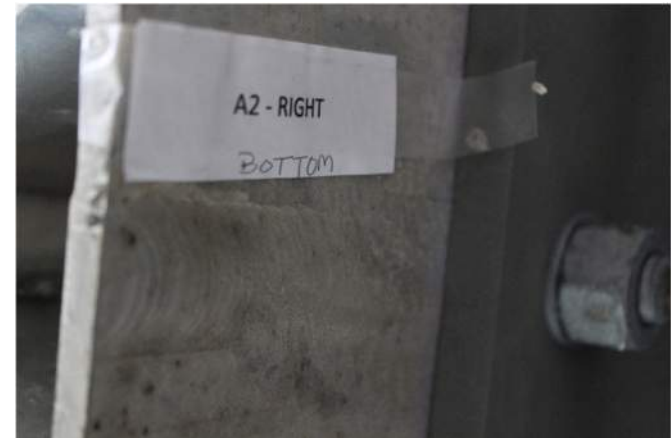
A2-LEFT



A2-LEFT-BOTTOM



A2-RIGHT



A2-RIGHT-BOTTOM



A3-1.1



A3-1.2



A3-1.3



A3-1.4



A3-1.5



A3-2.1



A3-2.2



A3-2.3



A3-2.4



A3-2.5



A3-LEFT



A3-LEFT-BOTTOM



A3-RIGHT



A3-RIGHT-BOTTOM



A4-1.1



A4-1.2



A4-1.3



A4-1.4



A4-1.5



A4-2.1



A4-2.2



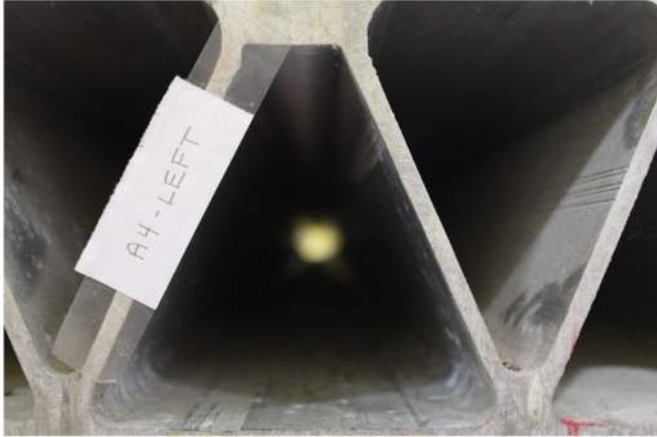
A4-2.3



A4-2.4



A4-2.5



A4-LEFT



A4-LEFT-BOTTOM



A4-RIGHT



A4-RIGHT-BOTTOM



A5-1.1



A5-1.2



A5-1.3



A5-1.4



A5-1.5



A5-2.1



A5-2.2



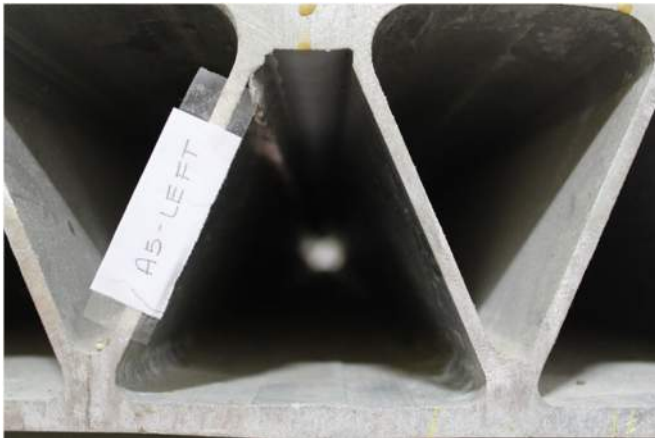
A5-2.3



A5-2.4



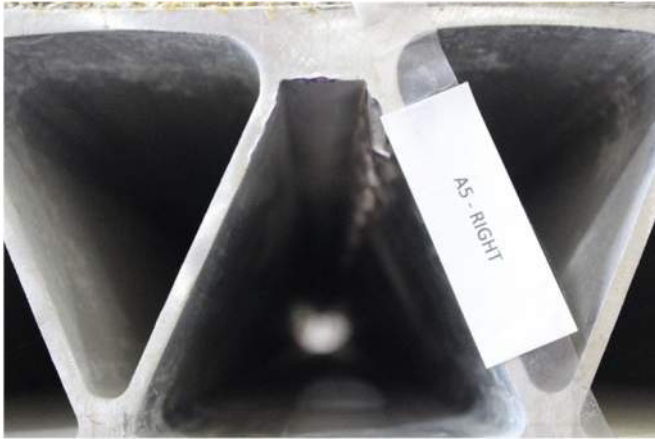
A5-2.5



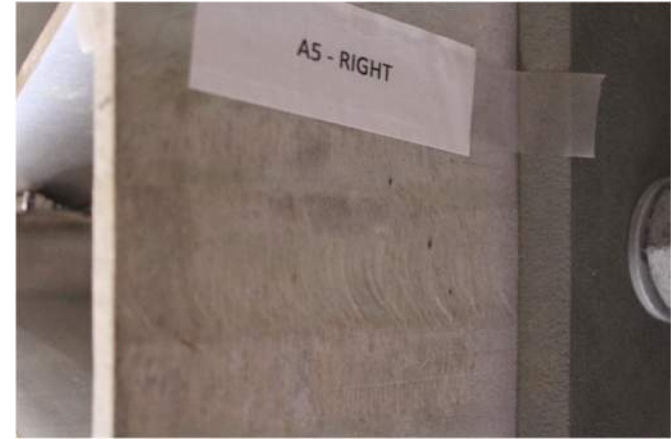
A5-LEFT



A5-LEFT-BOTTOM



A5-RIGHT



A5-RIGHT-BOTTOM



A6-1.1



A6-1.2



A6-1.3



A6-1.4



A6-1.5



A6-2.1



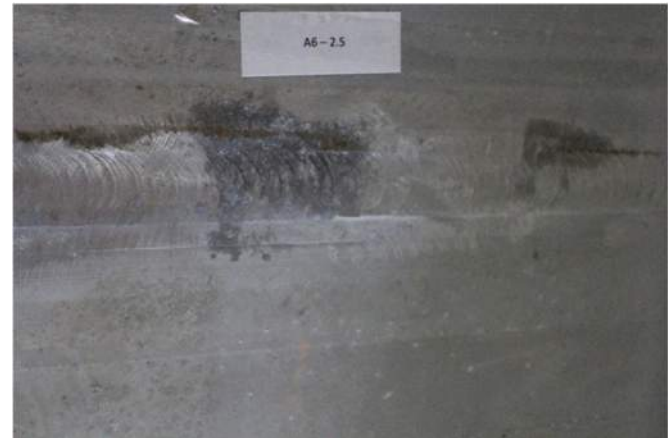
A6-2.2



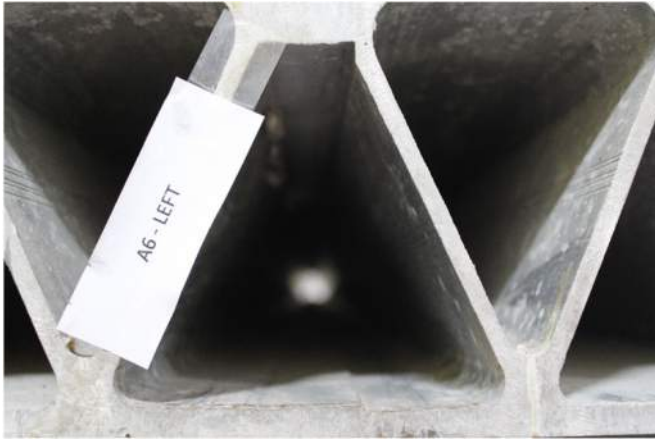
A6-2.3



A6-2.4



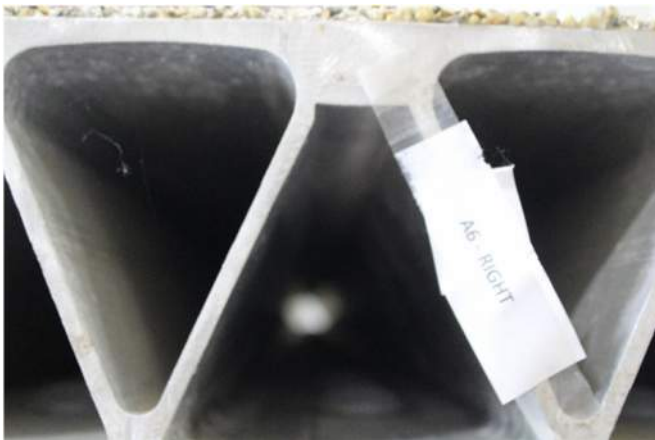
A6-2.5



A6-LEFT



A6-LEFT-BOTTOM



A6-RIGHT



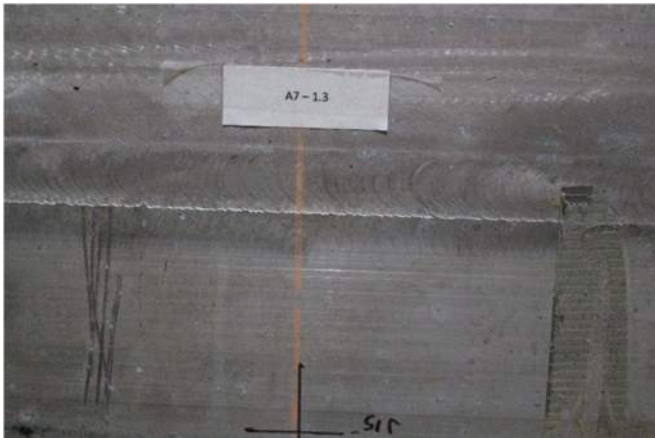
A6-RIGHT-BOTTOM



A7-1.1



A7-1.2



A7-1.3



A7-1.4



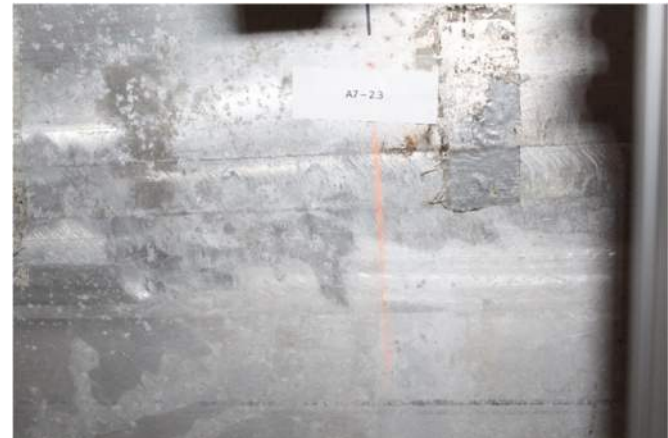
A7-1.5



A7-2.1



A7-2.2



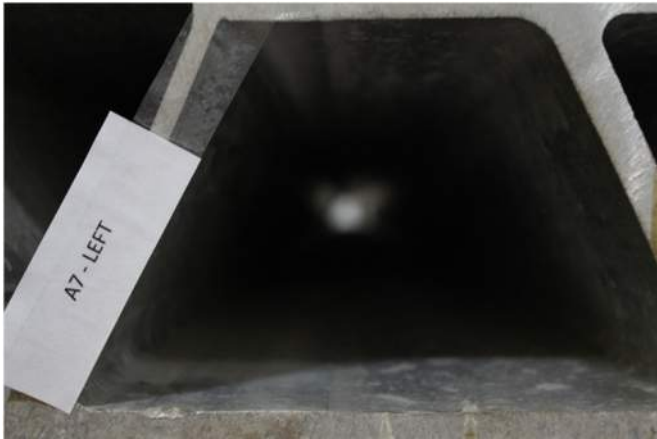
A7-2.3



A7-2.4



A7-2.5



A7-LEFT



A7-LEFT-BOTTOM



A7-RIGHT



A7-RIGHT-BOTTOM



B1-1.1



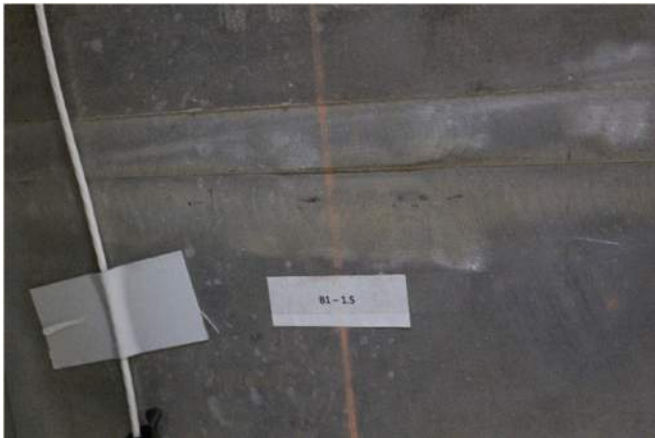
B1-1.2



B1-1.3



B1-1.4



B1-1.5



B1-2.1



B1-2.2



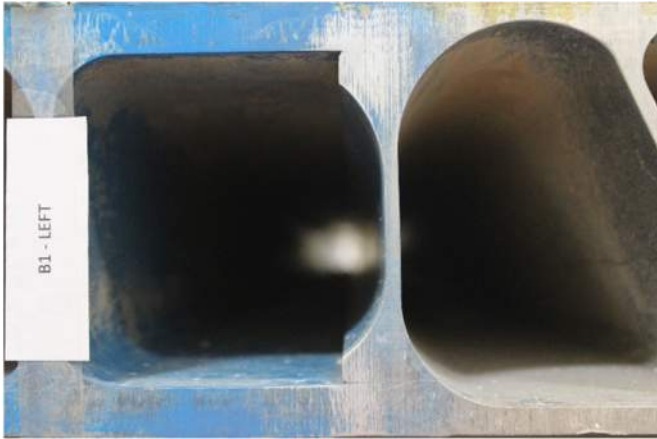
B1-2.3



B1-2.4



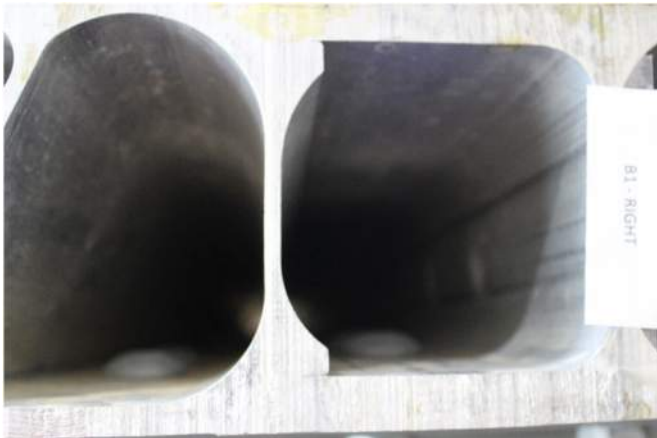
B1-2.5



B1-LEFT



B1-LEFT-BOTTOM



B1-RIGHT



B1-RIGHT-BOTTOM



B2-1.1



B2-1.2



B2-1.3



B2-1.4



B2-1.5



B2-2.1



B2-2.2



B2-2.3



B2-2.4



B2-2.5



B2-LEFT



B2-LEFT-BOTTOM



B2-RIGHT



B2-RIGHT-BOTTOM



B3-1.1



B3-1.2



B3-1.3



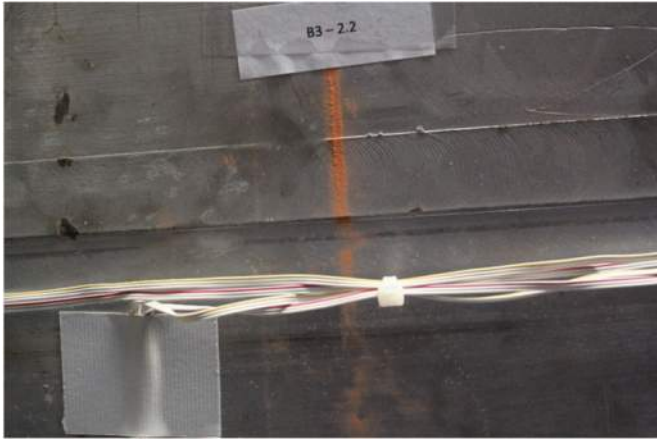
B3-1.4



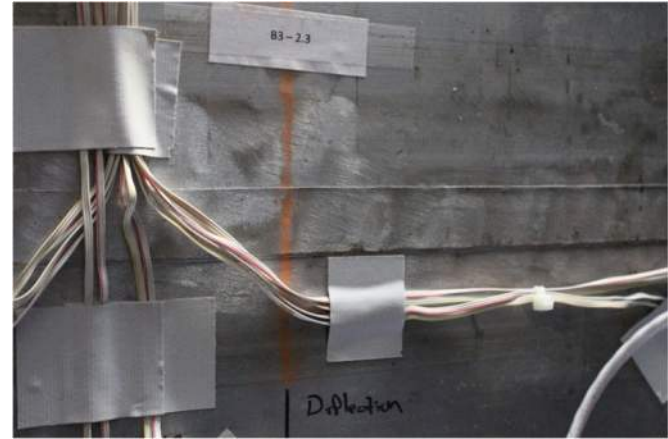
B3-1.5



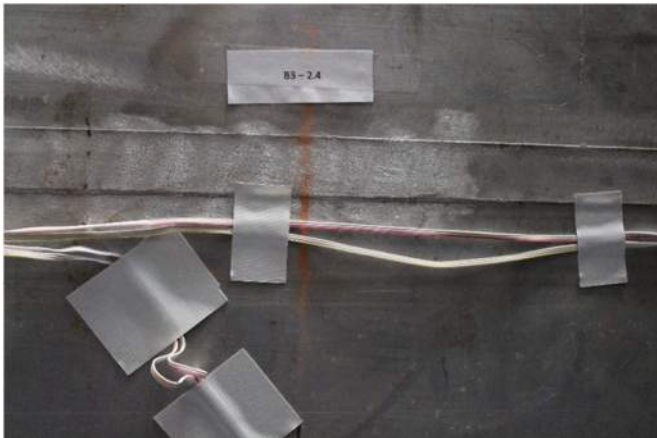
B3-2.1



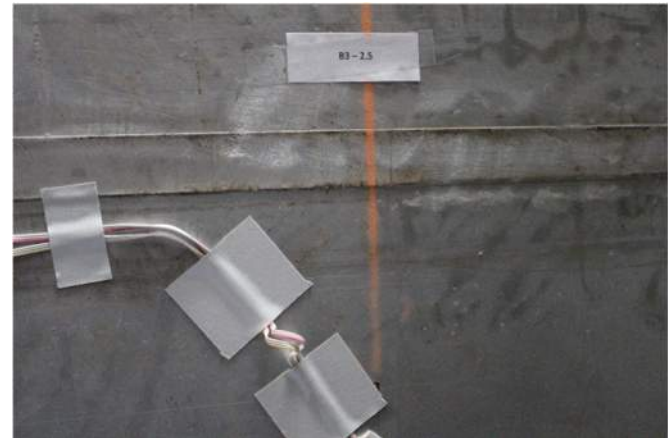
B3-2.2



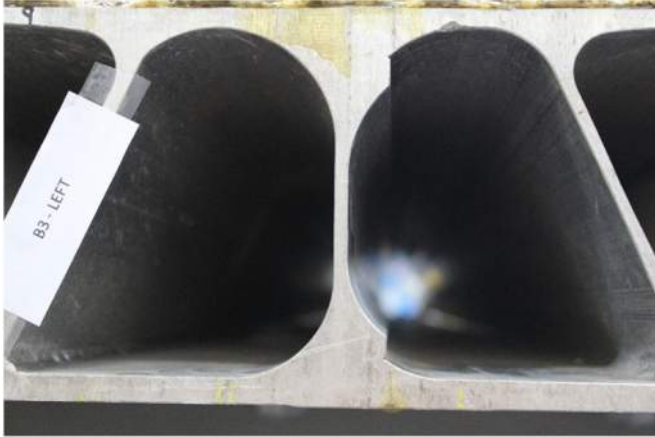
B3-2.3



B3-2.4



B3-2.5



B3-LEFT



B3-LEFT-BOTTOM



B3-RIGHT



B3-RIGHT-BOTTOM



B4-1.1



B4-1.2



B4-1.3



B4-1.4



B4-1.5



B4-2.1



B4-2.2



B4-2.3



B4-2.4



B4-2.5



B4-LEFT



B4-LEFT-BOTTOM



B4-RIGHT



B4-RIGHT-BOTTOM



B5-1.1



B5-1.2



B5-1.3



B5-1.4



B5-1.5



B5-2.1



B5-2.2



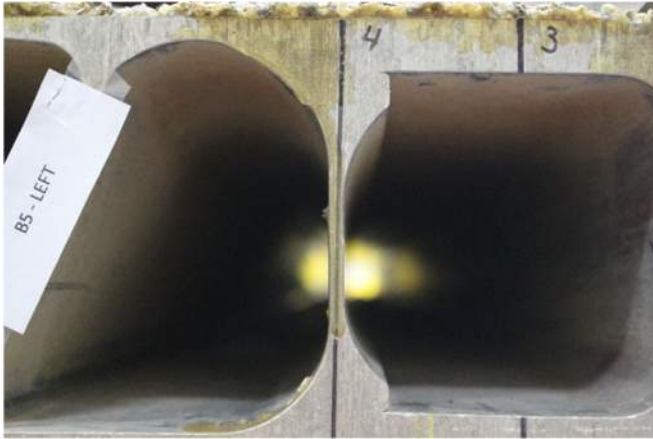
B5-2.3



B5-2.4



B5-2.5



B5-LEFT



B5-LEFT-BOTTOM



B5-RIGHT



B5-RIGHT-BOTTOM

Photo Inventory:

Final Inspection



A1-1.1



A1-1.2



A1-1.3



A1-1.4



A1-1.5



A1-2.1



A1-2.2



A1-2.3



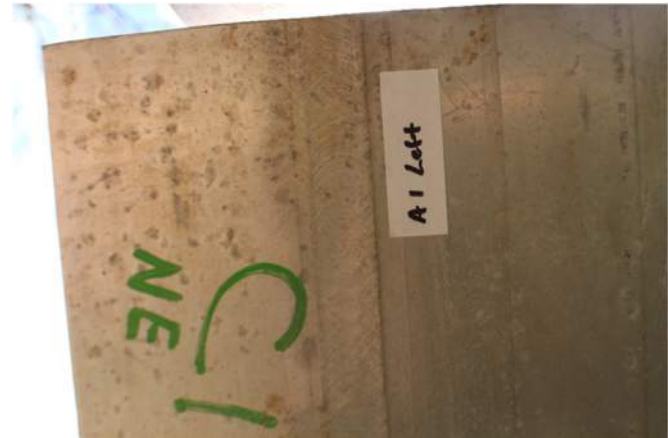
A1-2.4



A1-2.5



A1-LEFT



A1-LEFT-BOTTOM



A1-RIGHT



A1-RIGHT-BOTTOM



A2-1.1



A2-1.2



A2-1.3



A2-1.4



A2-1.5



A2-2.1



A2-2.2



A2-2.3



A2-2.4



A2-2.5



A2-LEFT



A2-LEFT-BOTTOM



A2-RIGHT



A2-RIGHT-BOTTOM



A3-1.1



A3-1.2



A3-1.3



A3-1.4



A3-1.5



A3-2.1



A3-2.2



A3-2.3



A3-2.4



A3-2.5



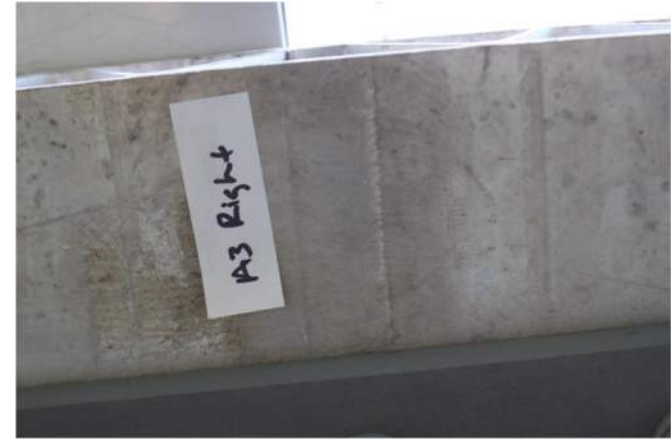
A3-LEFT



A3-LEFT-BOTTOM



A3-RIGHT



A3-RIGHT-BOTTOM



A4-1.1



A4-1.2



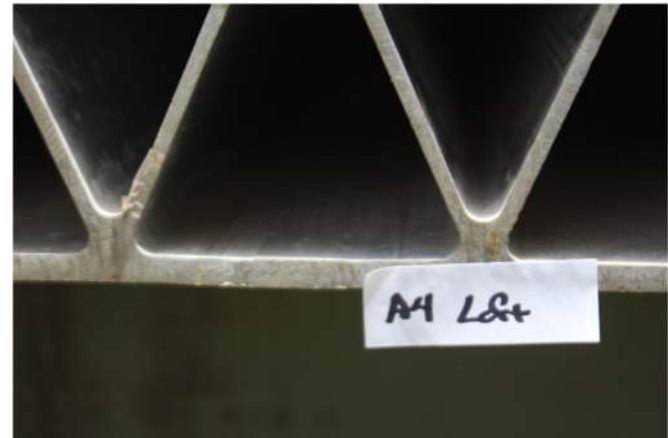
A4-1.3



A4-1.4



A4-1.5



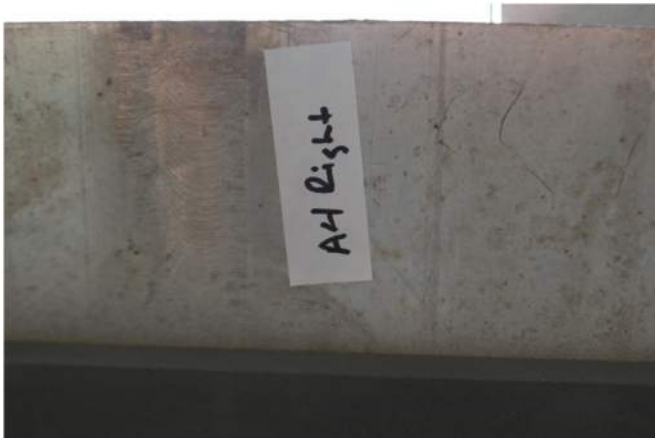
A4-LEFT



A4-LEFT-BOTTOM



A4-RIGHT



A4-RIGHT-BOTTOM



A5-1.1



A5-1.2



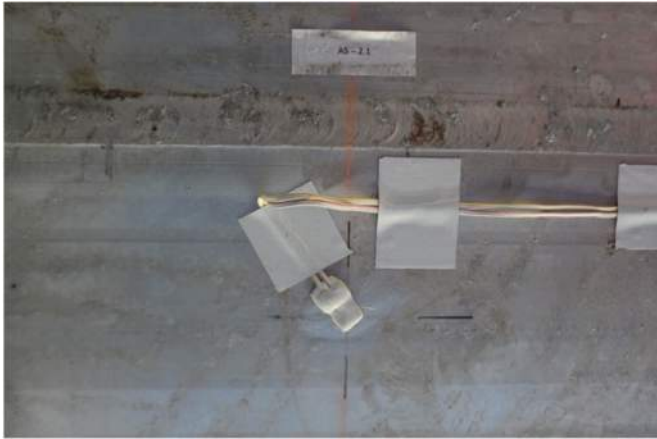
A5-1.3



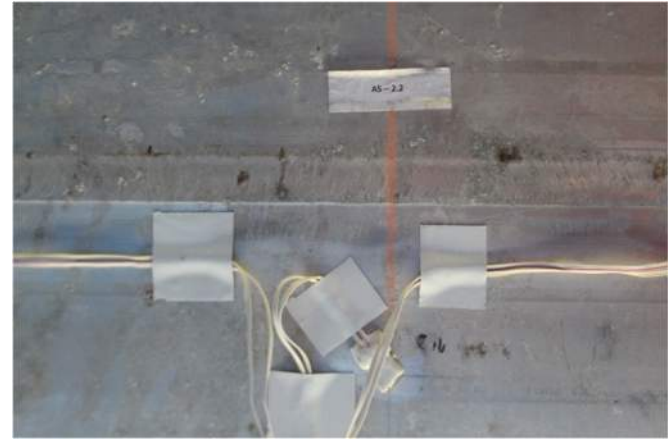
A5-1.4



A5-1.5



A5-2.1



A5-2.2



A5-2.3



A5-2.4



A5-2.5



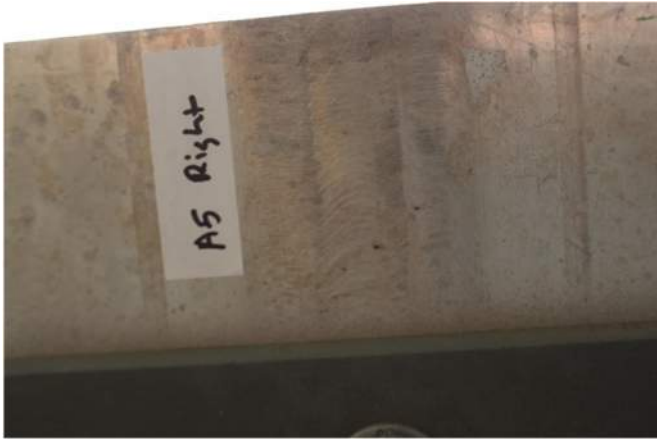
A5-LEFT



A5-LEFT-BOTTOM



A5-RIGHT



A5-RIGHT-BOTTOM



A6-1.1



A6-1.2



A6-1.3



A6-1.4



A6-1.5



A6-2.1



A6-2.2



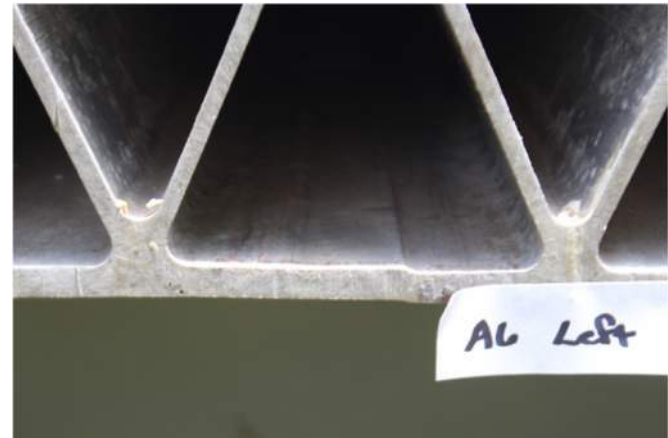
A6-2.3



A6-2.4



A6-2.5



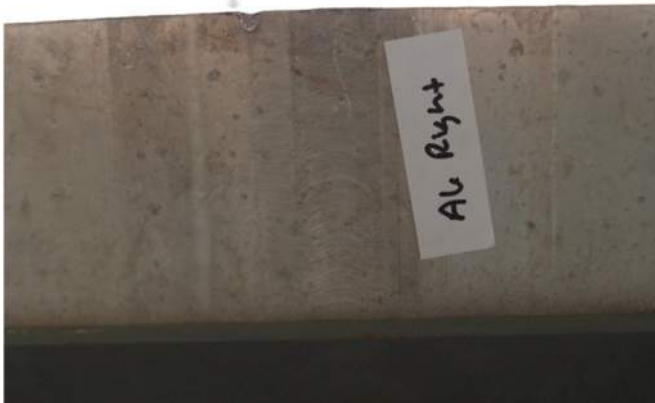
A6-LEFT



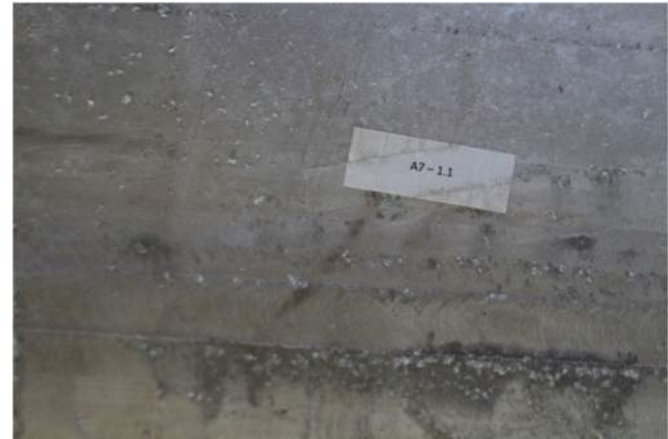
A6-LEFT-BOTTOM



A6-RIGHT



A6-RIGHT-BOTTOM



A7-1.1



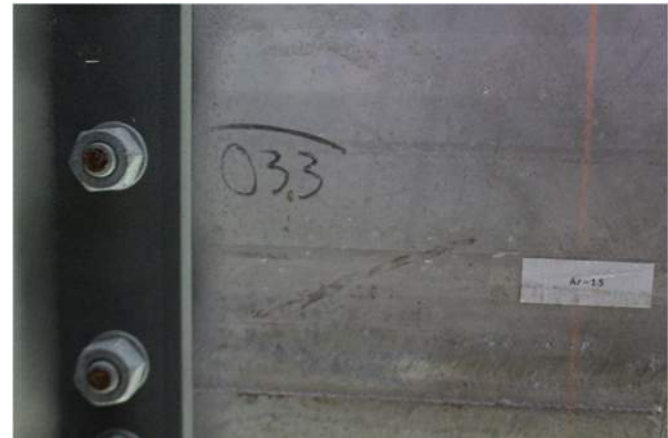
A7-1.2



A7-1.3



A7-1.4



A7-1.5



A7-2.1



A7-2.2



A7-2.3



A7-2.4



A7-2.5



A7-LEFT



A7-LEFT-BOTTOM



A7-RIGHT



A7-RIGHT-BOTTOM



B1-1.1



B1-1.2



B1-1.3



B1-1.4



B1-1.5



B1-2.1



B1-2.3



B1-2.4



B1-2.5



B1-LEFT



B1-LEFT-BOTTOM



B1-RIGHT



B1-RIGHT-BOTTOM



B2-1.1



B2-1.2



B2-1.3



B2-1.4



B2-1.5



B2-2.1



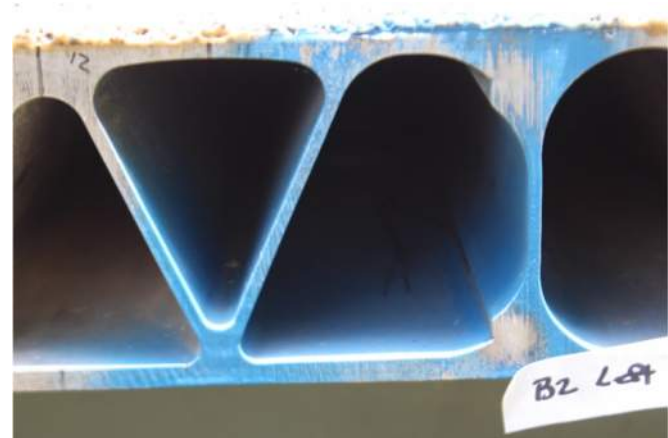
B2-2.2



B2-2.4



B2-2.5



B2-LEFT



B2-LEFT-BOTTOM



B2-RIGHT



B2-RIGHT-BOTTOM



B3-1.1



B3-1.2



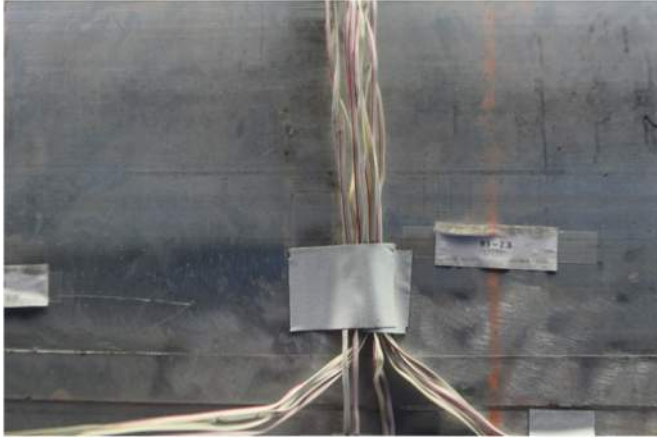
B3-1.3



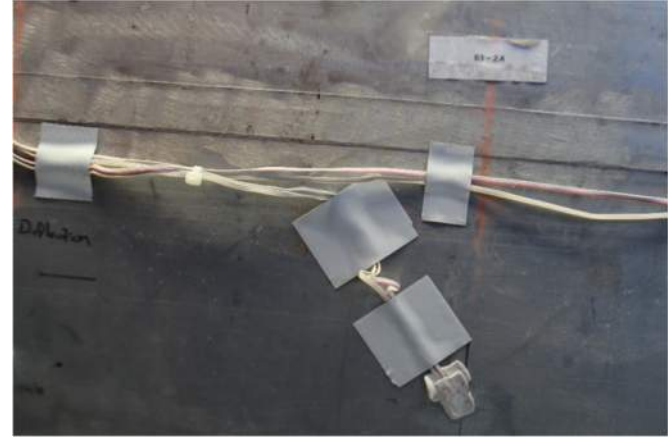
B3-1.4



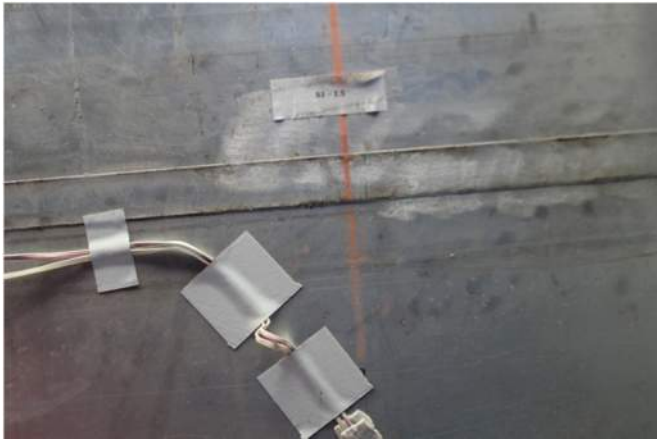
B3-1.5



B3-2.3



B3-2.4



B3-2.5



B3-LEFT



B3-LEFT-BOTTOM



B3-RIGHT



B3-RIGHT-BOTTOM



B4-1.1



B4-1.2



B4-1.3



B4-1.4



B4-1.5



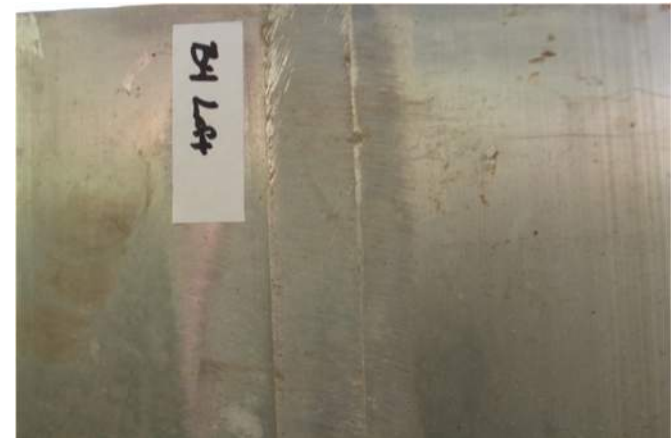
B4-2.2



B4-2.3



B4-LEFT



B4-LEFT-BOTTOM



B4-RIGHT



B4-RIGHT-BOTTOM



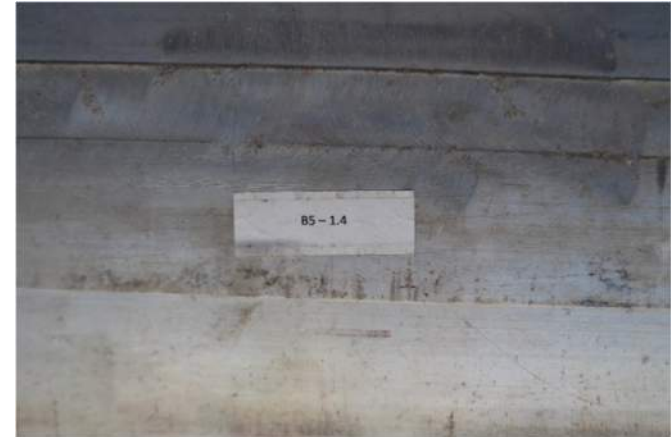
B5-1.1



B5-1.2



B5-1.3



B5-1.4



B5-1.5



B5-2.1



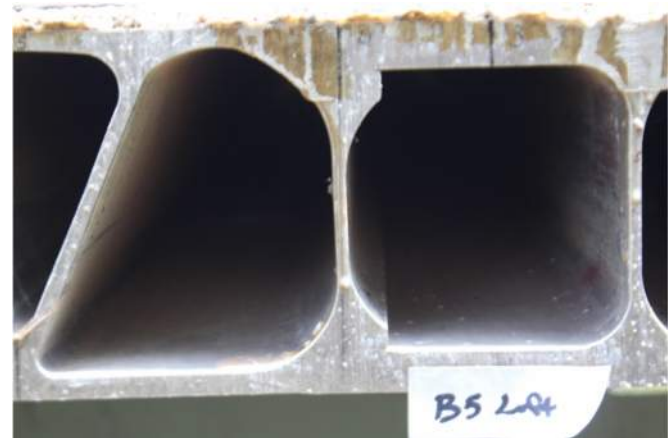
B5-2.2



B5-2.3



B5-2.4



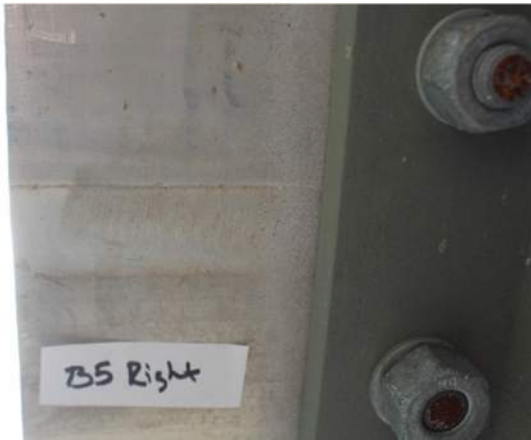
B5-LEFT



B5-LEFT-BOTTOM

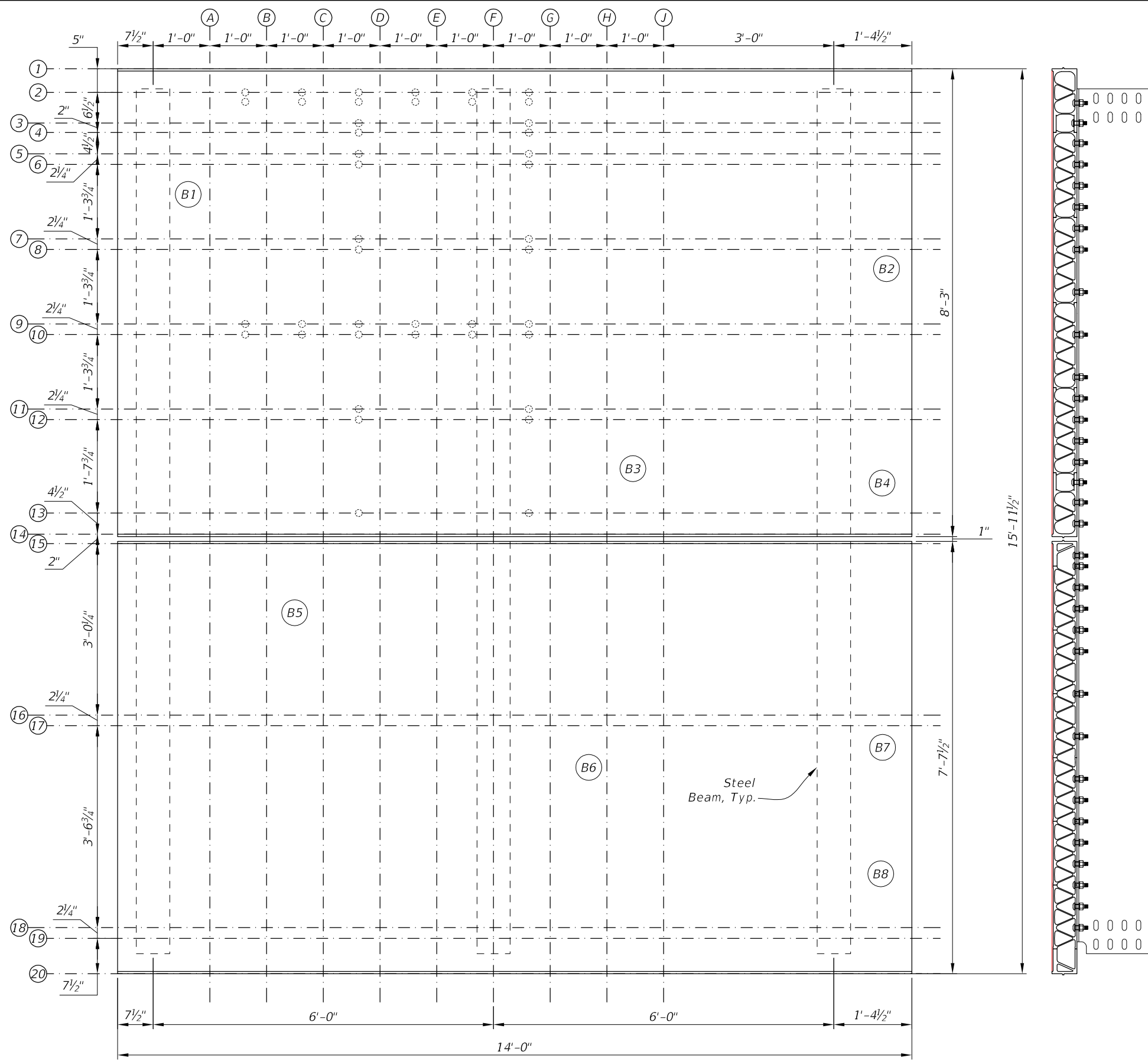


B5-RIGHT



B5-RIGHT-BOTTOM

Appendix F: Bond Test Location Plan and Photo Inventory



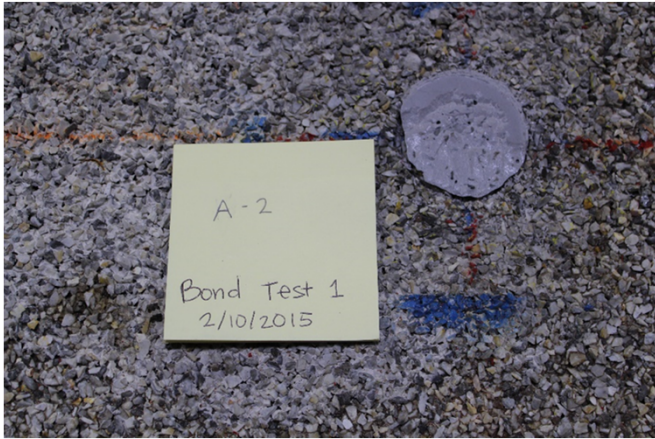
LEGEND
 (B#) Denotes Bond Test Location and Number

PLAN

REVISIONS						DRAWN BY: CJF 12-15	STATE OF FLORIDA DEPARTMENT OF TRANSPORTATION			SHEET TITLE: Bond Test 1B Plan	REF. DWG. NO.
DATE	BY	DESCRIPTION	DATE	BY	DESCRIPTION		ROAD NO.	COUNTY	FINANCIAL PROJECT ID.		
---	---	---	---	---	---	??					
---	---	---	---	---	---	DESIGNED BY: CJF 12-15	RD #	COUNTY	FPID #	PROJECT NAME: Lightweight Aluminum Deck Testing	SHEET NO. D-1
---	---	---	---	---	---	CHECKED BY: ??					

Photo Inventory:

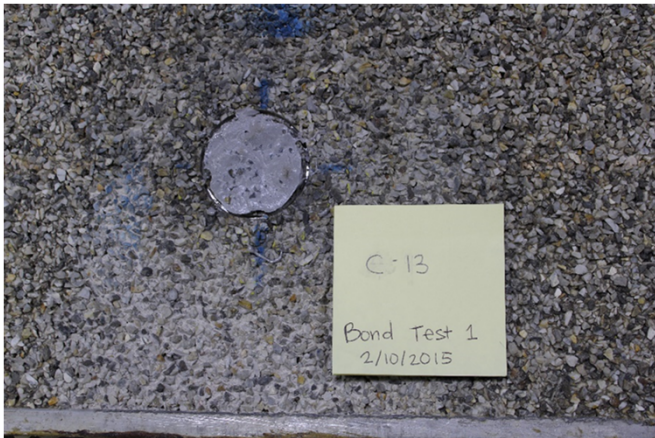
Bond Test 1A



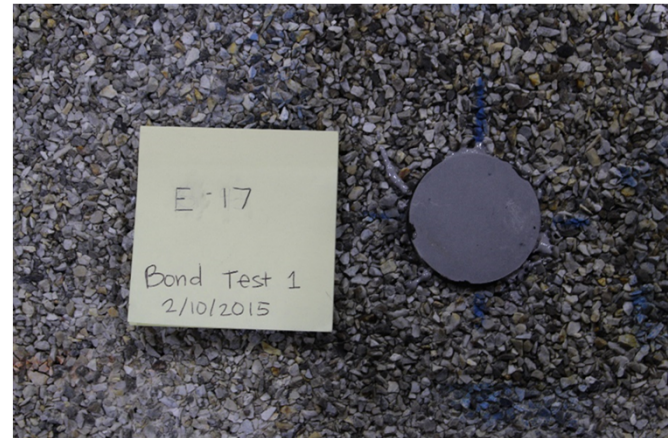
A-2



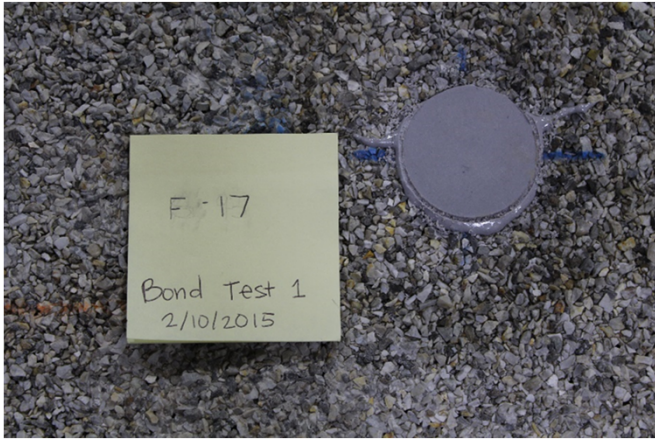
A-9



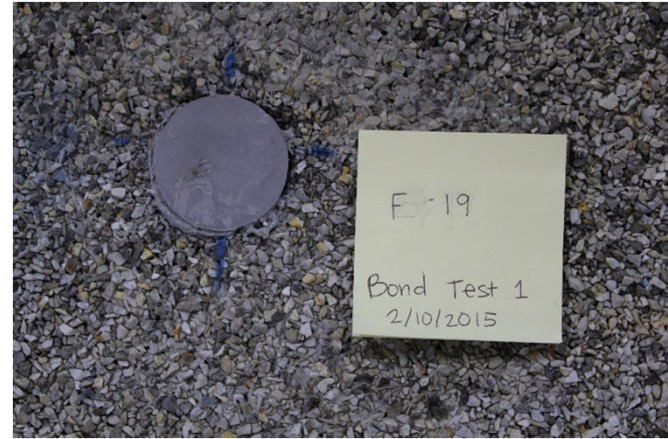
C-13



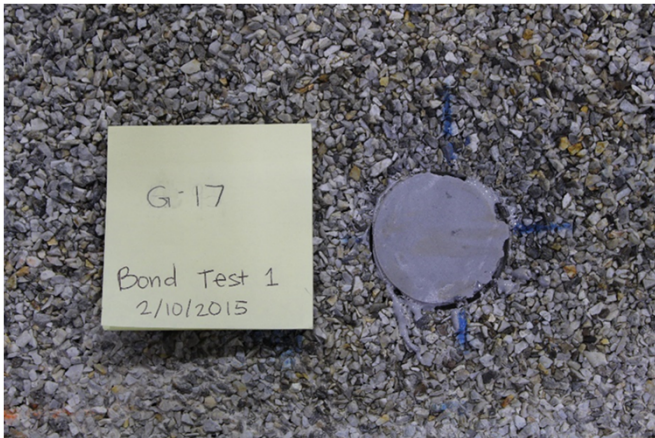
E-17



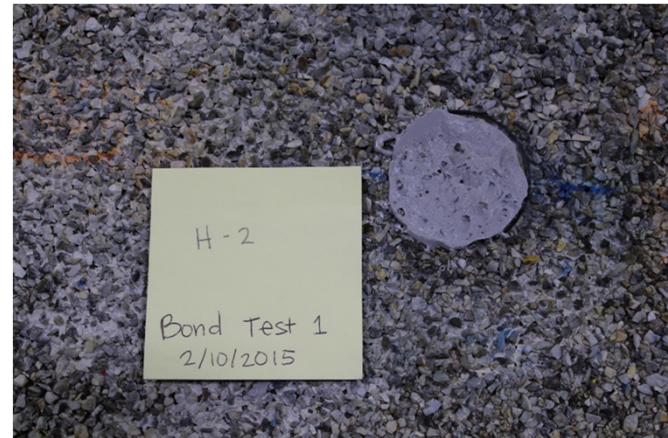
F-17



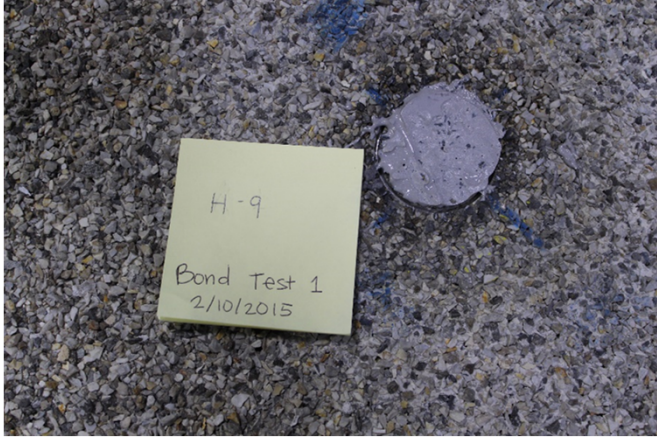
F-19



G-17



H-2



H-9

Photo Inventory:

Bond Test 1B



Test 1B - Location 1



Test 1B - Location 2



Test 1B - Location 3



Test 1B - Location 4



Test 1B - Location 5



Test 1B - Location 6



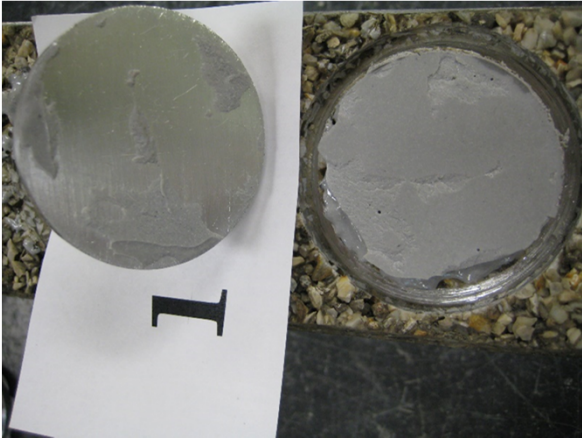
Test 1B - Location 7



Test 1B - Location 8

Photo Inventory:

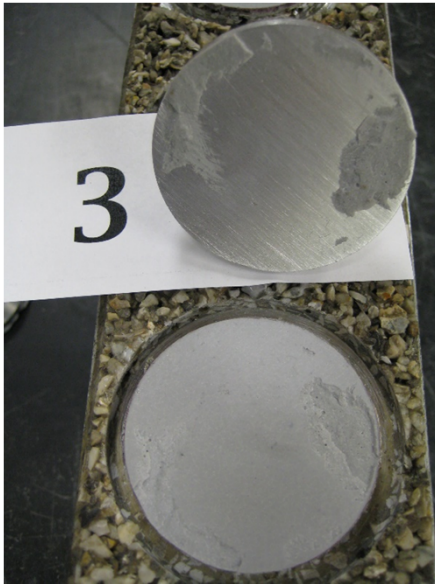
Bond Test 1C



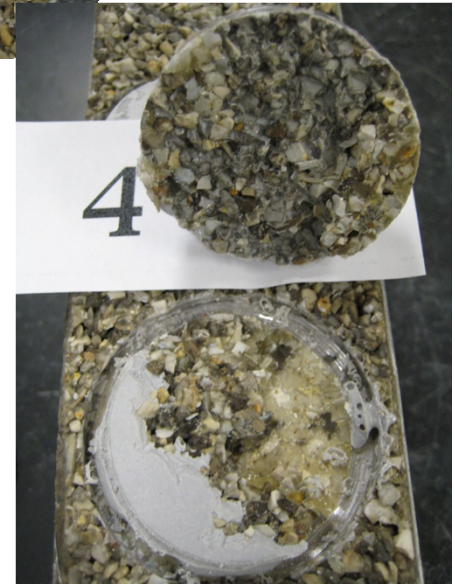
Location 1a



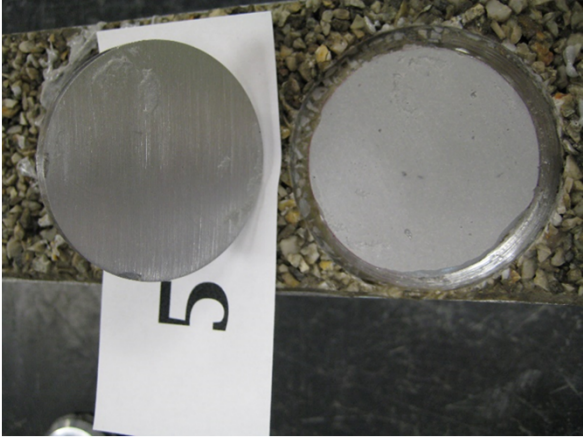
Location 2a



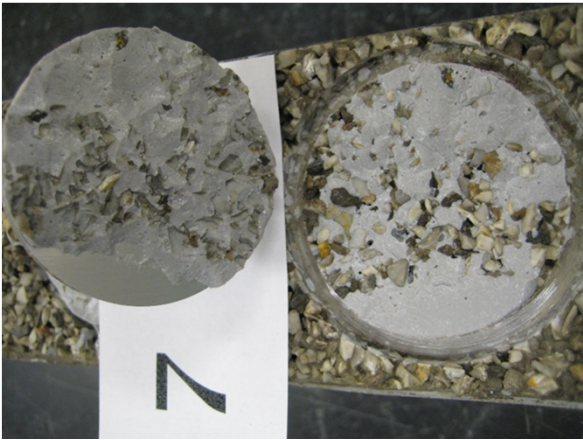
Location 3a



Location 4a- Incorrect Dolly



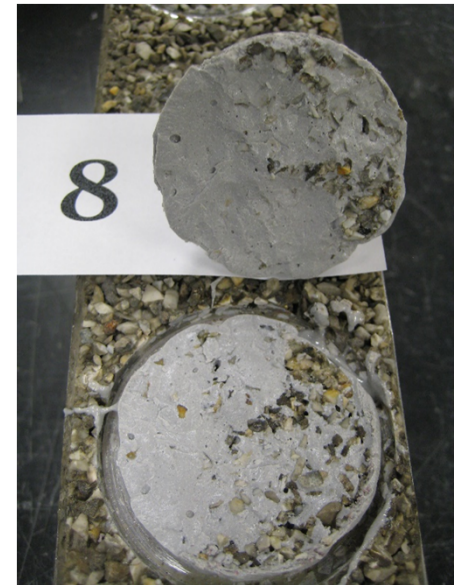
Location 5a



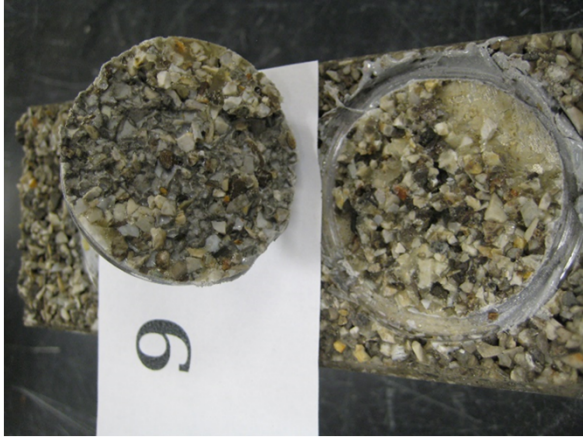
Location 7a



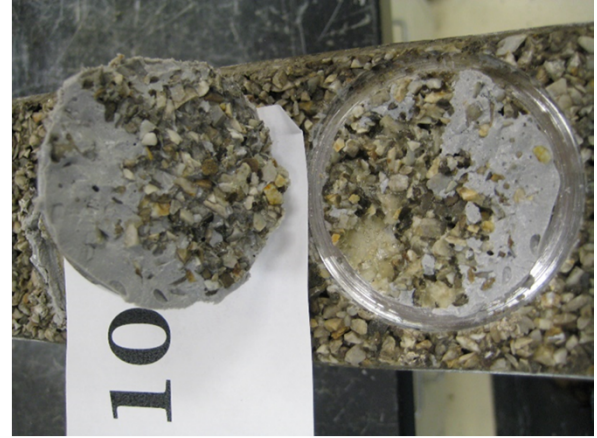
Location 6a



Location 8a



Location 9a



Location 10a

Appendix G: Friction Testing Report



Florida Department of Transportation

RICK SCOTT
GOVERNOR

605 Suwannee Street
Tallahassee, FL 32399-0450

JIM BOXOLD
SECRETARY

MEMORANDUM

DATE: June 21, 2016

TO: Christina Freeman, Structures Research Engineer

FROM: Charles Holzschuher, State Pavement Performance Engineer

COPIES: Bouzid Choubane, State Pavement Material Systems Engineer

SUBJECT: Dynamic Friction Tester (DFT), Circular Texturemeter (CTM), and Walking Texturemeter TM2 Testing on Aluminum Bridge Deck Surface

BACKGROUND

A special request was made to evaluate the friction and texture characteristics on an aluminum bridge deck overlaid with a skid-resistant wearing surface under three loading phases: (1) preload, (2) 1st 300,000 Heavy Vehicle Simulator (HVS) passes on dried surface condition at an elevated temperature of 120° F and (3) 2nd 300,000 HVS passes on wet surface condition. The skid-resistant wearing surface is a ¼” overlay, which consists of the Flexolith two-part epoxy resin mixed with basalt aggregate. Figure 1 shows the picture of the aluminum bridge deck with a close up view of the aggregate.

Three tests were performed, namely Dynamic Friction Tester (DFT) in accordance with ASTM E 1911, Circular Track Meter (CTM) test in accordance with ASTM E 2157, and Walking Texturemeter (TM2) test in accordance with ISO 13473. It should be noted that both CTM and TM2 measure macrotexture Mean Profile Depth (MPD), in which CTM measures MPD in a discrete way while TM2 measures MPD in a continuous way. A typical testing plan is presented in Figure 2. As shown, under each loading phase, both CTM and DFT will be performed at four spots (A, B, C and D) while TM2 will make three repeatable runs in the HVS wheel path.

This memo provides the testing results for the preload phase, the 1st 300,000 HVS passes loading phase and the 2nd 300,000 HVS passes loading phase.

SUBJECT: Dynamic Friction Tester (DFT), Circular Texturemeter (CTM), and Walking Texturemeter TM2 Testing on Aluminum Bridge Deck Surface



Figure 1. Aluminum bridge deck with a close up view of the aggregate.

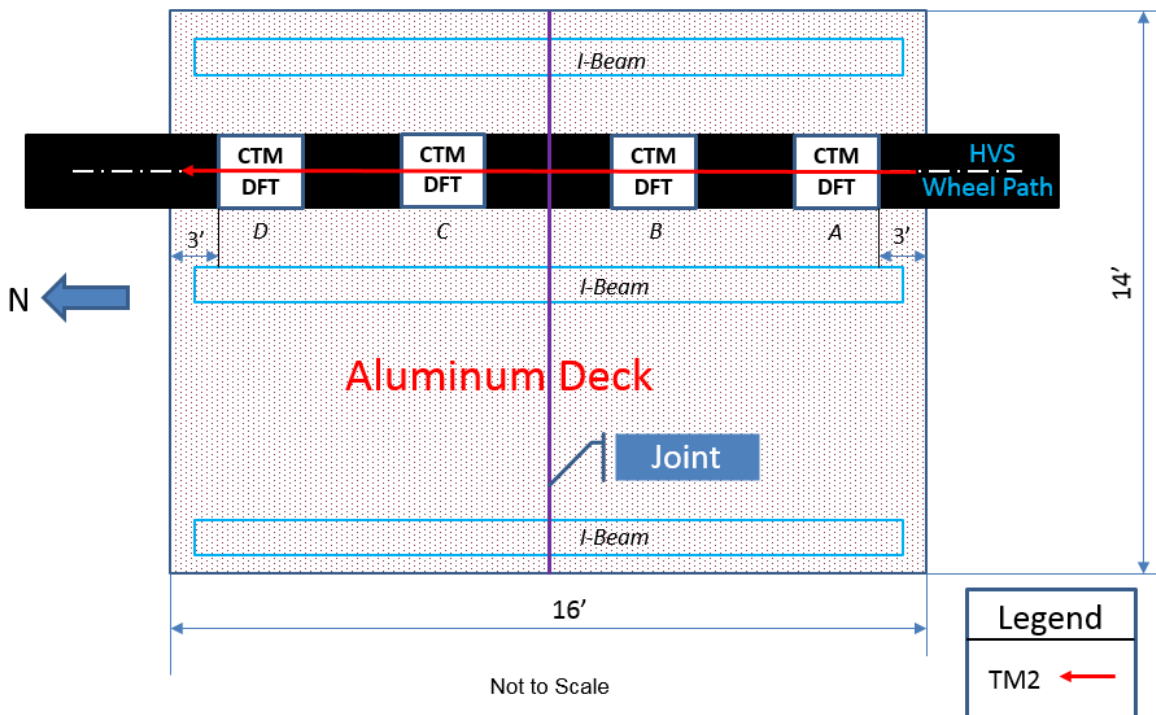


Figure 2. Test Plan for Aluminum Bridge Deck under HVS Loading Conditions

SUBJECT: Dynamic Friction Tester (DFT), Circular Texturemeter (CTM), and Walking Texturemeter TM2 Testing on Aluminum Bridge Deck Surface

RESULTS

DFT

The results of the DFT measurements for three loading phases are presented in table 1. As shown for multiple speeds, the average coefficient of friction for preload phase is between 0.85 and 0.90. The DFT coefficient at a 40 mph (designated as DFT40) is 0.897, which is equivalent to a friction number of 95. This value is determined when converting to a friction number measured at 40 mph using a locked wheel tester and ribbed test tire (designated as FN40R) using the following equation (1):

$$FN40R = 134 \times DFT40 - 24.7 \quad (1)$$

After the 1st 300K HVS passes at multiple speeds, the average coefficient of friction dropped between 0.71 and 0.77. After adjustment, the DFT40 is equal to 0.773 which is equivalent to a friction number of 79 when converting to FN40R. After the 1st 300K HVS passes, the deck surface was saturated and another 300K HVS passes were applied on the deck. The final average coefficient of friction dropped between 0.65 and 0.72 after 600K HVS passes in total. After adjustment, the DFT40 is equal to 0.722 which is equivalent to a friction number of 72 when converting to FN40R.

The equivalent FN40Rs for three loading phases exceed the requirement of 55 according to the developmental specification 403-Epoxy Overlay for Sealing and High Surface Treatment on Concrete Bridge Decks. Figure 3 shows the comparison between preload phase and the 1st 300K HVS passes. As shown, the coefficient of friction dropped about 20% on averaged after 600K HVS passes.

Table 1. Summary of DFT measurements for three loading phases

Loading Phase	Speed (mph)	A	B	C	D	Average	Equivalent FN40R
Preload	20	0.820	0.852	0.867	0.862	0.850	/
	30	0.840	0.874	0.914	0.915	0.886	/
	40	0.797	0.909	0.938	0.943	0.897	95
300K Passes	20	0.707	0.743	0.713	0.682	0.711	/
	30	0.716	0.753	0.735	0.717	0.730	/
	40	0.773	0.798	0.784	0.738	0.773	79
600K Passes	20	0.669	0.652	0.652	0.633	0.651	/
	30	0.684	0.673	0.664	0.666	0.672	/
	40	0.740	0.727	0.711	0.708	0.722	72

SUBJECT: Dynamic Friction Tester (DFT), Circular Texturemeter (CTM), and Walking Texturemeter TM2 Testing on Aluminum Bridge Deck Surface

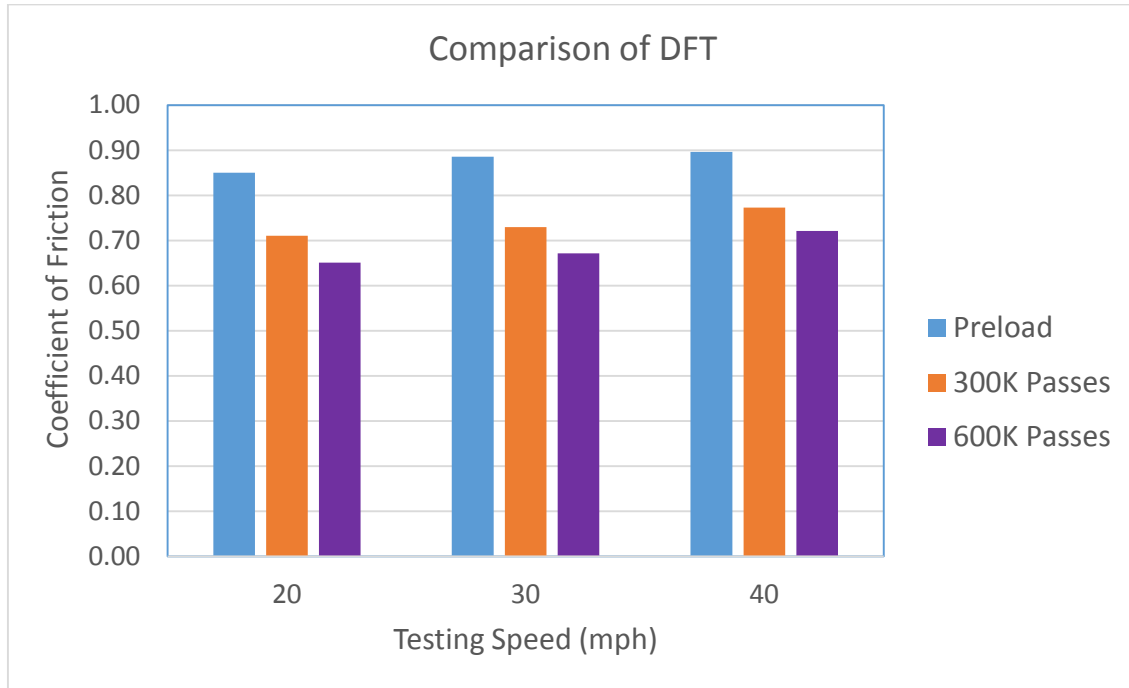


Figure 3. Comparison of average DFT measurements between Preload and 300K HVS Passes

CTM

The results of CTM measurements for three loading phases are presented in table 2. Detailed measurements are provided in Appendix I. As shown, the average MPD values are 2.016 mm for preload phase, 1.839 mm after 300K HVS passes and 1.836 mm after 600K HVS passes. For comparison purposes, the average MPD for the aluminum bridge deck section is higher when compared to a typical MPD for newer in-service longitudinal diamond grinding (LGD) concrete pavement (typically 0.6 mm) and longitudinal grind and transverse grooved bridge deck (typically 1.3 mm). Figure 4 shows the comparison among three loading phases. As shown, the MPD has dropped about 9% on average after 300K HVS passes. However, the MPD doesn't change much after 600K HVS passes as compared to the MPD after 300K HVS passes. Figure 5 shows the comparison of the surface texture between preload phase and after 600K HVS passes. As shown the texture seems to show minor aggregate wear and loss after 600K HVS passes. As a side note, due to the high friction surface texture of the deck surface, noticeable tire wear was observed as shown in Figure 6.

Table 2. Summary of CTM measurements for preload phase and 1st 300K HVS passes

Test Spots	MPD (mm)		
	Preload	300K HVS Passes	600K HVS Passes
A	2.043	1.844	1.705
B	2.153	1.676	1.821
C	1.999	1.884	1.776
D	1.870	1.951	2.043
AVG	2.016	1.839	1.836

SUBJECT: Dynamic Friction Tester (DFT), Circular Texturemeter (CTM), and Walking Texturemeter TM2 Testing on Aluminum Bridge Deck Surface

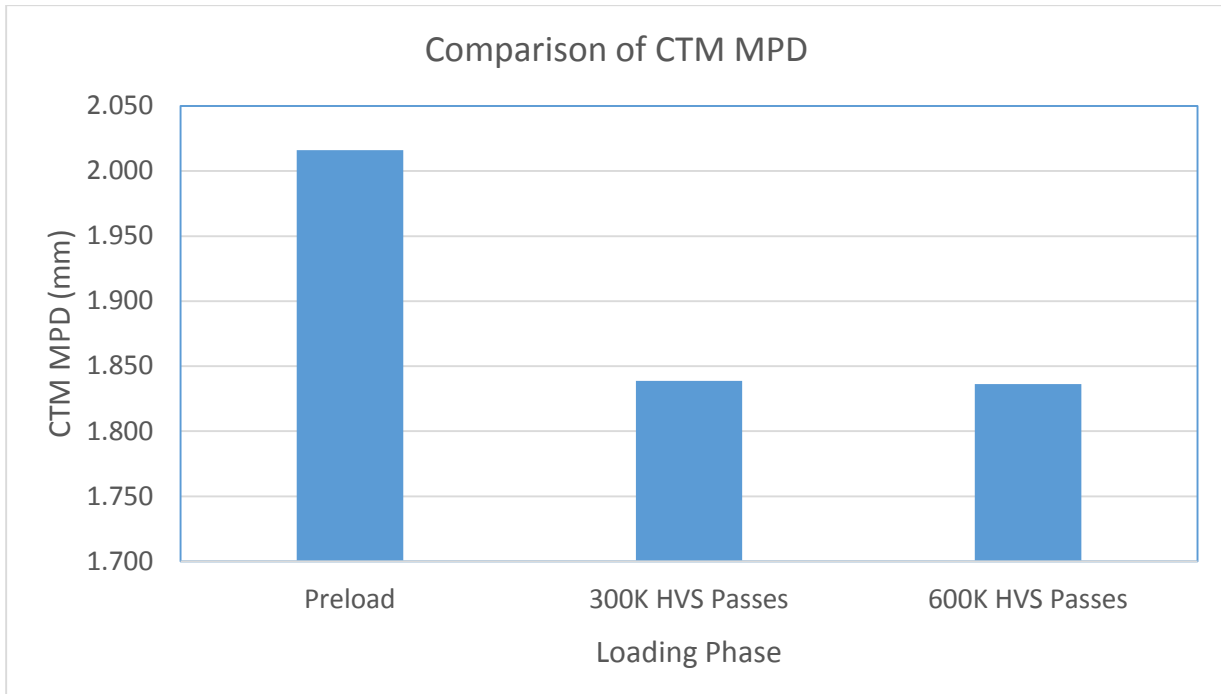


Figure 4. Comparison of average CTM measurements among three loading phases

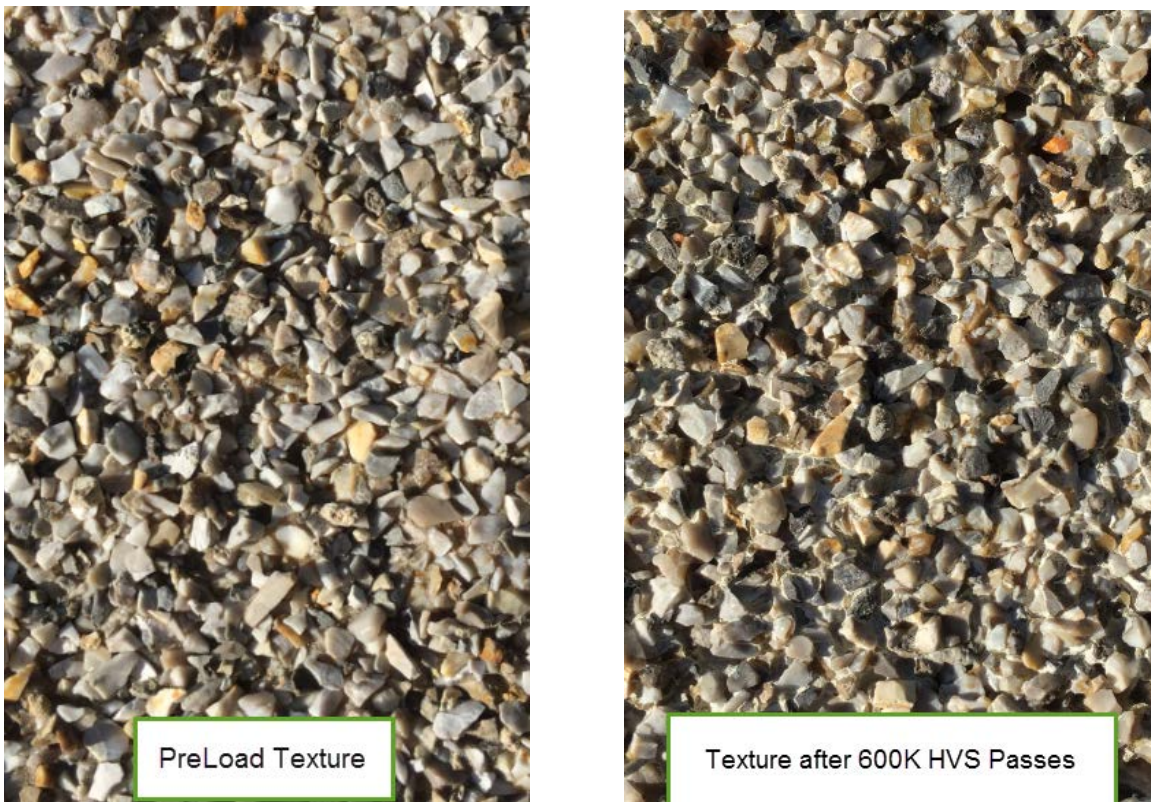


Figure 5. Comparison of texture before load and after 600K HVS passes.

SUBJECT: Dynamic Friction Tester (DFT), Circular Texturemeter (CTM), and Walking Texturemeter TM2 Testing on Aluminum Bridge Deck Surface

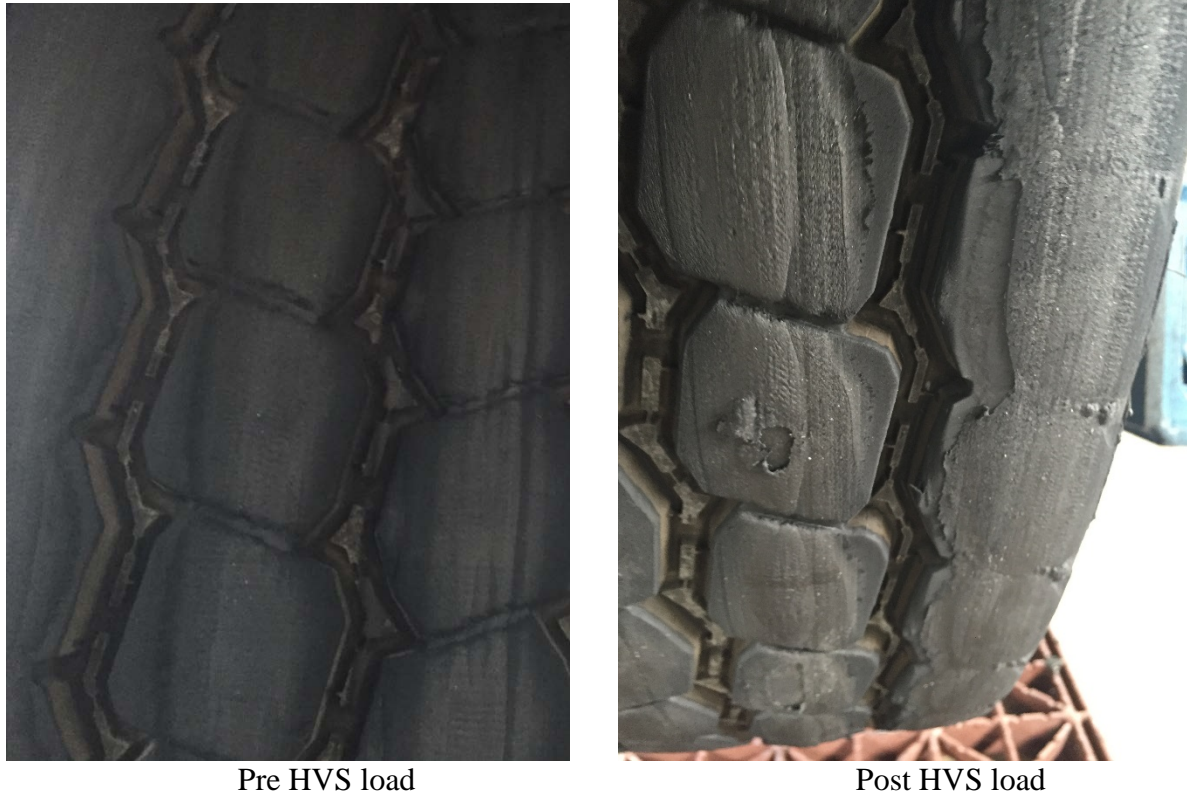


Figure 6. Comparison of tire wear before load and after HVS load.

TM2

The TM2 device shown in Figure 7 is a texturemeter that is capable of measuring the pavement texture in a continuous way in accordance with ISO 13473, while being pushed at a walking speed. The texture is measured over a 4.0 in. (100 mm) laser footprint projected transversely to the direction of travel at approximately every 0.08 in. (2 mm). The texture values calculated over these transverse profiles are averaged and can be reported at any desired interval between 4.0 in. (100 mm) and 164 ft. (50 m).

SUBJECT: Dynamic Friction Tester (DFT), Circular Texturemeter (CTM), and Walking Texturemeter TM2 Testing on Aluminum Bridge Deck Surface

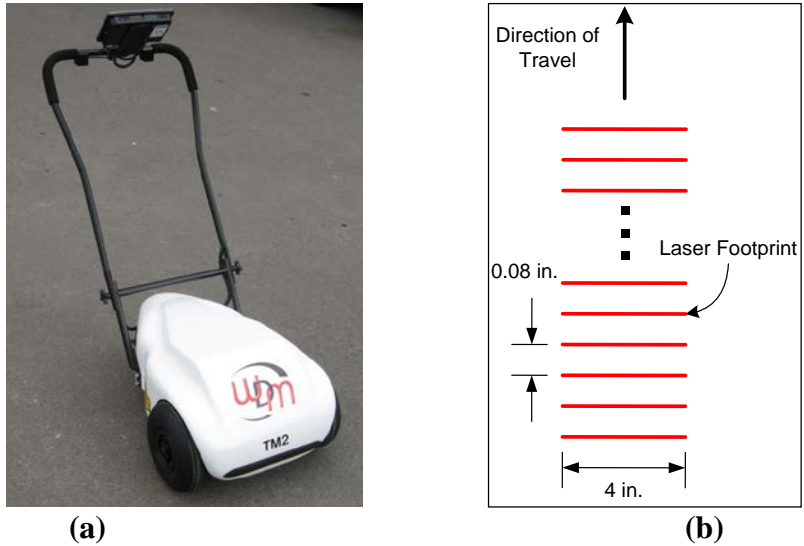


FIGURE 7 (a) Walking Texturemeter TM2 and (b) Schematics of Texture Collection

The results of TM2 measurements for three loading phases are presented in table 3. A detail dataset is provided in Appendix II. As shown, the average MPD values are 1.819 mm for preload phase, 1.719 mm after 300K HVS passes and 1.664 mm after 600K HVS passes. Figure 8 shows the comparison among three loading phases. As shown, the MPD is dropped about 9% on averaged after 600K HVS passes, which is similar to CTM test.

Table 3. Summary of TM2 measurements for three loading phases

TM2 Run#	MPD (mm)		
	Preload	300K HVS Passes	600K HVS Passes
Run1	1.810	1.767	1.664
Run2	1.828	1.702	1.662
Run3	1.819	1.687	1.666
AVG	1.819	1.719	1.664

SUBJECT: Dynamic Friction Tester (DFT), Circular Texturemeter (CTM), and Walking Texturemeter TM2 Testing on Aluminum Bridge Deck Surface

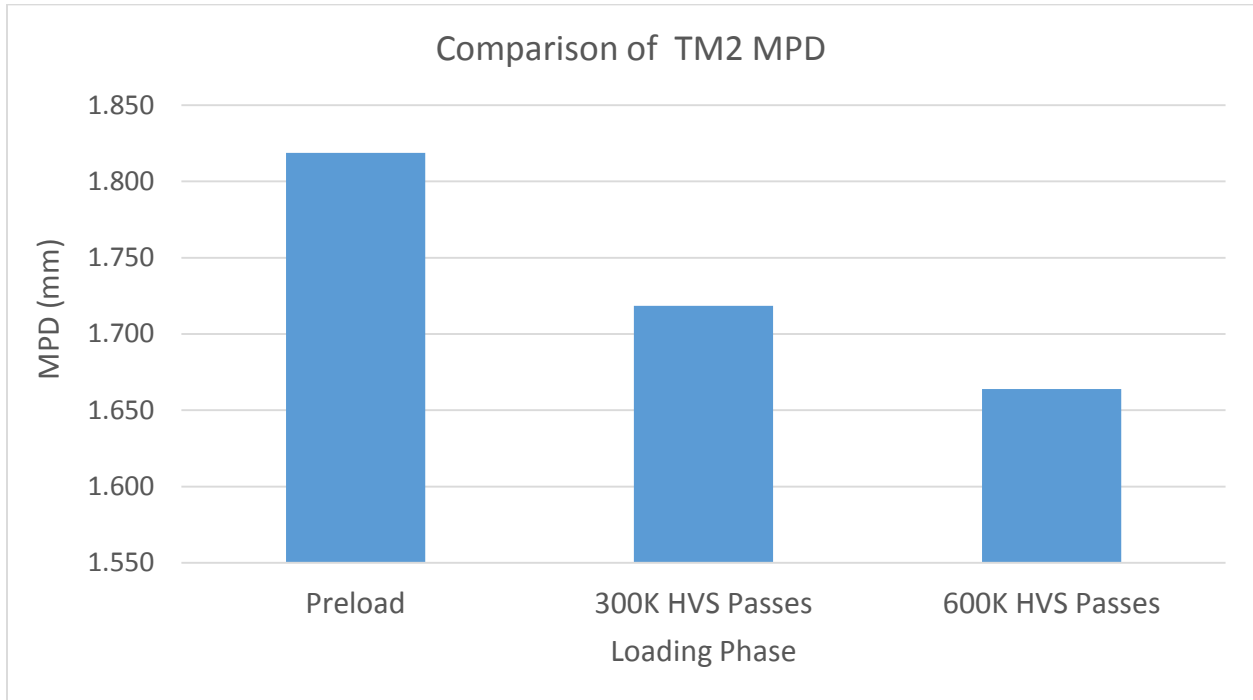


Figure 8. Comparison of average TM2 measurements among three loading phases

CONCLUSION

Based on testing results on three loading phases, some key points and observations are summarized below:

1. The results of DFT measurements show that the coefficient of friction dropped about 20% on average after 600K HVS passes. However, the equivalent FN40R after 600K HVS passes is 72, which still exceeds the requirement of 55 according to the developmental specification 403.
2. After 600K HVS passes, the results of both CTM (1.86 mm) and TM2 (1.66 mm) measurements show that the MPD has dropped about 9% on average and exceed newer in-service longitudinal diamond grinding (LGD) concrete pavement (typically 0.6 mm) and longitudinal grind and transverse grooved bridge decks (typically 1.3 mm).
3. Final observations indicate no physical distresses of the deck substrate and only minor aggregate wear and loss after 600K HVS passes. However, noticeable tire wear was observed during the evaluation due to the high friction surface texture.

CH/gm

SUBJECT: Dynamic Friction Tester (DFT), Circular Texturemeter (CTM), and Walking Texturemeter TM2 Testing on Aluminum Bridge Deck Surface

REFERENCE

1. Wilson, Bryan and Anol Mukhopadhyay. *Performance Evaluation of High Friction Surface Treatment and Development of Design and Construction Guidelines. Research Draft Submitted to Florida Department of Transportation, Report No. FHWA/FL-16/BDR74 977-05, Tallahassee, FL, May, 2016.*

SUBJECT: Dynamic Friction Tester (DFT), Circular Texturemeter (CTM), and Walking Texturemeter TM2 Testing on Aluminum Bridge Deck Surface

Appendix I: CTM Measurements

Loading Phase	Test ID	CTM_MPD (mm)											
		A	B	C	D	E	F	G	H	MAX	MIN	STD	AVG
Preload	A	2.220	2.340	2.670	1.780	1.900	1.890	1.940	1.600	2.670	1.600	0.345	2.043
	B	1.440	1.790	2.670	2.030	2.270	1.740	2.650	2.630	2.670	1.440	0.475	2.153
	C	1.750	1.800	1.840	2.770	2.320	1.780	1.990	1.740	2.770	1.740	0.366	1.999
	D	2.160	1.980	1.470	2.250	1.980	1.770	1.610	1.740	2.250	1.470	0.269	1.870
	Overall									2.770	1.440	0.368	2.016
300K HVS Passes	A	1.460	1.350	1.540	2.060	2.010	2.310	2.100	1.920	2.310	1.350	0.348	1.844
	B	2.070	1.920	1.140	1.410	1.410	1.500	1.710	2.250	2.250	1.140	0.379	1.676
	C	2.460	1.510	1.730	1.760	1.820	2.640	1.750	1.400	2.640	1.400	0.437	1.884
	D	1.690	2.070	2.100	1.600	1.970	1.890	2.370	1.920	2.370	1.600	0.242	1.951
	Overall									2.640	1.140	0.356	1.839
600K HVS Passes	A	1.900	1.880	2.520	1.390	1.370	1.600	1.490	1.490	2.520	1.370	0.387	1.705
	B	1.700	1.820	1.650	1.700	1.610	1.720	2.910	1.460	2.910	1.460	0.452	1.821
	C	1.410	1.230	2.290	1.500	1.710	1.920	2.090	2.060	2.290	1.230	0.374	1.776
	D	2.370	1.660	1.810	2.130	2.860	1.820	2.060	1.630	2.860	1.630	0.415	2.043
	Overall									2.910	1.230	0.408	1.836

SUBJECT: Dynamic Friction Tester (DFT), Circular Texturemeter (CTM), and Walking Texturemeter TM2 Testing on Aluminum Bridge Deck Surface

Appendix II: TM2 Measurements

Distance	Preload			300K HVS Passes			600K HVS Passes		
	MPD (mm)			MPD (mm)			MPD (mm)		
	RUN1	RUN2	RUN3	RUN1	RUN2	RUN3	RUN1	RUN2	RUN3
0.2	1.89	1.95	1.95	1.77	1.63	1.68	1.77	1.54	1.72
0.4	1.91	1.88	1.85	1.77	1.77	1.76	1.75	1.69	1.71
0.6	1.82	1.82	1.81	1.73	1.66	1.67	1.57	1.7	1.65
0.8	1.96	1.89	1.89	1.79	1.66	1.67	1.61	1.64	1.57
1	1.87	1.84	1.86	1.7	1.59	1.59	1.64	1.54	1.58
1.2	1.82	1.82	1.79	1.71	1.64	1.59	1.63	1.64	1.6
1.4	1.78	1.79	1.78	1.72	1.66	1.61	1.72	1.6	1.74
1.6	1.7	1.69	1.63	1.68	1.75	1.77	1.61	1.67	1.63
1.8	1.68	1.73	1.74	1.76	1.64	1.66	1.69	1.61	1.6
2	1.53	1.58	1.53	1.74	1.66	1.64	1.51	1.61	1.5
2.2	1.85	1.81	1.86	1.72	1.55	1.62	1.62	1.59	1.65
2.4	1.81	1.81	1.83	1.64	1.65	1.62	1.53	1.6	1.6
2.6	1.88	2	1.95	1.72	1.58	1.59	1.69	1.6	1.62
2.8	1.76	1.82	1.82	1.72	1.62	1.62	1.63	1.61	1.73
3	1.81	1.79	1.8	1.78	1.77	1.75	1.63	1.6	1.69
3.2	1.73	1.76	1.76	1.8	1.77	1.72	1.72	1.67	1.67
3.4	1.79	1.79	1.77	1.75	1.7	1.7	1.67	1.72	1.66
3.6	1.84	1.87	1.84	1.71	1.7	1.74	1.78	1.72	1.76
3.8	1.82	1.93	1.94	1.77	1.82	1.7	1.78	1.74	1.81
4	1.89	1.99	1.98	1.96	1.88	1.86	1.83	1.79	1.89
4.2	1.86			1.97	1.88	1.85		1.9	
4.4				1.96	1.79				
AVG	1.810	1.828	1.819	1.767	1.702	1.687	1.664	1.662	1.666
STD	0.094	0.100	0.107	0.090	0.094	0.082	0.086	0.084	0.092